"EVALUATION OF PARALLEL FEED WATER HEATING IN INTEGRATED SOLAR THERMAL POWER PLANT"

A DISSERTATION

SUBMITTED IN PARTIAL FULFILLMENT OF THE REQUIREMENTS FOR THE AWARD OF THE DEGREE OF

MASTER OF TECHNOLOGY

IN

THERMAL ENGINEERING

Submitted by:

NEERAJ KUMAR SHUKLA

(Roll No. 2K16/THE/15)

Under the supervision of

DR. SAMSHER

PROFESSOR

DEPARTMENT OF MECHANICAL ENGINEERING

DELHI TECHNOLOGICAL UNIVERSITY

(Formerly Delhi College of Engineering)

Bawana Road, Delhi-110042

JUNE, 2018

DELHI TECHNOLOGICAL UNIVERSITY

(Formerly Delhi College of Engineering)

Bawana Road, Delhi-110042

CANDIDATE'S DECLARATION

I, NEERAJ KUMAR SHUKLA, Roll No. 2K16/THE/15 student of M.Tech (Thermal Engineering), hereby declare that the project Dissertation titled "Evaluation of Parallel Feed Water Heating in Integrated Solar Thermal Power Plant" which is submitted by me to the Department of Mechanical Engineering, Delhi Technological University, Delhi in partial fulfillment of the requirement for the award of the degree of Master of Technology, is original and not copied from any source without proper citation. This work has not previously formed the basis for the award of any Degree, Diploma Associateship, Fellowship or other similar title or recognition.

Place: Delhi **NEERAJ KUMAR SHUKLA**

Date:

DEPARTMENT OF MECHANICAL ENGINEERING

DELHI TECHNOLOGICAL UNIVERSITY

(Formerly Delhi College of Engineering)

Bawana Road, Delhi-110042

CERTIFICATE

I hereby certify that the project Dissertation titled "Evaluation of Parallel Feed Water Heating in Integrated Solar Thermal Power Plant" which is being submitted by NEERAJ KUMAR SHUKLA, Roll No. 2K16/THE/15, Department of Mechanical Engineering, Delhi Technological University, Delhi in partial fulfillment of the requirement for the award of degree of Master of Technology, is a record of the project work carried out by the student under my supervision. To the best of my knowledge this work has not been submitted in part or full for any Degree or Diploma to this University or elsewhere.

Place: Delhi **(DR. SAMSHER)**

Date: **SUPERVISOR**

PROFESSOR

DEPARTMENT OF MECHANICAL ENGINEERING

ACKNOWLEDGEMENT

Any accomplishment is a result of positivity of thoughts and efforts. It is important here to appreciate contribution, encouragement and support from persons who stood as 'Light House' throughout the voyage.

I wish to express my sincere gratitude for my project supervisor and mentor, DR. SAMSHER, Professor, Department of Mechanical Engineering, Delhi Technological University (Delhi). It was a golden opportunity to work under his kind supervision. His scholastic guidance and sagacious suggestions helped me to complete the project.

I wish to thank DR. VIPIN, Head, Department of Mechanical Engineering, Delhi Technological University (Delhi), for constantly motivating and providing able guidance.

I am also thankful to the faculty and staff of Department of Mechanical Engineering, Delhi Technological University (Delhi) for their continual support and cooperation.

Finally, but importantly, I would like to express my heartfelt thanks to my beloved family and friends who have endured the long working hours and whose motivation kept me going.

NEERAJ KUMAR SHUKLA

(Roll No. 2K16/THE/15)
M.Tech. (Thermal Engineering)
Delhi Technological University, Delhi, India

ABSTRACT

The integration of steam power plant to solar thermal energy is a research area based on modern day challenges of higher power production with lower emission. The steam power plant solar integration can be done in many ways detailed in this project. One such method is to replace feed water heaters of a regenerative steam power plant with solar heating system. This is the most recent scheme and requites least modification in existing plant. It is also very flexible integration scheme as the control systems provide methods to operate plant in solar integrated mode as well as base mode. The analysis is done based on two methods; analytical method and simulation method. The analysis is performed by formulating entire case and then analyzing it with data available with on 'Engineering Equation Solver' (EES) software. The concept of solar thermal energy storage to increase overall efficiency of integrated model is also introduced and analyzed. This model is then simulated in 'System Analyzer Model' (SAM) software to get the trend analysis results of the project. The 'Integrated Solar Thermal Power Plant, Dadri' is chosen as the base model of this work. The solar thermal integration at this plant is modeled on 'Compact Linear Fresnel Reflector' (CLFR) Technology. In this work the CLFR is replaced with 'Heliostat Field Collector' (HFC). This model is having higher solar thermal collection efficiency as well as more heat available to aid the steam cycle. The solar thermal storage addition had added system ability to operate with integrated mode for a longer duration. Talking to the environmental front, this type of integrating with optimum integration mode had proved better on emission front. The carbon dioxide and sulphur dioxide emissions are reduced in the integrated mode as obtained from the analysis results. The other pollutants are also assumed to be reduced in the same pattern. In economical terms, the project is also analyzed on coal saving front. The hourly coal saving in different integration modes is provided. This shows the economical benefits of the project. Carbon dioxide emission reduction is also a good step to save carbon tax as well. Thus the benefits of such schemes are worth noting and further research should also be continued on the technology for betterment of existing results.

CONTENTS

LIST OF FIGURES

LIST OF TABLES

ABBREVIATIONS

CLFR	Compact Linear Fresnel Reflector
CSP	Concentrated Solar Power
CST	Combined Solar Thermal
CW	Cooling Water
DNI	Direct Normal Irradiance
FWH	Feed Water Heater
GCV	Gross Calorific Value
HFC	Heliostat Field Collector
HPT	High Pressure Turbine
IPT	Intermediate Pressure Turbine
ISTPP	Integrated Solar Thermal Power Plant
LCV	Lower Calorific Value
LFR	Linear Fresnel Reflector
LPT	Low Pressure Turbine
MNRE	Ministry of New and Renewable Energy
NCPS	National Capital Power Station
NREL	National Renewable Energy Laboratory
NTPC	National Thermal Power Corporation
SAM	System Advisor Model
SG	Steam Generator
TES	Thermal Energy Storage

LIST OF SYMBOLS

Letters

A	Area (m^2)
c	Specific heat (kcal/kg)
CV	Gross calorific value (kcal/kg)
F	Amount of coal (Ton/hr)
h	Enthalpy (kJ/kg)
L	Latent Heat (kcal/kg)
m	Mass flow rate (Ton/hr)
M	Mass (kg)
η	Efficiency
P	Power (MW)
P	Pressure (N/m^2)
Q or q	Heat (kJ/kg)
ρ	Density (kg/m^3)
R	Rate of production (kg/hr)
S	Solar Irradiance (W/m^2)
SH	Solar heat (W)
T	Temperature (^{0}C or K)
v	Specific volume
V	Volume (m^3)
W or w	Work (kJ/kg)

Subscripts

1, 2, 3, 4,.....26	Points as shown in corresponding schematic diagram or cycle
I,II,III,IV,V,VI,VII	Corresponding cases of FWH replacement
A	Feed water heater A
B	Feed water heater B
BFP	Boiler Feed Pump
c	Collector
C	Feed water heater C
CO_2	Carbon dioxide
Case	Corresponding case

CEP	Condensate extract pump
CT	Colder fluid at thermal storage
Cycle	Of corresponding cycle being studied
d	Average annual value of solar parameter
D	Feed water heater D or Deaerator
Drip	Drip pump
e	At entrance
E	Feed water heater E
f	Saturated liquid state
F	Feed water heater F
g	Saturated vapour state
G	Of coal
gen	Generated
HT	Hot Fluid at thermal storage
i	At exit
in	Coming in to the system
net	Net value of said parameter
out	Coming out from the system
P	Pump
pump,in	Input to the pump
Salt	Thermal Storage Salt
SO_2	Sulphur dioxide
T	Turbine
Tank	Thermal Storage Tank
th	Thermal
turbine,out	Output from the turbine

CHAPTER 1

INTRODUCTION

1.1 GENERAL

Before beginning of modern civilization, there were three basic needs for social survival; Food, cloth and shelter. Modernization of civilization has added another basic need i.e. Power (or electricity). The digitization of modern world has boosted the global power needs. India that recently took a remarkable jump to become the sixth mammoth economy of the world is also among the world's leading consumer of electricity [1].

The consumption of electricity should meet with production for an appropriate balance. In terms of production as well as consumption of electricity in the world, India is now third in the world, behind China and United States of America. The net production of electricity in Financial Year 2016 was 1423 billion units (BU) [2].

Fig. 1.1 depicts the on-grid power production in India in different sessions. India has a capacity to produce surplus power but is unable to do so because of under developed infrastructure and poor transmission together with distribution system.

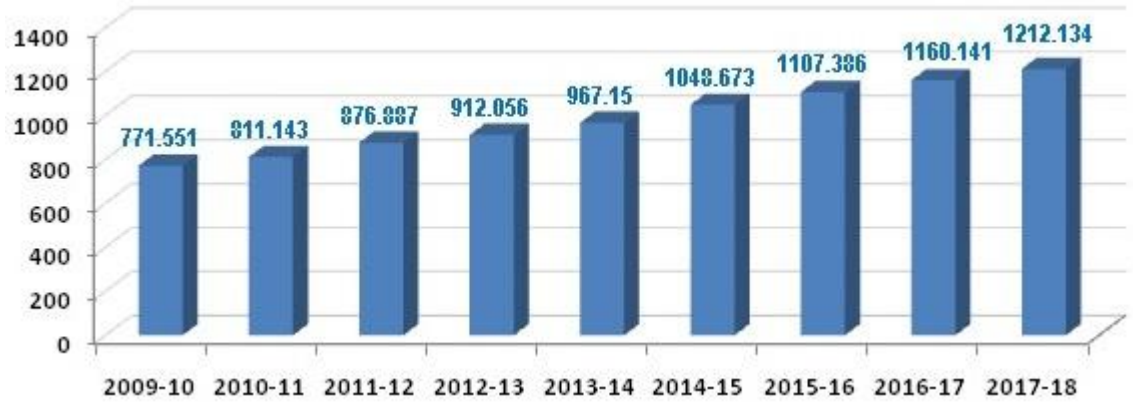

Fig.1.1 On-grid power production across years in India [3]

1.2 INDIA'S POWER PRODUCTION: AN OVERVIEW

The generation of electrical power needs some source. The power sector of India is shown briefly by 'Ministry of Power', GoI. Following important data was retrieved as presented in table 1.1 below;

Table 1.1 Summary of power production in India [3].

Fuel	MW of Production	% of Total
Total Thermal	222693	64.8
Coal	196958	**57.3**
Gas	24897	7.2
Oil	838	0.2
Hydro	45293	13.2
Nuclear	6780	2.0
Renewable Energy Sources	69022	**20.1**
Total	**344002**	

From above table, it is clearly evident that Indian power production is majorly dependent on coal. Not only India, but coal is main power producing fuel in the world owing to its certain merits such as;

- Coal is most reliable and economically stable fuel of world.
- It is simple to burn coal and produce high energy.

The power production from coal needs setting up a thermal power plant, driven by coal as primary fuel. The coal being fuel of power has certain lacks and limitations [4].

- Coal is an exhaustible energy source i.e. the world should be none left of coal in coming time.
- Green house gases emission is other prime disadvantage of coal burning.
- Coal mining trigger ecological imbalances.
- Coal burning is genesis of thousands tons of waste.

- Harmful particles as Mercury, Selenium, Arsenic, Carbon etc. are also emitted.
- Coal transportation is also not very economical.

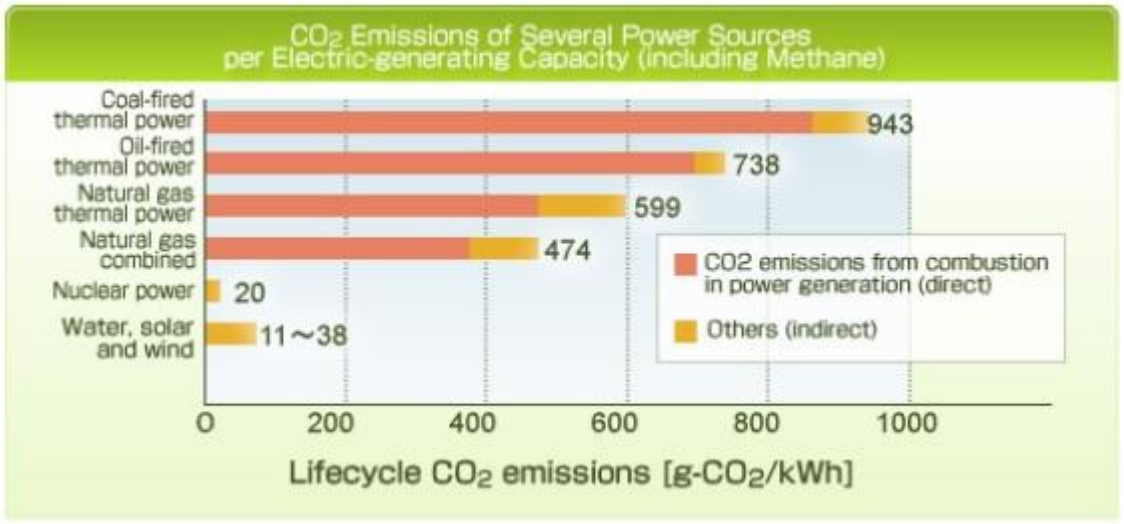

Fig. 1.2 Carbon dioxide production from various sources with estimation [5]

From above discussion it is evident that there is greater number of disadvantages than advantages of coal utilizing power production technology [4], [6]. However, the dependency on coal is still there and shall also remain in future because of non-availability of other reliable technology [7].

Table 1.1 also lists the power production from renewable resources. The renewable sources mentioned above include;

- Hydro projects (Smaller),
- Biomass power,
- Biomass gasifier,
- Industrial and urban waste power,
- Solar Energy, and
- Wind energy.

The utmost advantage with these sources is there inexhaustible and non-polluting nature. Renewable energy is one which is obtained using sources provided by nature. The exhausting nature of major fossil fuels of world and their harmful environmental impact has drawn world attention towards renewable resources of energy.

1.3 RENEWABLE ENERGY STATUS

To take an idea on renewable energy status, first we have to take a look on world energy status. Following fig. 1.3 shows the same;

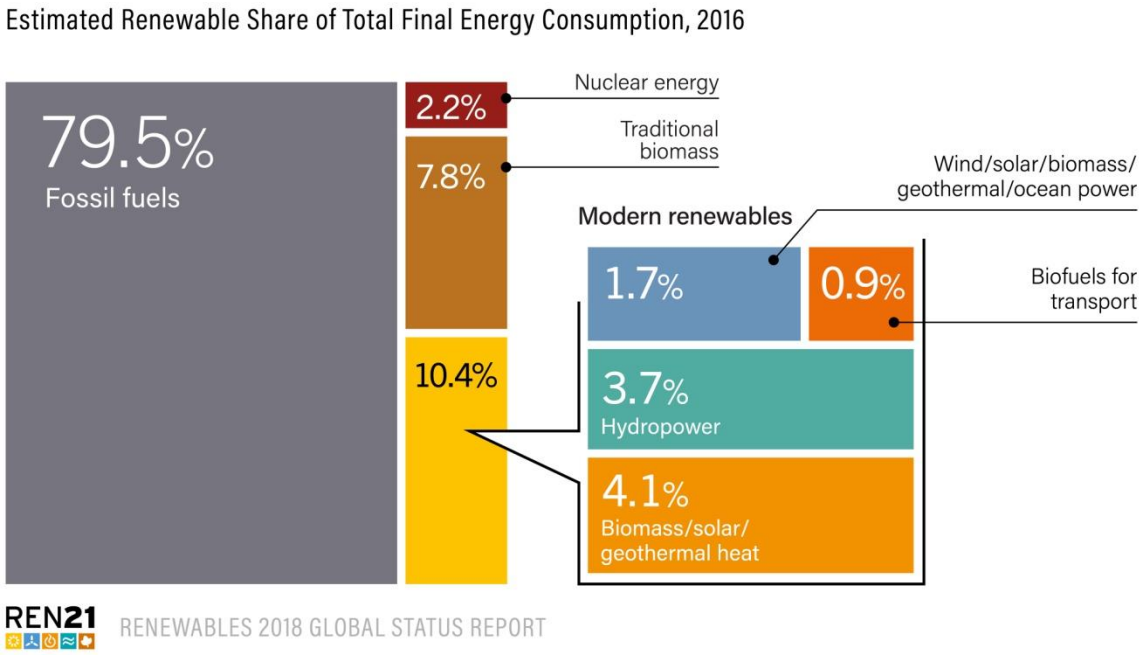

Fig. 1.3 World total energy consumption utilizing different sources [8].

There is significant increase in global renewable energy capability in recent years. Among renewable energy major sources, three are; Solar, Wind and Hydroelectricity.

India has clear target, '175 GW renewable energy infrastructure developments till 2022' [9]. The India's renewable energy status presented by 'Ministry of New and Renewable Energy', GoI, is summarised in following table 1.2.

Table 1.2 Grid interactive power from renewable energy [10].

Sector	Financial Year 2018-19		Net Achievement (Till 31/05/2018) (MW)
	Total Target (MW)	Achievements (Till May 2018) (MW)	

Wind Power	4000	48.2	34193.2
Ground Mounted Solar Power	10000	530.8	21118.6
Roof Top Solar Power	1000	147.1	1210.7
Smaller Hydro Power	250	7.4	4493.2
Biomass (Bagasse) Cogeneration	250	0	8700.8
Biomass (non-bagasse) Cogeneration)/Captive Power	100	12	674.8
Waste to Power	2	0	138.3
Total	15602	745.3	70529.7

1.4 SOLAR ENERGY POTENTIAL IN INDIA

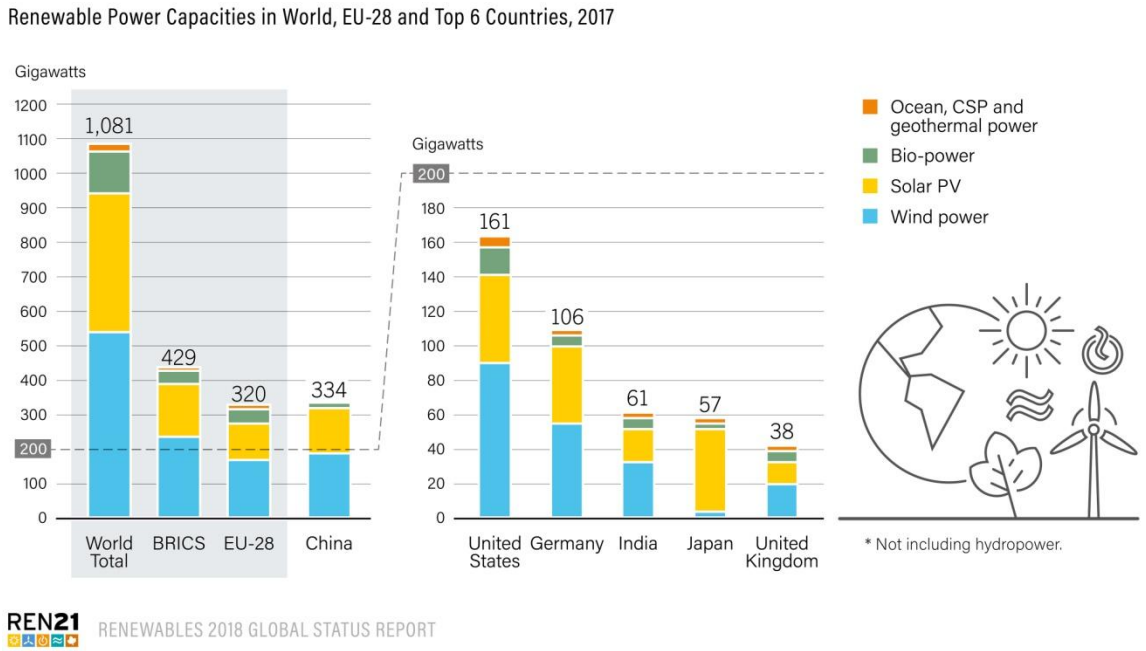

Fig. 1.4 Renewable energy production potential in world with top six countries [8]

Renewable energy development has a challenge. It is non-uniformly available across the globe. There are few nations in globe having high renewable energy potential. The recent report shows the same in fig. 1.4.

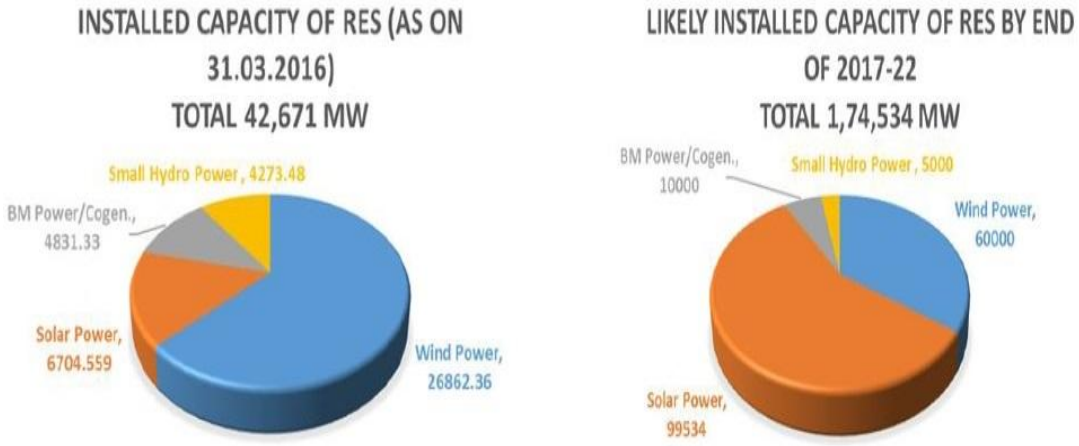

Fig. 1.5 Indian renewable energy capacity addition in coming future [11]

In India's target to reach the renewable energy of 175 GW up to 2022 [9], following capacity addition is projected as presented in fig. 1.5. Thus, the solar capacity addition is most important in recent future [12].

1.5 FRAMEWORK OF THE DISSERTATION

From above discussion, it is evident that coal, as source of energy, can't be neglected in coming future. Also, there is growing market of solar energy in our country, as a major renewable energy source [13]. Hence, some method should be there to integrate the coal energy to solar energy. The Integrated Solar-Thermal Power Station is one such solution. Integration of solar collected energy with thermal power plant minimizes the fossil fuel utilization and hence benefits of renewable resource aids the system. In this dissertation, the project discusses is solar-thermal integration of power station. The framework of the dissertation is:

- In first chapter of the project, the general introduction of the scenario is given to visualize need of project as per present time energy status.

- In second chapter, the literature exposition and intent of project is specified.
- Third chapter presents basic overview of methodology to power production from coal as a fuel and its components. Then solar energy collection techniques are briefed in light of the project. In later part of this chapter, the various techniques to integrate solar power to thermal systems are given.
- In fourth chapter, a case discussion of NTPC, Dadri "Integrated Solar Thermal Power Plant" is presented as base of this project. The analytical model of the base case is also developed for better understanding of the technology.
- In fifth chapter, the improved methodology to integrate same plant to solar energy is described. The improved collector model for better solar thermal collection efficiency is proposed and analyzed. Also, a storage system for solar thermal is integrated analytically for better performance. At last in this chapter, analytical model is simulated on SAM software for further analysis.
- In sixth chapter, results of analytical and simulated models are presented and discussed.
- The seventh chapter presents the conclusion of study with the future outlook to model and its betterment ahead.
- At last, the references of the study and a few appendixes are provided to aid this project report.

CHAPTER 2

LITERATURE REVIEW

2.1 STEAM POWER STATIONS

A machine which is used to generate electricity is called alternator or generator. The electricity is produced due to rotation of the generator coil in magnetic field. The alternator or generator coil needs an external torque to rotate. This rotation is provided by some external means, called prime mover. The power stations differ in type of prime mover they use to drive the generator coil. In a steam power plant, the rotation to generator coil is provided by a steam turbine, so it is named steam power station. The basic representation of steam power station is provided in fig. 2.1.

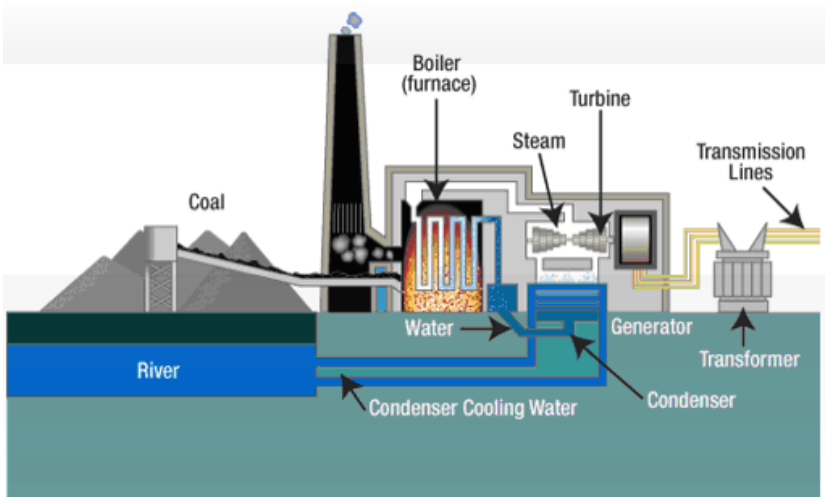

Fig. 2.1 Steam power plant basic representation.

The rotation of steam turbine axel is done by steam expansion on turbine blades. This steam is generated in boiler by fossil fuel (coal etc.) burning. The fossil fuel burning also causes generation of some harmful byproducts and environmental pollutants.

The project discussed in this dissertation is an integration of steam power plant to solar energy hence a literature survey of steam power plant is important as a base of the project. Few important researches are described as under:

Mishra U. C. (2004) investigated environmental impact of thermal power stations and coal industry in India. As per his study the scale of environmental condition in this century will be determined by energy generation plans of developing countries like India. A few of the suggestions had been implemented in new plants and their situation is much better [7].

Raghuvanshi S. P. et.al (2006) theoretically analyzed emission of carbon di-oxide from coal fueled power stations in India. Their study shows that CO_2 generated as a by-product of coal (or fossil fuels) combustion is cause of more then 60% of the increase in global warming. Their work also provides a brief examination of CO_2 generation from coal fueled power stations in India. Methodology for examination of carbon emissions and possibility of sinks is also provided [4].

Sengupta S. et.al (2007) numerically investigated exergy analysis of 210 MW coal fired thermal power station at NTPC, Dadri. The analysis was based on operating data collected from plant visit. It was observed by the authors that boiler is the major reason behind irreversibility in cycle and it accounts for an exergy loss of about 60%. The operations on part load also increase the plant cycle irreversibilities and these irreversibilities enlarge with reduction of load. Their basic observational data of plant cycle operation is important for analysis presented in this report as well [14].

Hashimoto T. (2008) talked about technological changes in modern power plants and enhances their efficiency as well as reduces emissions. The project was centered to increase the power cycle efficiency to enhance power production and also to minimize the CO_2 emission [15].

Graus W. et.al (2010) developed a model for calculating CO_2 intensity due to power generation and utilization at the global level. Their study concluded that method

chosen could have a larger impact on the CO_2 intensity for countries that have relatively greater number of heating and power plants [16].

International Energy Agency (IEA) (2010) presented its report titled 'Power Generation from Coal: Measuring and Reporting Efficiency, Performance and CO_2 Emissions' against 'Plan of Action' on change in climate , which was released with the G-8 'Gleneagles Summit' in July 2005. This report reviewed the ways to calculate and express coal power station's efficiency and CO_2 emissions [17].

Mittal M. L. (2011) studied about emission of oxides of carbon, nitrogen and sulphur from Indian thermal power plants for a time of 9 years. He performed analytical calculation of mass emission factor using basic principles of combustion at actual operating conditions of the power station. An estimation of emissions up to 2021 was also provided based on the study. This study provided useful method for inventory preparation in power sector as measured value for emission factor is important in this field [6].

Murehwa G. et.al (2012) carried out energy efficiency improvement analysis of coal stimulated thermal power stations. The energy analysis was compared with exergy analysis and their difference was presented. This study was important to have an idea of the gap between energy demand and generation [18].

Geete A. et.al (2013) studied numerically the variation effect in inlet temperature at constant inlet pressure on a 120 MW coal power station. Parametric graphs relating power produced and heat rate at specific pressure and temperature conditions at various points were plotted. The trend analysis of curves showed plant performance variation with variation in plant input parameters of pressure and temperature [19].

Ravinder K. et.al (2014) thermo-economically investigated 210 (MW) thermal power station. Thermodynamic study with 'mass' and 'energy' balance equations and empirical correlations was also done. The economic analysis was also performed. The impact of efficient operation of condensate pump was more important than the drip pumps [20].

Xiao W. et.al (2015) reviewed steam power station in three different aspects; first its design, second its configuration and third its control system. In order to enhance operation of the steam power plant, study of control system from both safety and economical aspects as well is necessary. Concluding the review, new steam power plant control systems were also introduced for research as well as implementation purposes [21].

Satish V. et.al (2016) examined theoretically energy and exergy study of a 'Vijayawada Thermal Power Plant' (VTPS). From their study, the researchers have shown that in low pressure turbine the exergy is lost more. The comparison of cycle efficiency with exergy efficiency was also presented. This comparison is important to minimize overall losses [22].

Buckley T. et.al (2017) presented a report titled 'NTPC: A Force in Indian Electricity Transition' for 'Institute for Energy Economics and Financial Analysis', U.S. They reported NTPC as key associate in Indian energy scenario. NTPC's new drive towards solar energy utilization was also highlighted. Major world investors in Indian solar sector were also highlighted. The upcoming era is going to be renewable energy time and NTPC is emerging as a strong leader in this field as per the report [23].

Schesack M. (2017) carried out comparative analysis at Dadri and Simhadri in thermal prospects in Indo-German Energy Forum. The transition situation of Indian power plants was presented. This was important as renewable energy can lead key role in development of future flexible plants. The above quoted two plants were just representing the coming scenario. Detailed study of next phase of flexible plants was also suggested [24].

Sutrakar A. K. et.al (2018) did experimental work to explore firing characteristics of coal and biomass in different blends. To meet global emission challenges this is found to be a competitive and cheaper solution. The 'proximate analysis' and 'ultimate analysis' results of different blends provided various significant results in their lab testing but more research is suggested before large scale implementation. The NTPC boiler firing characteristics were considered during the

study. Pulverization, Combustion, ash deposition characteristic of pure coal, pure biomass as well as intermediate blends was tested based on NTPC Dadri power plant data for 210 MW unit [25].

2.2 SOLAR ENERGY: EVOLUTION, EXECUTION AND ECONOMICS

The name of solar energy is being used in a misleading sense in modern world. Actually sun is the most basic of energy in the solar system. When we burn wood or other fuels, it releases the stored energy of the sun. Taking it deeper, the sun is base of all the life on the earth, whether it is in the form of photosynthesis in plants or indirectly the basic needs of survival for living beings. The modern solar energy scientists are interested harnessing the energy of sun through the use of solar panels. Though the modern solar energy utilization concept is new, but the fact that solar energy utilization is being done since the origin of solar system, is universal truth.

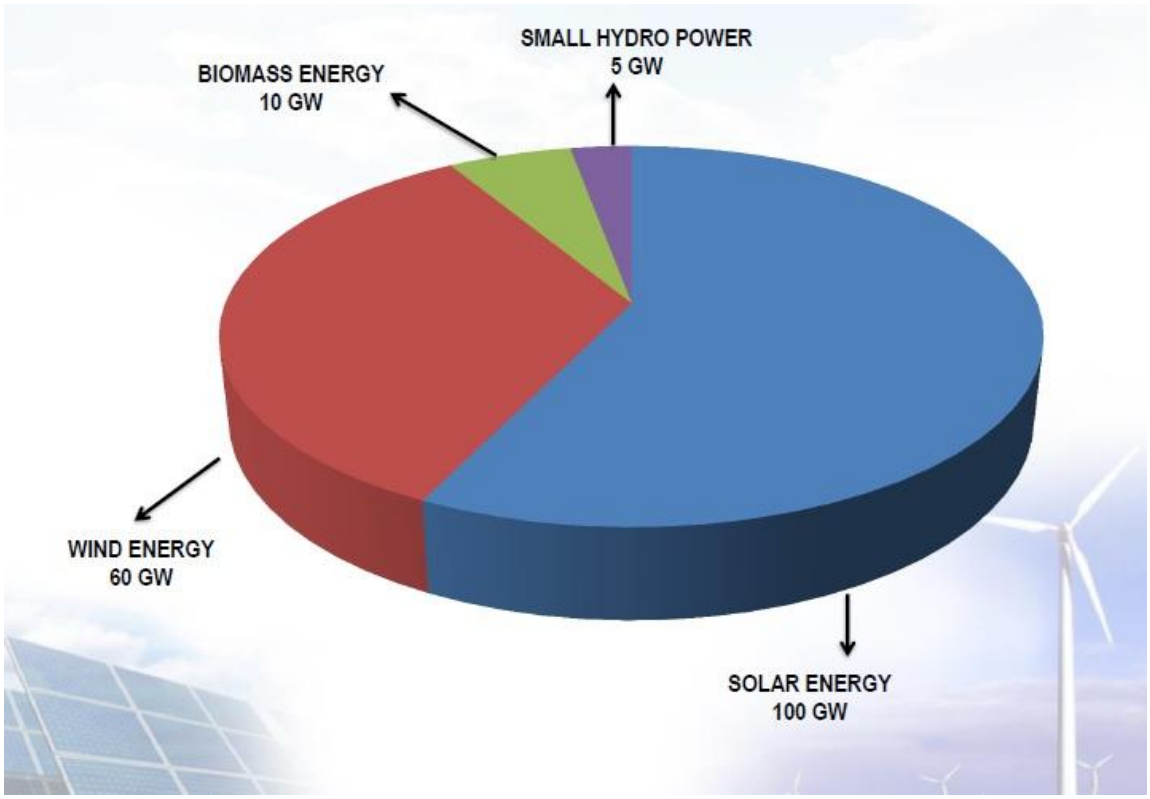

Fig. 2.2 Renewable energy target: 175 GW up to 2022 [9].

The solar energy utilization is not only economical but also environment friendly also. Hence attention is required in harnessing solar energy to achieve United Nations 'Affordable and Clean Energy' for India [26].

The solar energy utilization for heat generation at larger scale is a matter of research in modern energy technology. Different solar energy collection technologies are being used for this purpose based on needs.

A brief description of various solar energy concentration technologies for power plant operation is as under in fig. 2.3.

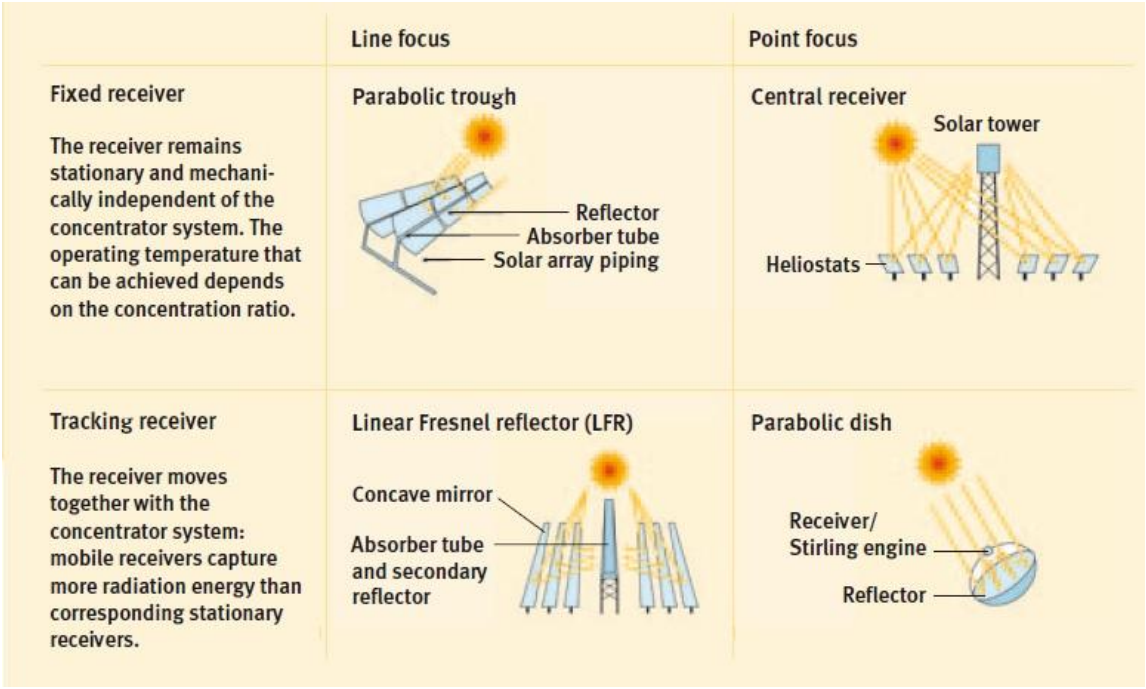

Fig. 2.3 Line and point focusing systems used in 'Solar Thermal Power Plants' [27]

The project discussed in this dissertation is using solar heat to be integrated to steam power station. Thus a deep technological understanding should always be in mind for better results. Few important researches of this field are as discussed below:

Feuermann D. et.al (1991) did the numerical analysis of two-stage 'Linear Fresnel Reflector' (LFR) solar concentrator. The concentrator configuration included basic LFR setup with curved mirrors and tube type receiver. The case was simulated

computationally to find a variable model and the key parameters such as sensitivity analysis, optical errors and mode of tracking using same as well as different mirrors were studied. The economic study of the project found the technology to be cheaper than parabolic trough collector, but lasses in energy output were significant. Reflectors were important as the efficiency improvement parameter of such systems [28].

Kalogirou S. A. (2004) presented a survey of different solar thermal collectors with their uses. The study was started with environmental discussion of solar energy benefits. A brief time history of different collector systems was also presented. After this, the study outlined the technical aspect of collectors as their optical and thermal analysis. The uses of different collector technologies were also outlined [29].

Clifford K. H. (2008) prepared a review on software along with coding for computational study of 'Concentrating Solar Power' (CSP) technologies. These codes are presented in different groups in order to have proper contrast in their study. These codings presented in detailed techno-economic manner. The probabilistic model of sensitivity analysis including uncertainty analysis is also modeled [30].

J. Fan et.al (2009) numerically investigated efficiency and solar collectors' life for 'solar heating' purposes. An important fact presented in their study was that between 2002 and 2007, thermal performance of solar collector had been increased significantly with increasing fluid temperature [31].

Nixon J. D. et.al (2010) presented a study on selecting the optimal 'Solar Thermal Collection Technology' to be used in India. All the available options were evaluated using the 'Analytical Hierarchy Process' (AHP). It included 'Parabolic Troughs Collector' (PTC), 'Heliostat Field Collector' (HFC), 'Linear Fresnel Reflector' (LFR), 'Parabolic Dish Collector' (PDC), 'Compound Parabolic Concentrator' (CPC) and 'Linear Fresnel Lenses' (LFL) and their comparative study based on techno-economical and other criteria. The study concluded on 'Linear Fresnel Reflector' (LFR) and 'Heliostat Field Collector' (HFC) to be preferred technology for India [32].

Sharma B. D. (2011) submitted his report titled 'Performance of Solar Power Plant in India' to 'Central Electricity Regulatory Commission, New Delhi.' He recommended the necessity to build up monitored database for future solar power plant works. Location based metrological study was also recommended [12].

Manikumar R. et.al (2012) examined design and analytical performance analysis of LFR solar collector with a tubular absorber, used in modern mid range temperature solar thermal operations. Parametric study for efficiency enhancement of system was also reviewed. Software based study was also performed to optimize results. Graphical results presented are important to study for proper understanding of LFR system working as well [33].

Guangdong Z. et.al (2013) presented detailed study of past, current and future of 'Linear Fresnel Reflector' (LFR). The paper presented utilization based review of the LFR based systems based on plant scale. Their study becomes important for parametric analysis of LFR power plants. Such a review has also helped for analytical design of the LFR based plant in this report [34].

Montes M. J. et.al (2014) performed LFR study. A new variable called useful energy efficiency was defined in this work. It is related to solar intensity at receiver. This study also compared 'Linear Fresnel Reflector' (LFR) with 'Compact Linear Fresnel Reflector' (CFLR). This comparison clearly specifies the minimized blocking and shading losses in CFLR systems [35].

McGoverna R. K. et.al (2014) evaluated mathematically the relation between receiver temperatures along with solar concentration in designing the Rankine cycle solar power plants. Various other mathematical relations regarding thermal performance and losses are also presented. Their study results that there is an increase in receiver temperature and decrease in receiver irradiance with increase in thermal resistance of solar receiver and condenser [36].

Gakkhar N. et.al (2014) performed numerical investigation on the parameters necessary for the setting up the 'Concentrating Solar Power' (CSP) plant in India. Under

the umbrella of technical and economical aspect, a total of 39 parameters are discussed. These parameters are important in designing and simulating the CSP plant in a developing country like India [37].

Ahmed M. H. (2016) simulated the 'Linear Fresnel Reflector' (LFR) numerically. The incident angle of incoming radiation was modified in his study. The numerical model presented in his research is suitable to obtain optimized model of solar thermal concentrator based on efficiency criteria [38].

Maithani P.C. (2017) presented a report titled 'Renewable Energy Development in India' at 'MNRE' as an advisor. As an important fact in our study, it was stated that India's renewable energy target by 2022 is 175 GW, from which 100 GW shall come from solar energy [9].

Tikariha M. K. et.al (2018) discussed the solar energy on grid and off grid forecasting for its future studies. An experimental model on 'Artificial Neural Network' (ANN) based system using 'Non Linear Auto Regressive with Exogenous Inputs (NARX)' for prediction of solar irradiance from the past metrological data is also presented. The software based simulation of such forecasting is also performed. The data from 'NREL', U.S. was used to aid the experiments [39].

2.3 SOLAR AUGMENTATION OF THERMAL POWER PLANT

In solar augmented thermal power stations, special mirrors are there to concentrate solar heat to provide it to power cycle. The heat obtained from solar concentration eliminates necessity of burning of fuel for heating. The solar collector system optimization is very necessary to achieve higher temperature during plant operation. In modern solar thermal systems, there is an integrated storage system enabling it to provide solar thermal power as per requirement. As a matter of fact, operative solar power stations in the world are having capacity of 2.5 (GW). Also, 1.5 (GW) capacity plants are being constructed [27].

Some important researches in the area of solar thermal augmentation with fossil fuel plant are disused as under:

Mills D. R. et.al (1999) performed an evaluation to check the suitability of 'Compact Linear Fresnel Reflector' (CLFR) based systems for power plant operations. The 'shading' and 'blockage' of incident radiation was also considered. Optical design was used to perform such a system which is having a low tower height. Such a system was advisable to incorporate a cost effective model of receiver. Such a modified structure of system also inherits the advantages of its parent system namely 'Linear Fresnel Reflector' (LFR). Alternate versions of such a CFLR model can also be prepared through ongoing research programs as per the author's predictions [40].

Suresh M. V. et.al (2010) presented an investigation to explore the solar integrated coal burnt thermal power stations in different aspects of design. The coal saving in power plant with solar augmentation was also discussed. The energy along with exergy analysis of base plant and solar aided plats are also compared. The environmental prospect of coal saving are also discussed in relation to emission reduction. Their study also concluded the need to improve such a system due to which net savings could be made more cost effective [41].

Popov D. (2010) modeled a regenerative steam cycle power station on software named 'Thermoflow'. The Fresnel based collector system was used for solar thermal input of studied model. The fuel saving model was also presented in this study. The author had suggested replacing all high pressure heaters and operating the cycle on a temperature higher than its design value at heaters. The solar share in thermal cycle was maximized up to 23 % in this study. This efficiency was increased with improvement of solar input [42].

Patel V. et.al (2010) studied coal saving in thermal stations with solar augmentation. The suitability of solar integration with coal plants is also presented in this work. The concept of preheated boiler water entry is presented in this research. This ultimately reduces fuel required for steam production in boiler. For maximization of fuel

saving, more the feed water heaters are suggested to be replaced. The environmental benefit of such a plant was also highlighted [43].

Mahtta R. et.al (2011) prepared technical note on discrete potential of solar power in India at localized level and its centralized harnessing system on 'Photo-Voltaic' (PV) based model. The 'Surface Meteorology and Solar Energy' program of 'NASA', U.S. were studied for basic data input to the study. Few important sites for installation of 'Concentrated Solar Power' (CSP) stations and centralized large scale Solar PV plants at national level were also highlighted in this study [13].

Zhai R. et.al (2013) presented an analysis on parametric view of solar augmented coal power plant. The study was completed considering a 600 MW plant as a base plant. The basic cycle analysis of plant had been done. The exergy destruction in boiler was presented as a contention to this model [44].

Peterseim J. H. et.al (2013) reviewed on hybridization technologies suitability for integration with conventional plants. Fresnel based technology was best suited at that point of time based on this research. Other technologies with their suitable temperature range were also compared. This study focused on location based technology selection for hybridization of plants with solar energy for optimal performance [45].

Wu J. et.al (2014) did thermal cycle and solar field coupling study. The matrix based model to study the integration was important in this study. This model was a direct integration of solar to thermal replacing entire boiler scheme with solar power input [46].

Hongbin Z. et.al (2014) came with solar coupled coal plant study with thermodynamic approach. The new approach of solar thermal integration of the time was presented in this study. The increased load to the base system improved performance of integrated approach. This model was then expected to be software simulated for model verification [47].

Yawen Z. et.al (2014) provided an evaluation standard for increased power plant performance after hybridization. Few analysis results were also presented for model

validation. The model duly verified was then presented for computational studies further [48].

Van R. W. L. (2015) presented solar augmentation at supercritical coal-fired power stations. 'Levelised Cost of Electricity' (LCOE) approach was presented in this study. This study presented that the LCOE of hybridized plant is less than LCOE of lone CSP plant at same conditions [49].

Zhai R. et.al (2015) analytically simulated method to evaluate solar contribution for enhanced operating conditions of solar hybrid power station. The performance of the system was studied on variable 'mass flow rate' of heating fluid. The economical model based on production rate of electricity and effective cost was established [50].

Khan N. H. et.al (2016) proposed a model of solar thermal integration. 'Parabolic Trough Collector' (PTC) was used as base solar energy generator. This was an advanced approach considering the performance models available for lone PTC plants. Impact of DNI at plant location was also highlighted. The other benefits of such an integrated plant were also highlighted [51].

Jiyun Q. et.al (2016) reviewed various possible combinations of solar integration to thermal power plant. Such a review provides a brief summary for new researchers to take a bird's eye view of the past researches and their limitations. This also helps in optimization study of such technologies. Various schematic diagrams were also presented by authors in support of their study [52].

Lei F. et.al (2016) presented the direct steam generation model for using in Rankine cycle after being superheated in boiler. An analytical method consisting of matrix approach was developed to balance the energy distribution. This method is best suited for further computational studies. A case study based on above model was also presented for model validation and its further uses [53].

Liqiang D. et.al (2016) presented integration of solar tower with coal fired power station to get a hybrid plant model. TRANSYS software was used for system simulation and get the best possible results. The localized irradiance based study was

also performed in this study. The model presented in this study gave technical, environmental, optical and thermal analysis as well of the plant [54].

Gholamreza A. et.al (2017) presented case study based on Iran situated power station integrated to solar heating. Seven different integration cases are discussed for comparative analysis of solar thermal integration. The replacement of high pressure 'feed water heater' was suggested in this model for optimal results of integrated model [55].

Jiyun Q. et.al (2017) investigated the feed water replacement model of solar thermal integration of fossil fuel powered station. Their work suggested that variation in mass flow rate proved to be a better strategy of efficiency enhancement of the integrated plant at constant temperature operation than its reverse operation. This conclusion is important at lower DNI operation of integrated plant [56].

Wei Z. et.al (2017) developed a LOCE based model of for thermo-economic study of solar integrated thermal power plant model [57].

Yawen Z. et.al (2017) studied optimized solar field size for the solar–coal hybrid system. The values of solar multiple were also calculated. The methodology to optimize the solar multiple was also presented. Solar irradiance variance and plant load conditions was also plotted. The results modeled the design optimization of hybrid plants [58].

Deepak B. et.al (2017) modeled a LFR based model of solar thermal station with integrated storage using 'System Advisor Model' (SAM) software presented by 'National Renewable Energy Laboratory' (NREL). The software provides the model capability so that the simulation results can be visualized. The software also helps in economical modeling of the plant. The project presented in this research is an India based study with feasibility study of a 100 MW plant [59].

Omar B. (2018) reviewed a spitted modeling and component based study of solar thermal power station. The study is important to know the modeling of individual components. 15 different plants are studied for model understanding. Different plant cycles have also been modeled for comparative performance study. Many different

performance parameters are plotted for ease of understanding of results. The results are important for comparative study of model presented in present study too [60].

Habibollahzade A. et.al (2018) carried the study of ISTPP way forward, toward combining solar chimney for enhanced power production at night time and utilization of wastage energy. The metrological conditions like wind speed, pressure temperature, specific and relative humidity etc. are important in designing such a project. The average advantage of such a project is not up to the mark at present time, but the future research can provide pleasing results to the new technology. The inconsistency of power production in integrated plant is the origin of such a project [61].

Yong Z. et.al (2018) presented an optimization study centered towards medium and higher temperature CSP power stations. The lone CSP plants as well as hybridized CSP plants, both are presented in this study. The data presented in this study is also validated using trend analysis of running plants. The results suggest that replacement of reheater and feed water heater in power cycle by solar thermal technology is promising solution toward fossil fuel saving. The most optimal scheme generated more than 200 MW of energy at optimal DNI value. This study provides promising results for comparative study of our project also [62].

2.4 SOLAR THERMAL STORAGE TECHNOLOGY

'Thermal energy storage' (TES) system balances mismatch between supply and demand of energy. It also increases system reliability, generation capacity of electricity and reduces generation cost.

The solar thermal integration of power plant also becomes more fuel efficient by integration of storage as depicted in fig. 2.4 below.

A brief review of solar thermal storage technology till date is being provided below. The integrated storage mode of operation in CSP station is taken in light while reviewing thermal storage technology.

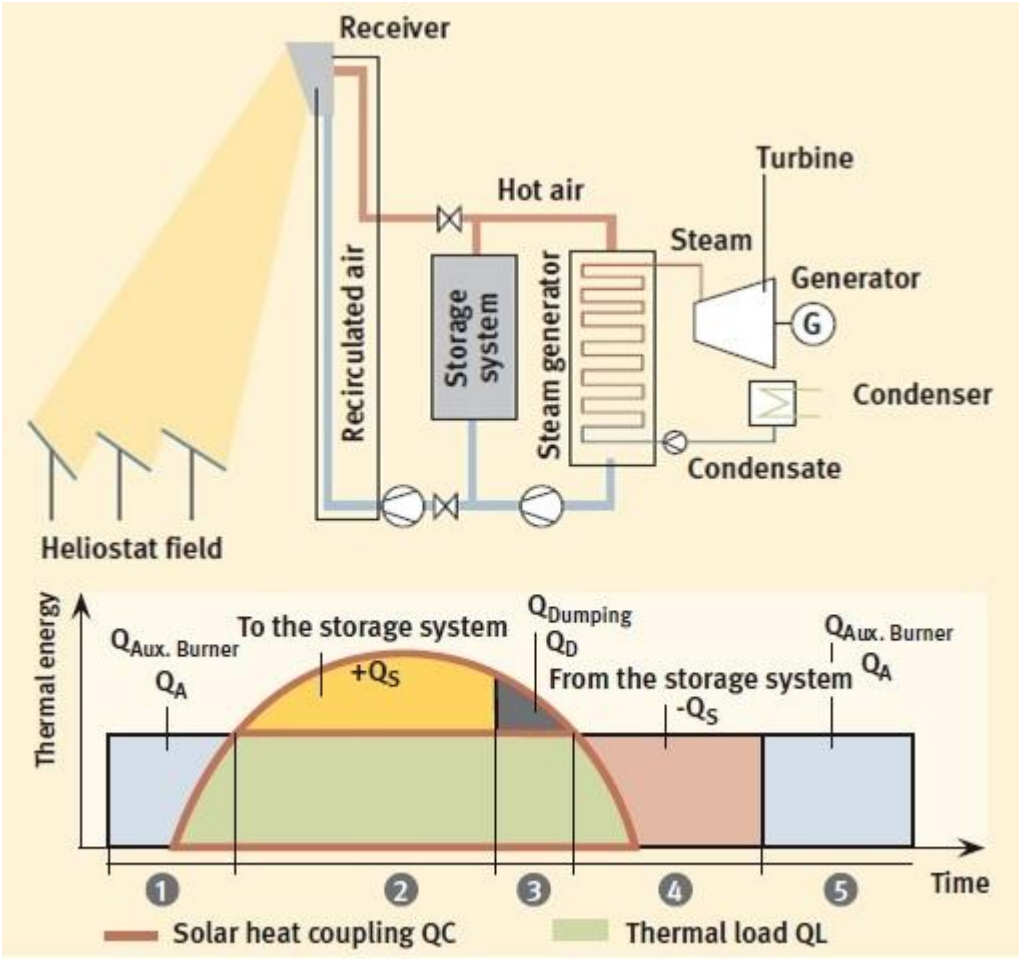

Fig. 2.4 Operating modes and energy balance of storage integrated solar thermal plant [18].

Sarada K. et.al (2013) reviewed the storage technology of solar thermal. The review study to start research was a best solution to get the information of historical development of thermal storage. The inconsistency of thermal power provided by solar thermal itself generates a need towards storage integration. The design, thermal as well as economical aspects of study are presented in this review [63].

Zohreh R. A. et.al (2013) prepared a control based model of direct thermal storage technology. The researchers agreed to argument that the storage type suitable for a plant operation varies based on needs of the plant. The tree aspects of design, as, discharge point temperature, inlet temperature and heat transfer fluid cycle are discussed in this study with plant analogy and dynamic modeling of storage technology. The study

of process control has presented a better access towards optimization of storage performance [64].

Steinmann W. D. (2015) examined the two tank ‘molten salt’ storage at innovative parameters. The exchange of molten salt material with a low cost material with steam heat transfer fluid for cheaper operation was proposed in this study. The model presented can be applicable for large scale operation also with different ‘Phase Change Materials’ (PCMs) in use. The model of storage presented this study provided a validation solution in our study [65].

Nunes et.al (2016) theoretically reviewed the ‘Thermal Energy Storage’ (TES) material. Nitrates and Nitrites of Alkaline materials with different blends are presented in this review. This review was important in data collection for our work [66].

Stutz B. (2017) theoretically and numerically reviewed the solar thermal storage with a variety of temperature range from ambient temperature to thousand degree Celsius. Also the storage time is another analysis criterion. Various technologies for solar thermal storage are put forward and critically reviewed [67].

Seitz M. et.al (2017) put forward the financial aspect of solar thermal storage for ISTPP with ‘Parabolic Trough Collector’ (PTC) in use for steam production to preheat storage material. ‘Levelised Cost of Electricity’ (LCOE) for 2 sites are compared with and without integrated storage mode. Also different storage systems are theoretically integrated to the same plant. Numerical methods are used to model the storage technology based on plant operating parameters and DNI at plant location [68].

Walczaka M. (2017) have detailed the degradation of storage system due to corrosive action of salts used for thermal storage. Such a study becomes important to select alloy for tank design of storage material casing. The material choice for safe operation of plant is important due to high temperature of storage material and overall plant efficiency and economy [69].

Cáceres G. et.al (2017) investigated PCM material for thermal storage in solar power stations. This work presented numerical tool for performance study of

encapsulates salt nitrate material for economical storage design at many quality control measures. One important outcome in this study is that there is a higher rate of heat flow at increased the thickness of storage material, keeping its density almost constant. The energy density concept of thermal storage was also used in this study [70].

Rodat S. et.al (2018) prepared a LFR based model consisting of a thermal storage. The modified ORC for such a plant operation was also presented. The simulated model can later be implemented on large scale for actual operation. The data of simulation is also compared with observational data for model validation. At last, a critical review and limitations of the model presented is performed. This is important for further research to the same model [71].

Zhao et.al (2018) performed an optimization study of two tank salt based storage system. The pressure and temperature criteria are varied for trend analysis of inlet parameters. The economical model of the same system is also developed. This economical model is presented to understand the large scale practicability of the same model on implementation [72].

Gerard et.al (2018) presented a case study on actual operation of hybrid solar integrated power plant with two tank thermal storage. Such a review provides data for quality assessment of the technology. This review was focused on study of medium operating temperature of thermal storage system. The overall optimization of operation in thermal, economical and environmental aspect was the key objective of this study. This work was important for our study as actual operating difficulties are identified in such a plant cycle operation by literature survey of the same [73].

2.5 INTENT OF STUDY

The modern day coal fueled thermal power stations in India are facing two distinct problems. One is Coal shortage and other is environmental effect of coal burning. In order to minimize the impact of these problems on power production, there is need to develop an optimal solution. Replacement of coal with some other fuel is one of them but it does not provide the complete solution. The environmental emissions of fuel

burning shall still be there. Therefore the integration of the coal fired plant with solar heating option becomes much better option. It minimizes the coal consumption of the plant and there is no harmful environmental emission of the technology as well. The objectives of the present study can be presented as below:

- To take a look at the model of 210 MW 'Integrated Solar Thermal Power Plant' at NTPC, Dadri, National Capital Region, Delhi.
- Analytical study of current 'Linear Fresnel Reflector' (LFR) based model of the 210 MW 'Integrated Solar Thermal Power Plant' at NTPC, Dadri.
- Case based shortcomings of LFR based system and possible improvements.
- Energy and environmental analysis of 'Heliostat Field Collector' (HFC) based model of NCPS 210 MW unit.
- Analytical integration of thermal storage to HFC based model.
- Simulation of 'Heliostat Field Collector' (HFC) based model to 'System Advisor Model' (SAM) simulator of 'National Renewable Energy Laboratory' (NREL).

CHAPTER 3

STEAM POWER STATION WITH SOLAR AUGUMENTATION

The solar integration of steam power station is a vast term in itself. For betterment of understanding the basic theory, this chapter is splitted in three sub parts:

- A brief introduction of working of steam power plant.
- An overview of the thermal applications to the solar energy option.
- Integration options of solar heat to steam power plants.

3.1 STEAM POWER PLANT LAYOUT

A power plant or station is a set of systems or subsystems integrated to generate and provide mechanical or electrical energy in an ‘efficient’, ‘economical’ and ‘environment friendly’ manner.

A steam power station utilizes energy of some fuel (be it fossil or fissile), after burning in presence of oxygen to generate heat, which is transformed in shaft work to produce electricity. There is some working fluid in plant cycle operation as a carrier of energy of fuel to turbine shaft rotation. This carrier fluid is water or steam in a ‘Steam Power Plant’. The modern day steam power station consists of following networks for smooth plant operation:

a. Coal and ash network

b. Air and gas network

c. Feed water and steam flow network

d. Cooling water network

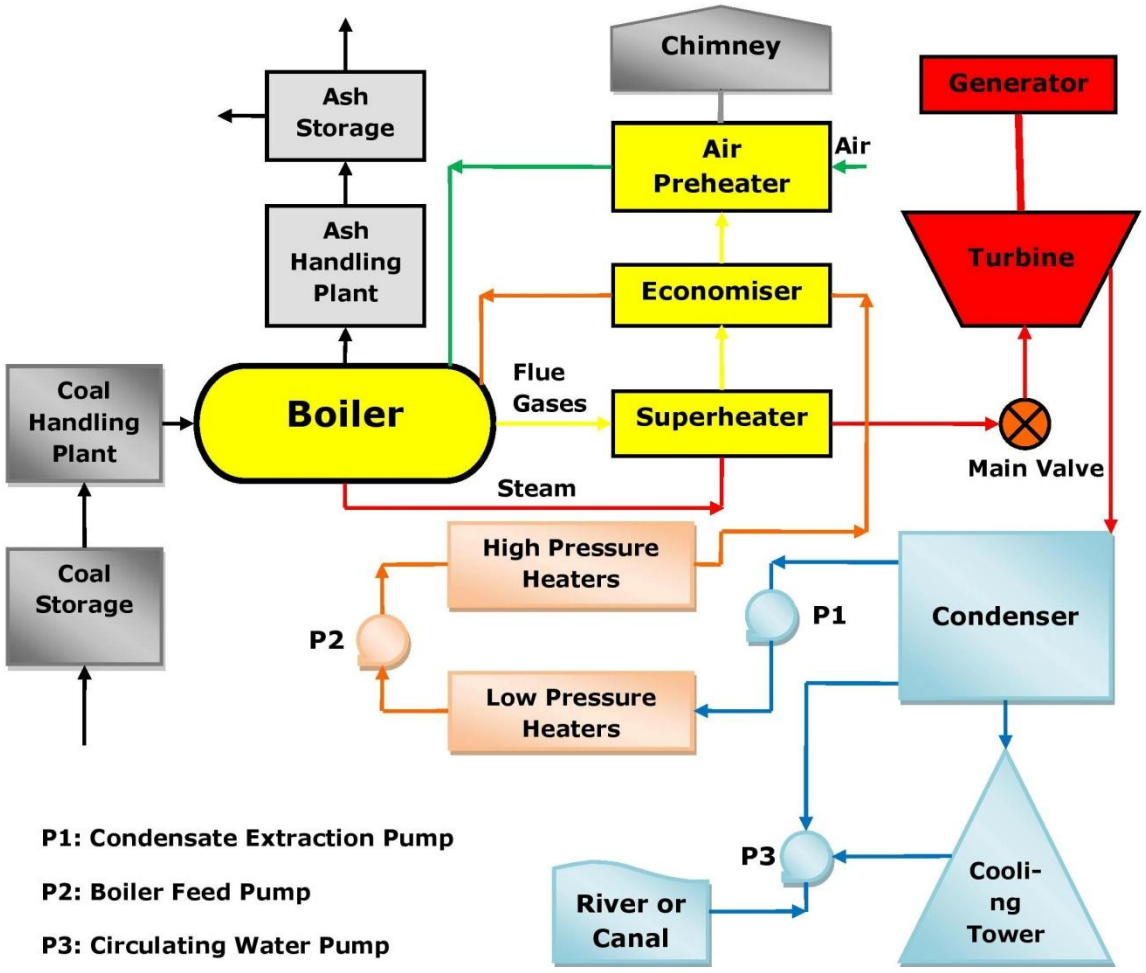

Fig. 3.1 Layout of a steam power plant

3.1.1 Rankine Cycle

It is previously stated, there is some fuel burning in steam power plant. The energy of burnt fuel is harnessed by the use of an energy carrying fluid. This carrier fluid is circulated in a cycle for continuous operation of the plant. The carrier fluid of this plant is water or steam. The water is fed into boiler to absorb the energy released by the burning of fuel and vaporise. This vapour is then allowed to expand in the turbine in controlled atmosphere to a low pressure to produce shaft work. The steam expanded in the turbine is sent to condenser. In condenser, there is some cooling fluid (generally river or stored water) to circulate and carry away the heat of condensed steam. This condensed water is then pumped again to boiler using a pump and thus the cycle continues again.

The above cycle, utilizing water vapour in energy transfer process is termed as 'Vapour Power Cycle'. A Rankine cycle is nothing but an ideal operating of all the above explained processes in a cyclic manner.

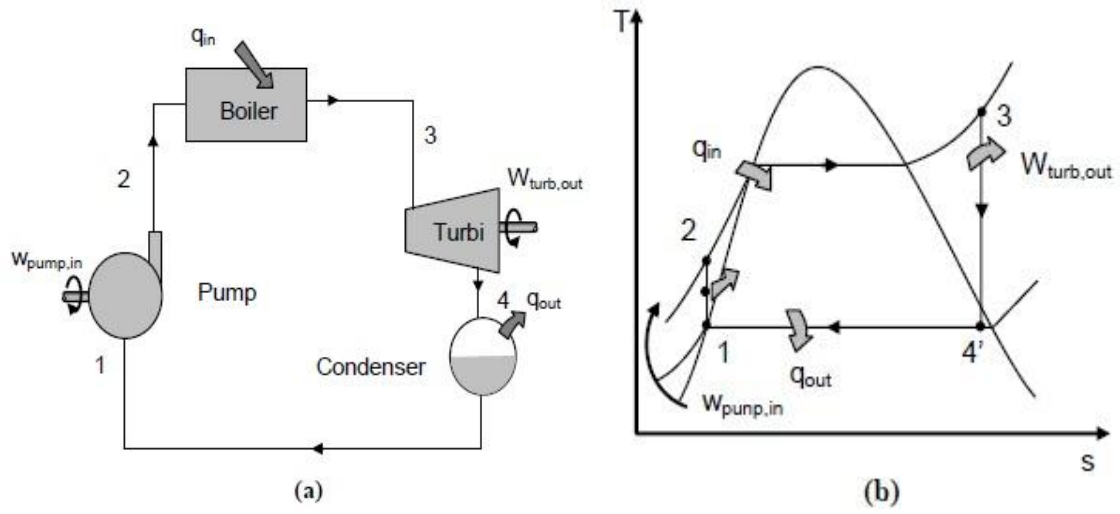

Fig. 3.2 (a) Simplified layout of Rankine Cycle; (b) Rankine cycle on T-s plot

The Rankine cycle, explained above, comprises the following 4 processes:

Process 1-2: Pump work (Isentropic compression); after being condensed in the condenser, the water is pumped back in the boiler. This pumping process is depicted in Rankine cycle as process 1-2. At point 1 the condensed water is in saturated liquid state. This saturated water is carried to state 2 by pumping at a higher pressure called boiler operating pressure. This pumping process from state 1 to 2 is called isentropic compression in thermodynamic terms. The water specific volume is reduced after this compression and thus its temperature increases slightly. The vertical space among stage 1 and 2 is very small actually, but is shown much larger for pictographic clarity.

Process 2-3: Steam generator assembly (Constant pressure heat addition); the water entering the boiler at stage 2 is vaporized in the boiler. The boiler is basically a vessel with water and fuel burning around it. Heat from fuel burning is transferred to boiler water by simple heat exchange process. The heat exchange process in boiler is isobaric process or constant pressure process. The steam generated in water is further

superheated in a separate circuit called superheater up to state 3. The boiler along with superheater completes the steam generator assembly.

Process 3-4: Turbine work (Isentropic expansion); the superheated vapour expands in the turbine from stage 3 to stage 4. This expansion is occurred on turbine blades producing thrust force to rotate the turbine axel. This constant entropy process (or isentropic process) is also stated turbine work production.

Process 4-1: Condenser heat rejection (Constant pressure heat rejection); the steam entering in condenser is a mixture of water and vapour. This mixture is cooled back to liquid stage at constant pressure. The process of condensation is heat transfer process in which a cooling liquid (generally river or lake water) is also involved for efficient operation. The condensed water is fed to pump to complete the cycle.

3.1.1.1 Energy Analysis of Ideal Rankine Cycle

All four processes of Rankine cycle (Compression, heat addition expansion and condensation) are steady-flow processes. Therefore, the steady flow energy equation of the system for unit mass of steam can be given as under:

$$(q_{in} - q_{out}) + (w_{in} - w_{out}) = h_e - h_i \quad \text{(kJ/kg)} \tag{3.1}$$

Pump ($q = 0$)

$$w_{pump,in} = h_2 - h_1 = v(P_2 - P_1) \tag{3.2}$$

Where, $h_1 = h_f$ at pressure P_1 and $v \approx v_1 \approx v_f$ at pressure P_1

Boiler ($w = 0$)

$$q_{in} = h_3 - h_2 \tag{3.3}$$

Turbine ($q = 0$)

$$w_{turbine,out} = (h_3 - h_4) \tag{3.4}$$

Condenser ($w = 0$)

$$q_{out} = h_4 - h_1 \quad (3.5)$$

Rankine cycle thermal efficiency is obtained using;

$$\eta_{th} = \frac{w_{net}}{q_{in}} = \frac{w_{turbine,out} - w_{pump,in}}{q_{in}} = 1 - \frac{q_{out}}{q_{in}} \quad (3.6)$$

3.1.2 Steam Condition Variation and Steam Power Station Thermal Efficiency

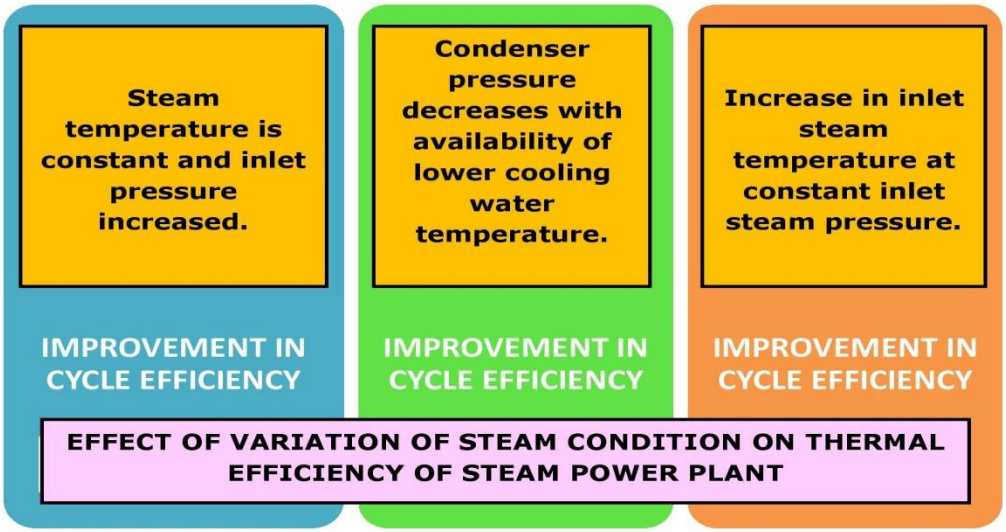

Fig. 3.3 Steam Condition Variation and Steam Power Station Thermal Efficiency

3.1.3 Reheating of Steam

Reheater is a part of the boiler assembly. The steam expanded in the higher pressure turbine is sent back to reheater. There the steam is heated again to produce work in intermediate and lower pressure turbine.

3.1.4 Regeneration

T-s diagram of Rankine cycle is shown in Figure 3.4. In this fig., it is shown that during process 2-2′, heat is transferred to the working fluid at relatively lower

temperature. This thing lowers the average heat addition temperature and hence the overall cycle efficiency.

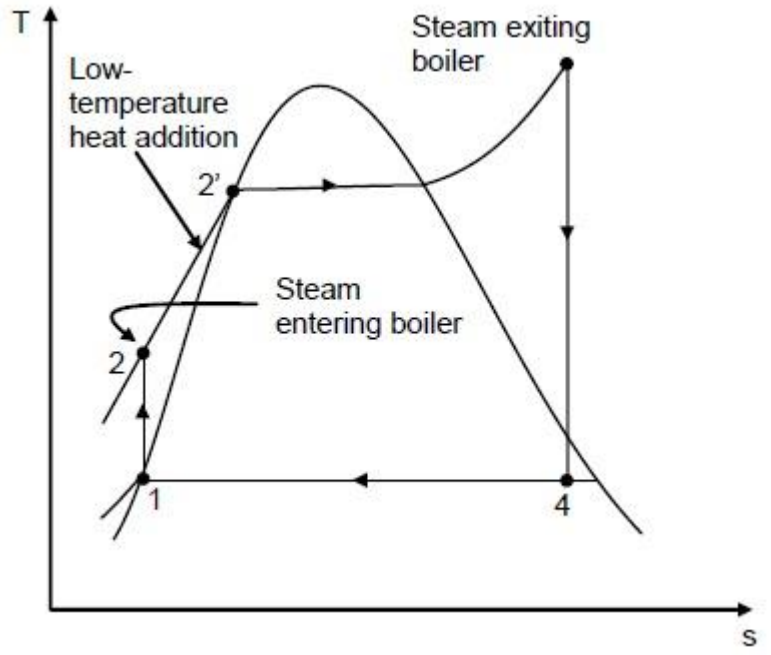

Fig. 3.4 Ideal regenerative Rankine cycle

To overcome this situation, the liquid water (also called Feed water) temperature before entering the boiler needs to be increased. This process is performed by a different way called ‘regeneration’. Regeneration is the process in which pumped liquid water (or feed water) is provided heat by bled off steam, extracted from discrete locations in turbine. This heating of feed water is completed in certain special heat exchange devices called ‘feed water heaters’ or ‘regenerators’.

3.1.5 Feed Water Heater(s)

A ‘Feed Water Heater’ (FWH) is heat exchanging device used to pre-heat pumped water before being entered to the boiler assembly. Preheating the feed water betters the system thermodynamic efficiency as explained above. The integration of feed water heater also reduces plant operating economy. There is reduced thermal vibration at boiler wall material when the pumped feed water is sent back into the steam cycle after regeneration.

In recent steam power plant, the use of feed water heater increases the temperature of feed water gradually to the saturation temperature. As a result of this, the heating to the feed water becomes more reversible.

The plant cycle system between the condensate pump discharge and boiler feed pumps is called condensate system. Low pressure FWH is operated in the condensate system. It utilizes steam extracted from low pressure turbine or auxiliary turbine to heat the pumped water.

The plant cycle system between 'boiler feed pump' discharge and the boiler is called feed water system. High pressure FWH is operated in the feed water system. It utilizes steam extracted from HPT and IPT to heat the feed water.

FWH(s) are of two types:

3.1.5.1 Open Feed Water Heater(s)

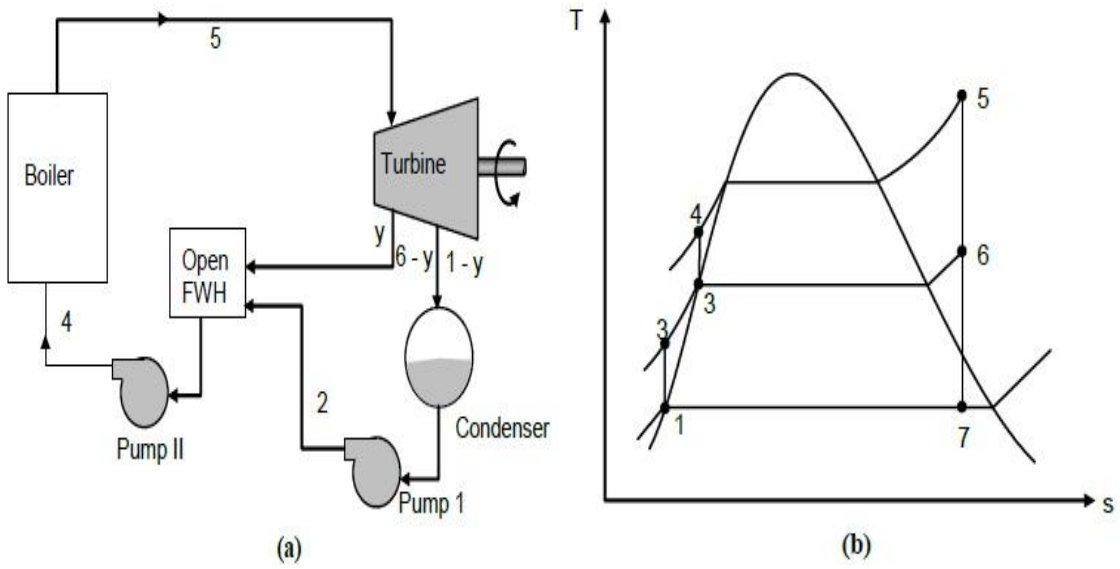

Fig. 3.5 (a) Open FWH in steam power plant (b) Rankine cycle representation of open FWH

An open FWH is also called direct-contact feed water heater. It is basically a chamber where the extracted turbine steam mixes with the pumped feed water. In ideal conditions a saturated liquid is obtained at the end of open feed water heating process.

The layout of steam power station having an open FWH and its T-s diagram on is depicted in the Figure 3.5.

3.1.5.2 Closed Feed Water Heater(s)

The closed feed water heater transfer heat to pumped water without mixing the steam and water. Because of independent flow of two fluids, there may be pressure difference between them. The layout of a steam power station with a closed FWH and its T-s diagram on is depicted in the Figure 3.6.

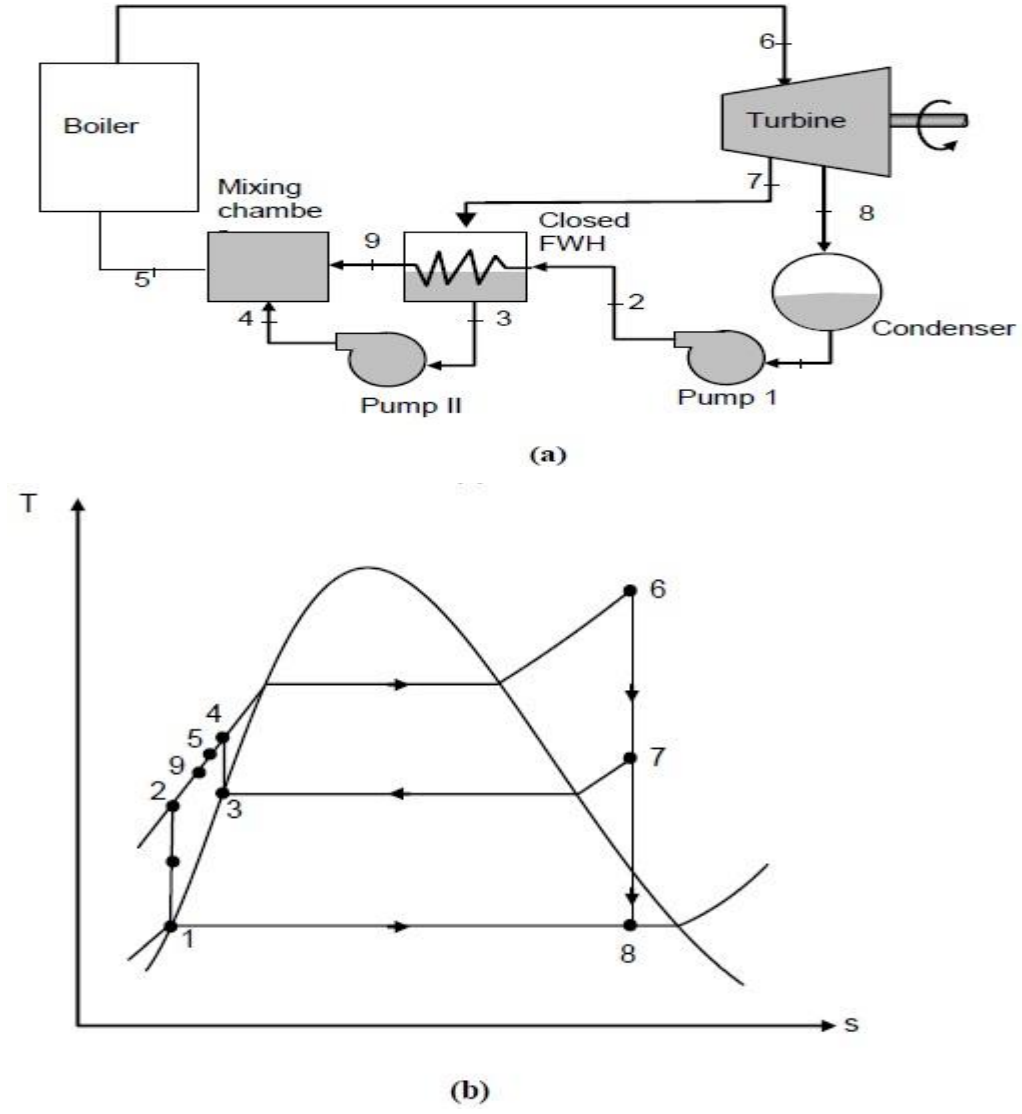

Fig. 3.6 (a) Closed FWH in steam power plant (b) Rankine cycle representation of closed FWH

3.1.6 Deaerator

Usually there is more than one heater in a feed water heating system. Minimum one feedwater heater among them is a direct contact or open feed water heater. It separates air bubbles from the feed water or deaerates it, thus also termed as deaerator.

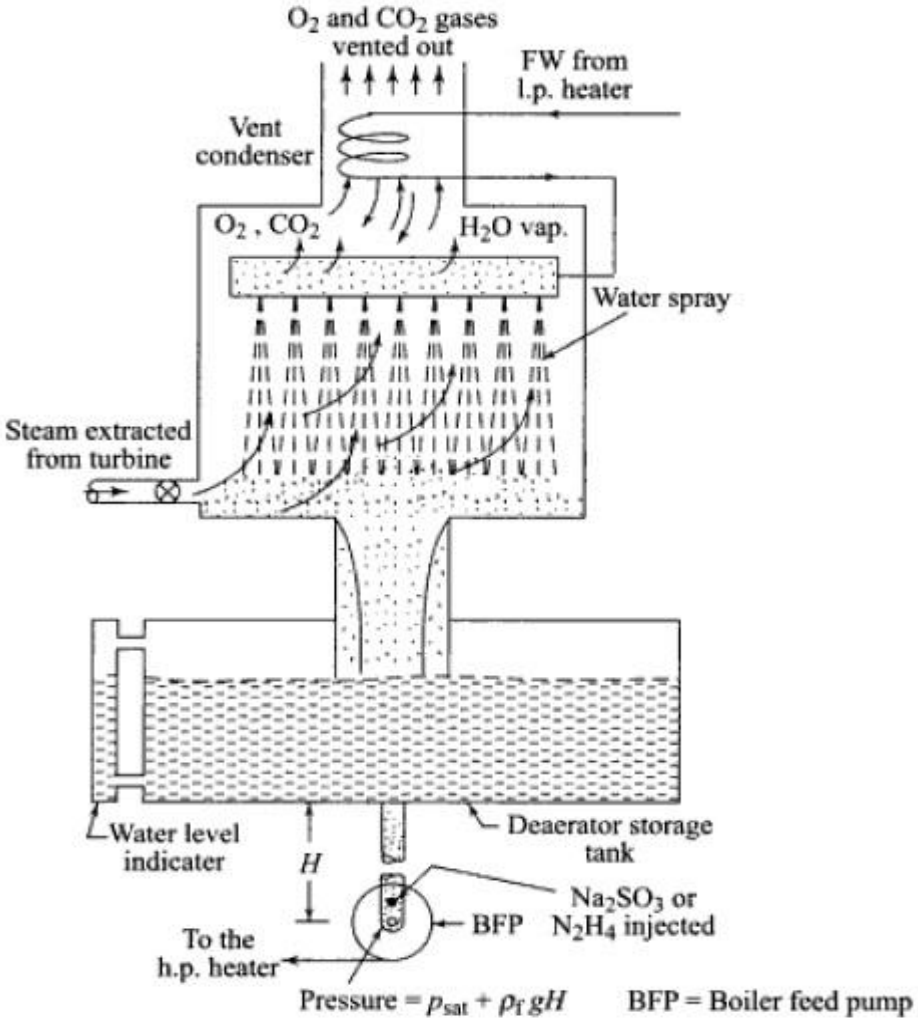

Fig. 3.7 Deaerator with storage tank [77]

There are gases dissolved in the water such as oxygen, CO_2 etc. The water at higher temperature becomes corrosive due to less solubility of dissolved gases at higher (i.e. saturation or boiling) temperature. It is desirable to remove these gases for smooth plant operation. Thus one FWH in the regenerative system is kept open FWH.

The mechanism of open FWH is quiet simpler. The pumped water is sprinkled in a chamber from top to expose more surface area. The turbine bleed steam is allowed to enter in the chamber from bottom. When the contact between these two streams happens, the steam condenses and the temperature of feed water rises to saturation temperature. The deaeration process i.e. separation of dissolved gases also takes place in this chamber as the gases leave the chamber with the vapour. This vapour gas mixture is sent back to condenser where the gases are vented out.

The deaerator is usually located approximately at centre of the regeneration system. It is done so to minimize the total pressure difference between the condensate pump and boiler feed pump. The feed water heaters between boiler feed pump and boiler are often called as high pressure (H.P.) heaters and those between the deaerator and condensate extraction pump are termed as low pressure (L.P.) heaters.

All the FWHs used in nuclear power plants are of closed type because of the chances of radioactivity leakage with deaeration.

3.2 THE SOLAR ENERGY OPTION: AN OVERVIEW OF THE THERMAL APPLICATION

3.2.1 Solar Energy

The light and heat radiations received from the sun are termed as solar radiation. The solar power is originated from continuous nuclear fusion process. The approximate life of sun is estimated to be 4 billion years. Theoretically, the energy emitted by sun over a minute is equal to energy required by the modern world in one year.

The modern utilization concept of solar power is not a very old idea. At first solar energy was used to produce heat. The first solar heat collector was built in 1767 by Horace de Saussure (a Swiss scientist). It was used for heating water and cooking food. Clarence Kemp (U.S.) patented the first marketed solar water heating system in 1891.

Two California executives bought this system from him. Later, the same system was used in one-third of houses in Pasadena, U.S. by 1897.

Then electricity was produced from solar energy. Edmund Becquerel (France) presented the thought of photovoltaic effect (‘photo’ means ‘light’ and ‘voltaic’ means ‘electrical potential’) in 1839. Selenium photovoltaic (PV) technology was developed in 1880. They were able to convert light into electricity on 1-2% efficiency, but the reason behind this conversion was not known. Albert Einstein presented a Nobel winning theory of the ‘photoelectric effect’ in the early 1900s.

3.2.2 Solar Energy Applications

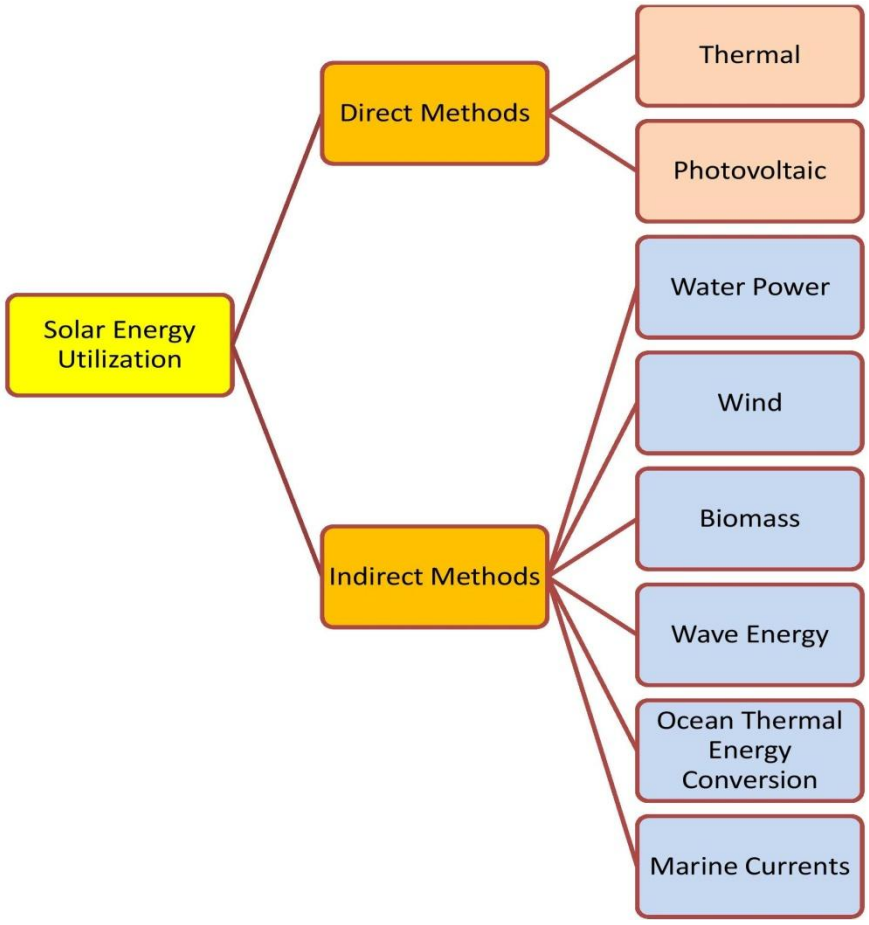

Fig. 3.8 Classification of methods for solar energy utilization

3.2.3 Solar Collectors and Commercial Utilization of Solar Energy

There are numerous methods to utilize of solar energy. In this study attention is on direct thermal approach of solar thermal utilization. The solar radiation on earth surface has certain value of annual average Direct Normal Irradiance (DNI) for a certain location. This variation of solar heat availability or DNI generates a need to develop a mechanism, which can intensify the solar heat, so that, the solar heat can also be utilized for higher heating applications, such as commercial purposes.

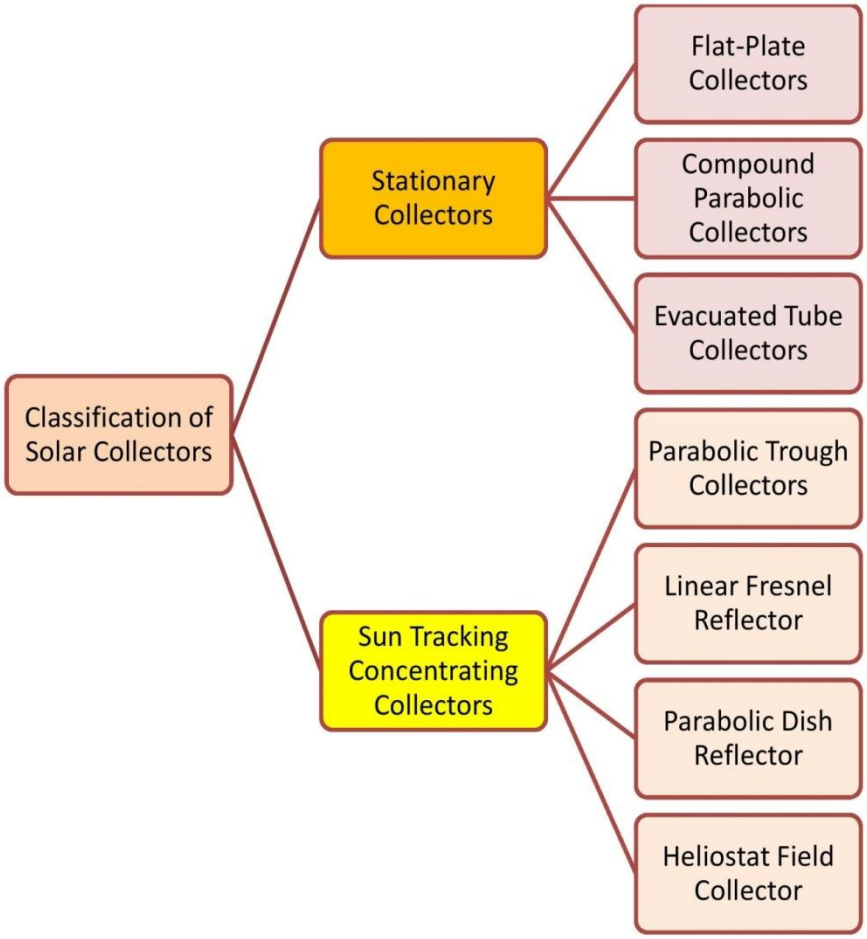

Fig. 3.9 Solar thermal collectors and their classification

A Solar collector aims the same. A **Solar Collector** is a mechanism to collect and/or concentrate solar radiation from sun. Classification of solar collectors is given in diagram above.

Curtailment of the above classification based on needs of this report implies the study of following two collectors:

3.2.3.1 Linear Fresnel Reflector (LFR)

LFR technology depends on a row of linear mirrors that concentrate thermal radiation of sun on a fixed linear pipe shaped receiver. The LFR field could be studied as a linearly broken differently shaped parabolic trough reflector (Fig. 3.10).

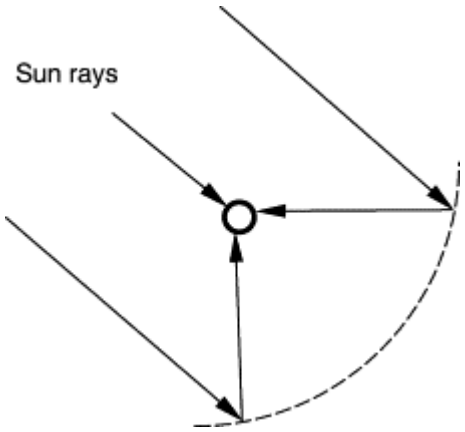

Fig. 3.10 Fresnel PTC [29]

A LFR model is presented in Fig. 3.11. It is cheaper than parabolic trough reflectors due to flat and simplified shape. Also LFR setup and maintenance cost is lesser due to its placement close to ground.

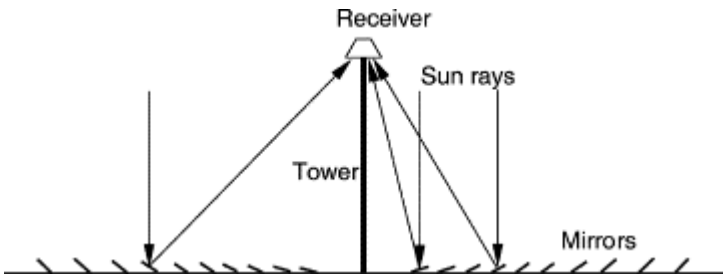

Fig. 3.11 Bottom facing receiver heated by LFR field [29]

The main operational difficulty in using the LFR is ‘blockage’ and ‘shading’ between the adjacent rows of reflectors. To minimize the losses incurred by these, the adjacent rows are separated by large spacing. This causes more land utilization. Sydney University in Australia had developed ‘Compact Linear Fresnel Reflector’ (CLFR) technology. In this technology, adjacent linear reflectors are inserted to counter shading problem. This extra reflector row in the system design provides denser array of mirrors. [29] The insertion of mirrors shared among two receivers is depicted in fig. 3.12.

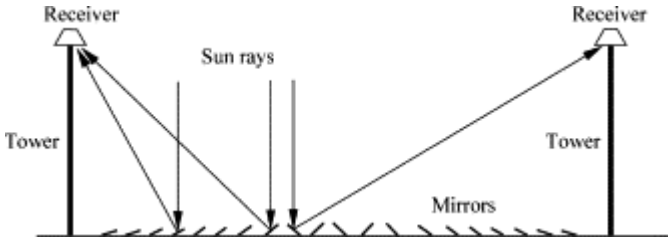

Fig. 3.12 Mirror sharing in a CLFR and reduced mirrors shading [29]

3.2.3.2 Heliostat Field Collector (HFC)

A number of flat mirrors or heliostats can be used to reflect incident solar radiation on them to a common receiver to get extremely high value of solar heat as depicted in fig. 3.13.

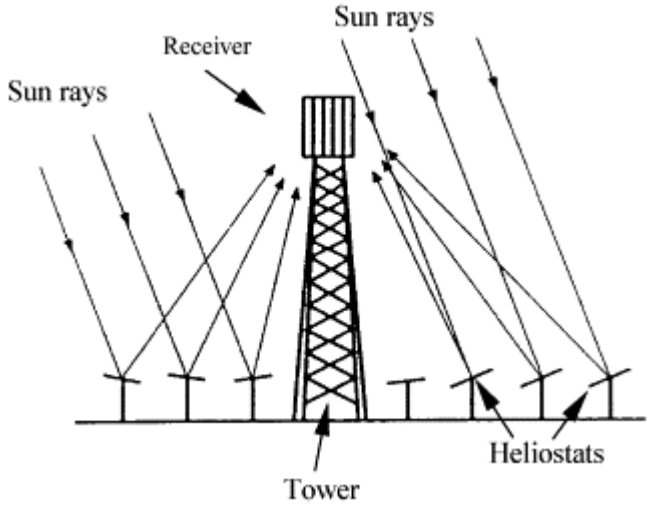

Fig. 3.13 Schematic of central receiver system [29]

This type of arrangement is called the HFC or 'Central Receiver Collector' (CRC). The mirrors used in this type of arrangement may be flat mirror or slightly concave mirror. Heliostat field collectors have many advantages:

1. Unlike flow channel energy losses in LFR system, there is optical transfer of solar energy to a central receiver.
2. A higher concentration ratios (of the range of 300–1500), collection efficiency.
3. Most suitable for large scale power production (generally >10 MW) at economical way.
4. Best suited for heat storage integration.

Each reflector in a heliostat field collector could be designed with 50 to 150 m^2 of surface area [29].

There are three configurations for Heliostat Field Collector:

a. Heliostats completely surround a cylindrical receiver tower having heat transfer external surface.
b. Heliostats being located in north of collecting tower in the northern hemisphere (and vice-versa for southern hemisphere) and the heat transfer surface of the receiver is closed.
c. Heliostats being located north of collecting tower in northern hemisphere (and vice-versa for southern hemisphere) like above, and a vertical plane shaped receiver heat transfer surface, which is north facing in northern hemisphere (and vice-versa for southern hemisphere), is situated.

3.2.4 Solar Thermal Storage

Termittent availability is the biggest drawback in using solar energy. The general scheme to sort out this problem is use of backup energy hybrid system in the form of fossil fuel etc. The modern day solution is use of 'Thermal Energy Storage' (TES) system. It stores the solar thermal energy at the time of larger availability and releases it as a backup heat on need. [Appendix 2.1]

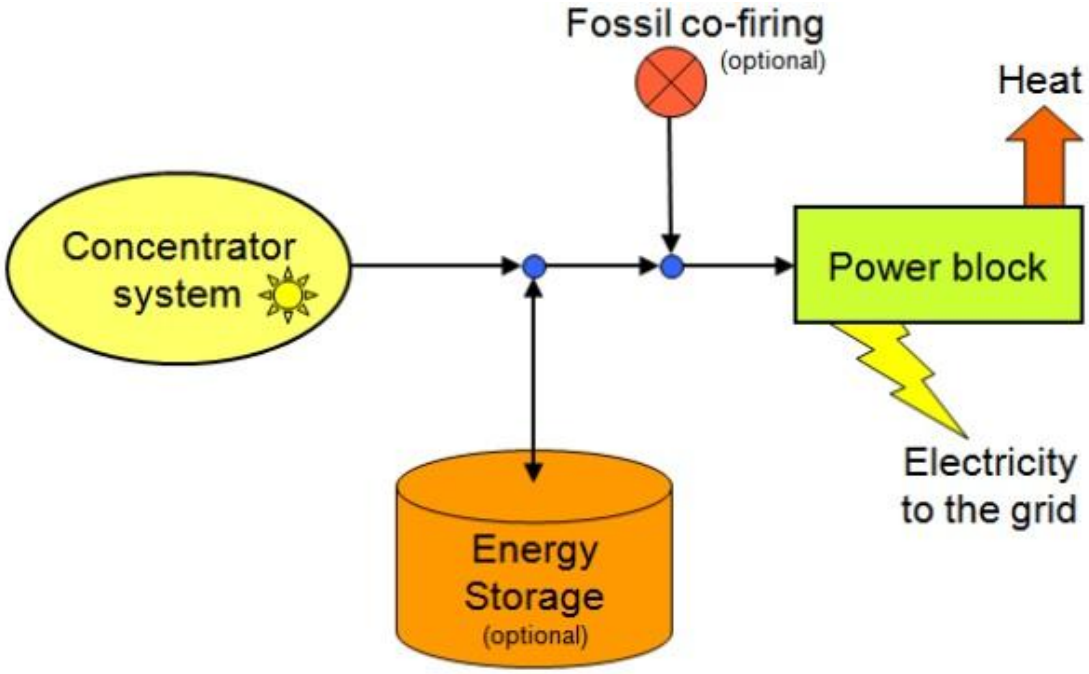

Fig. 3.14 Solar thermal storage integration advantage

3.2.4.1 Classification of Solar Thermal Storage:

There are three types of TES systems available at present:

a. Sensible heat storage

b. Latent heat storage

3. Thermo-chemical heat storage.

The brief description of each type of thermal storage is presented in fig. 3.15.

Sensible heat storage systems are dominant in terms of commercial availability among them.

They are greatly used in industrial applications. Most notable plants using this technology are:

- "PS10" and "PS20" projects (2007 and 2009), the "Andasol 1" and "Andasol 2" plants (2008) of Spain
- "Solar One", (1982) of USA

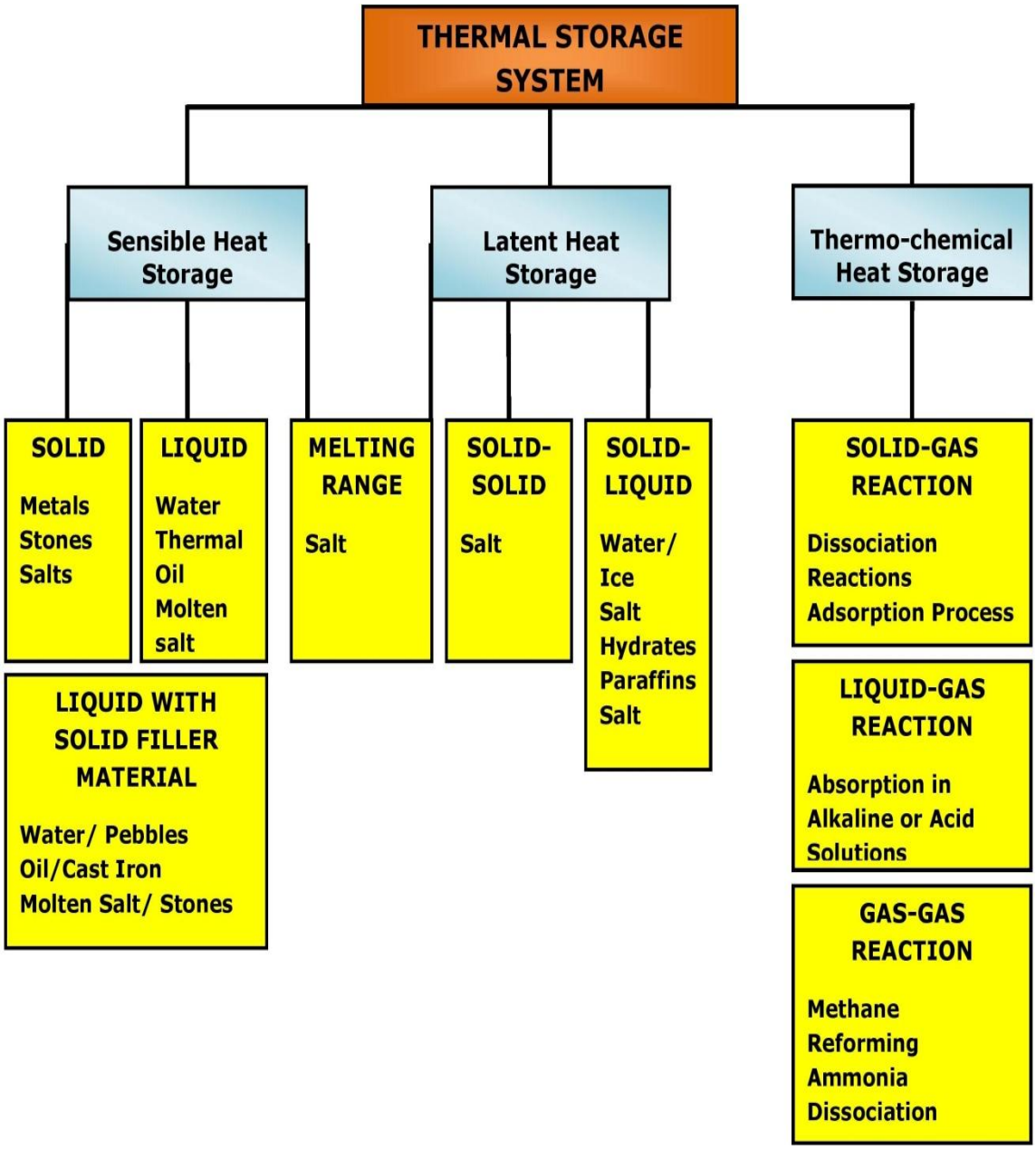

Fig. 3.15 Brief description of thermal storage classification

The latent heat storage system stores larger amounts of energy in compact spaces (high energy density) and is economical also. Among all the three techniques, thermo-chemical heat storage is under research now. [Appendix 2.2]

3.2.4.2 Solar Thermal Storage Design considerations at different levels:

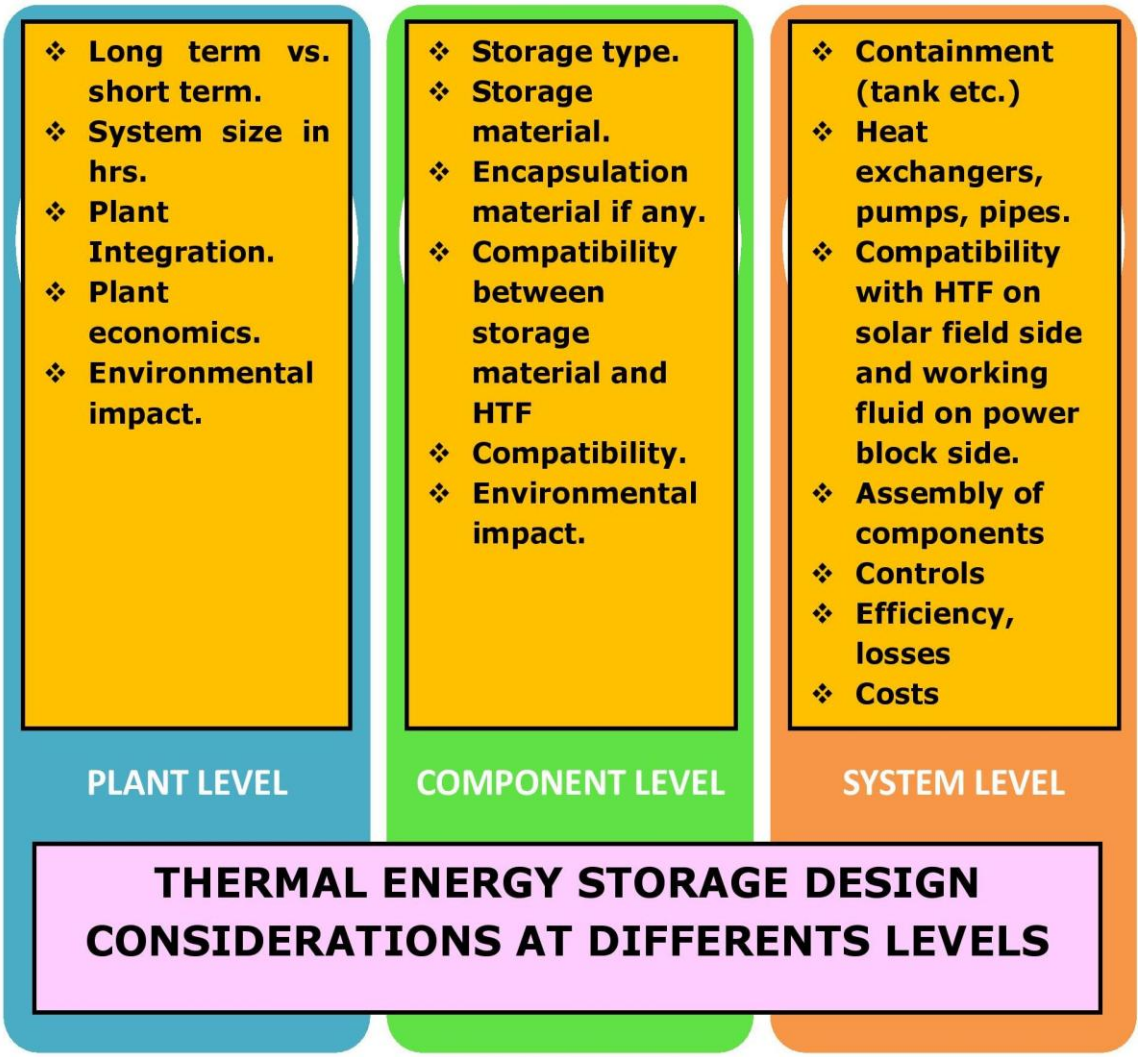

Fig. 3.16 Depiction of thermal storage design considerations levels.

3.3 INTEGRATION OPTION OF SOLAR THERMAL TO POWER PLANT

A methodology to combine solar thermal power in co-ordination with conventional power plants to minimize its fossil fuel requirements is called integrating the solar energy to thermal power plant. Integration of solar energy to thermal power plant could be done in both conventional as well as non-conventional plants.

Generally there are three classes of integrated solar thermal conventional power plants:

i. Hybrid solar ‘steam power plants’

ii. Hybrid solar ‘combined cycle power plants’

iii. Hybrid solar ‘gas turbine power plants’

This project is dealing with hybrid solar steam power plant. The steam power station integration with solar energy can be done in many ways. These are described as under. Following are the integration schemes presented by NTPC at ‘Indian Power Stations: International O&M Conference’ in a presentation [74].

3.3.1 Option 1: Solar Steam in HP/IP/LP Turbine

It is also called conventional solar thermal integration philosophy. In this method, the entire boiler is replaced with solar steam. There are two possibilities in this option; solar energy used to generate high pressure steam and solar energy used to generate low pressure steam. Both of the possibilities are presented in fig. 4.6 below.

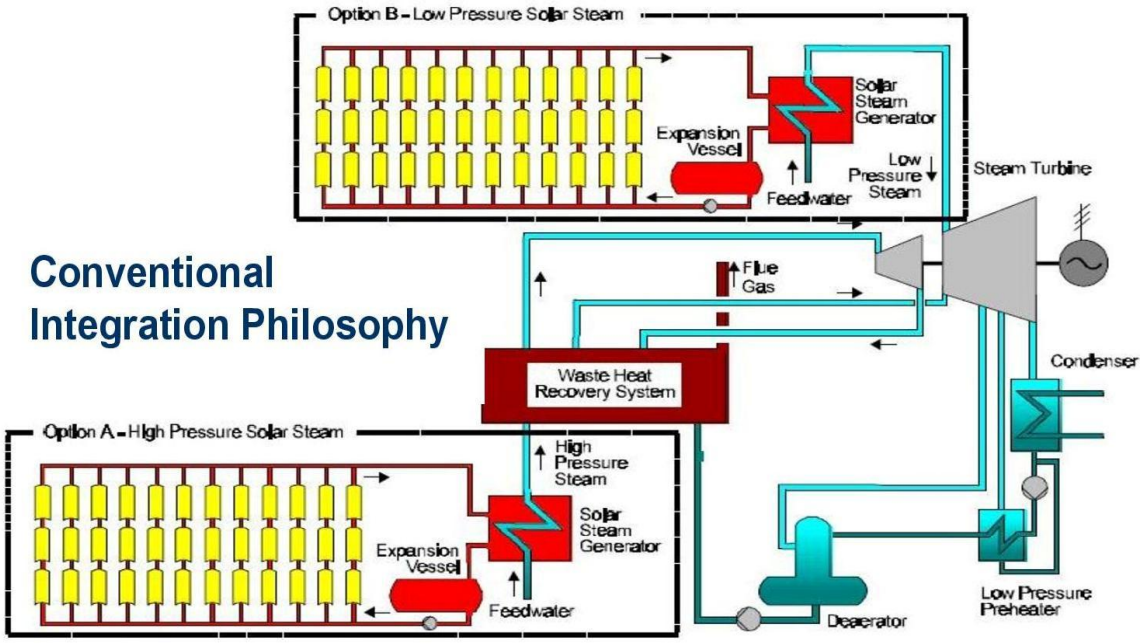

Fig. 3.17 Conventional Solar Thermal Integration Philosophy [74]

3.3.2 Option 2: Solar Steam to Replace Extraction Steam to Heaters

In this option solar steam is allowed to be a part of plant Rankine Cycle by bleeding it into heater steam directly without using any heat exchanger. The scheme of such type of plant is shown below in fig. 4.7.

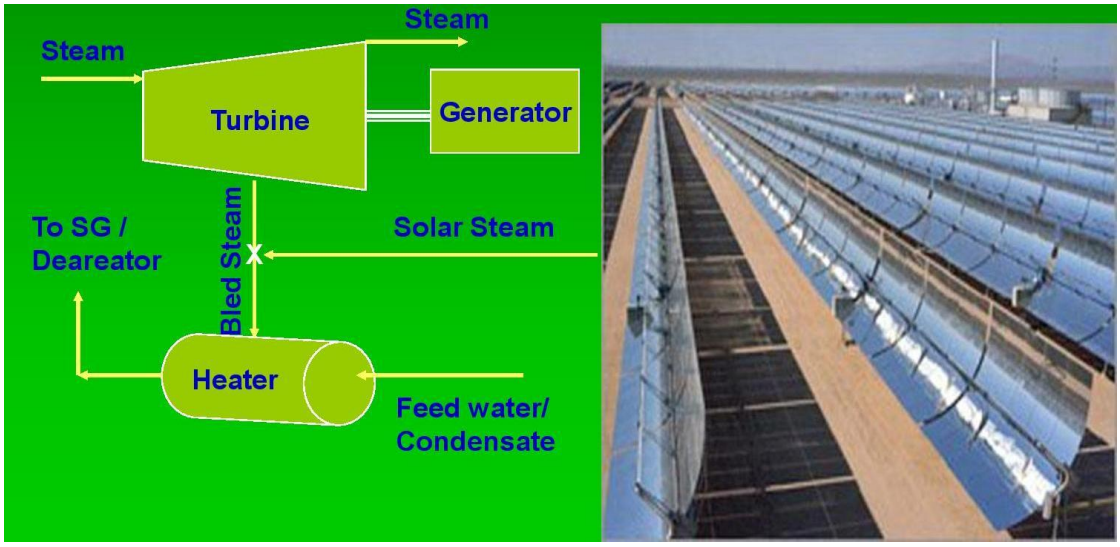

Fig. 3.18 Solar Steam to replace extraction steam to heaters [74]

3.3.3 Option 3: Solar Steam for Cooling CW Inlet

The schematic diagram for this option is shown below in fig. 3.19

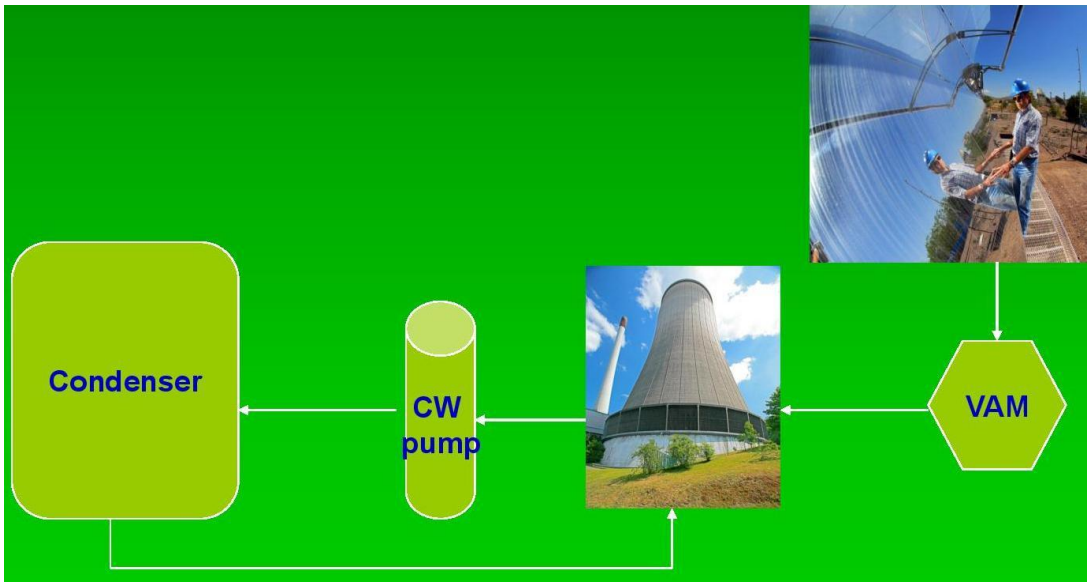

Fig 3.19 Solar steam for cooling CW inlet [74]

3.3.4 Option 4: Solar Steam for Pre-heating FW to SG

This is the latest approach to integrate solar heating to existing fossil-fuel fired plant. This can also be done in various forms. Fig 3.20 shows various options.

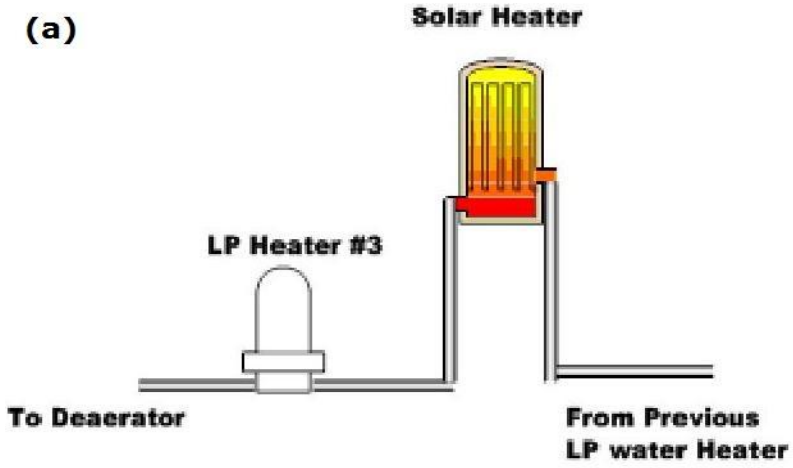

Fig. 3.20 (a) Solar steam for pre-heating feed water to steam generator first option [74]

In option (a), solar heating used to pre-heat LP section of feed water in series with LP heater. In this type of heater, there is a direct contact of solar steam with Rankine cycle steam.

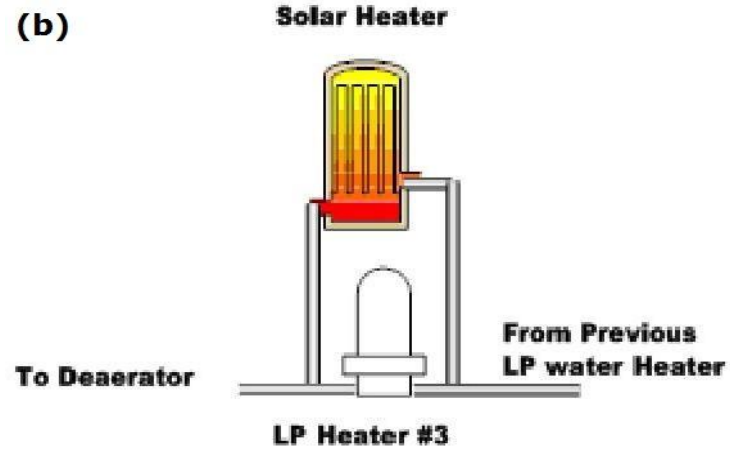

Fig. 3.20 (b) Solar steam for pre-heating feed water to steam generator second option [74]

In option (b), solar heat is used for pre-heating LP section feed water in parallel with LP heater. In this type of heater, there is also a direct contact of solar steam with Rankine cycle steam.

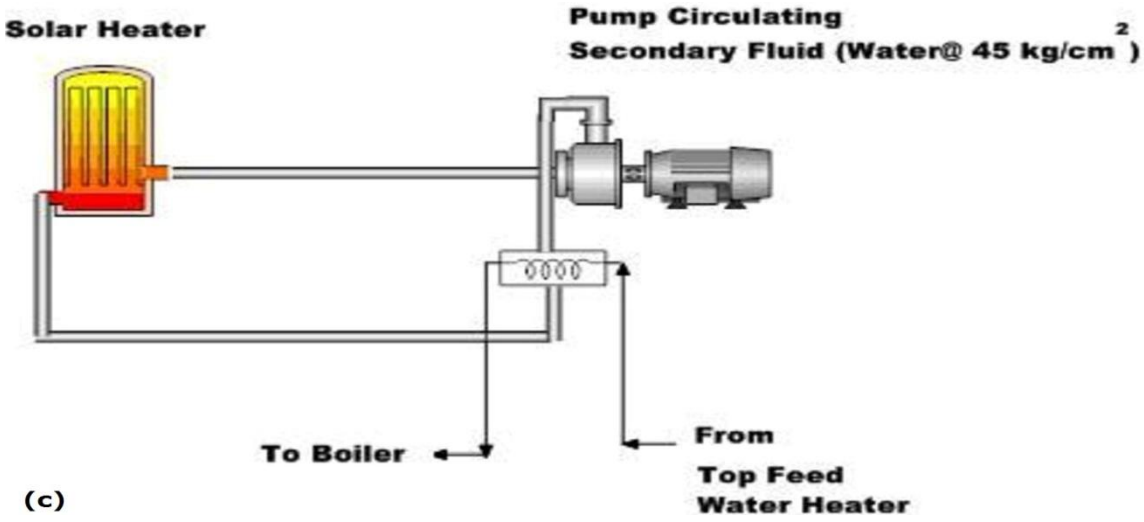

Fig. 3.20 (c) Solar steam for pre-heating feed water to steam generator third option [74]

In option (c), solar heat is used for pre-heating HP section feed water in parallel with HP heater. Heating is done after feed water heater section, before boiler entrance of feed water. In this heater, there is no contact of solar steam with Rankine cycle steam.

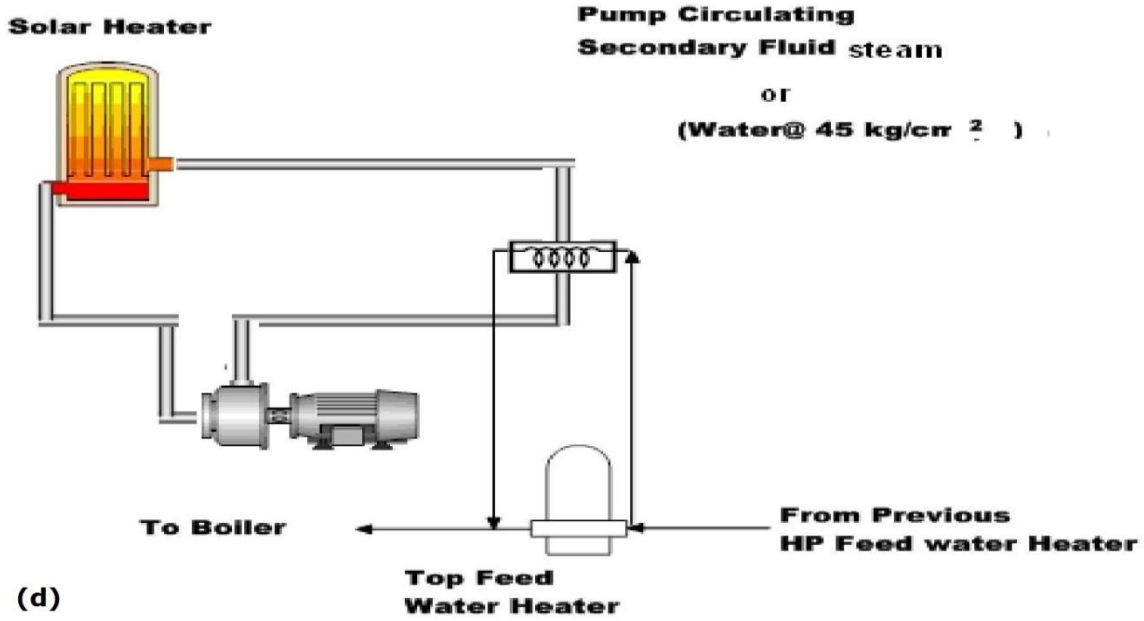

Fig. 3.20 (d) Solar steam for pre-heating feed water to steam generator fourth option [74]

In option (d), the solar heat is allowed to work in parallel with any heater (generally high pressure heater), without mixing with Rankine cycle fluid. This allows relaxation of pressure difference among the two streams. It is the best integration being used now a day for solar thermal integration of fossil-fuel fired plants. It allows flexibility in operating and integration.

CHAPTER 4

CASE DISCUSSION: LFR BASED INTEGRATED SOLAR THERMAL POWER PLANT OF NCPS

4.1 ABOUT NCPS

The important information of the base plant is provided as under:

Name of the plant: 'National Thermal Power Corporation' (NTPC), Dadri.

Location: Dadri, Gautam Buddh Nagar district of Uttar Pradesh.

Other name: 'National Capital Power Station' (NCPS) (This station provides power to National Capital Region (NCR), India.

Installed Capacity: 1820 MW coal-fired power plants;

817 MW gas-fired power plants;

5 MW solar thermal power plants.

Fig. 4.1 An introduction to NCPS (Source: India Today Education)

4.2 ABOUT THE INTEGRATION PROJECT

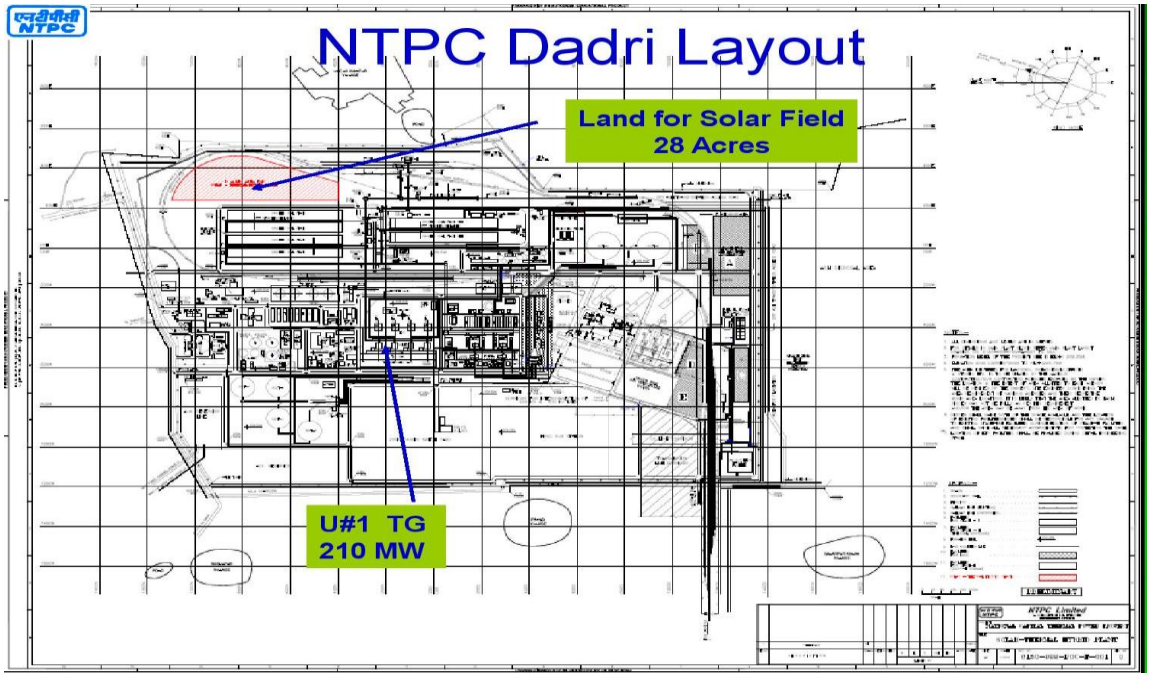

Fig. 4.2 NTPC Dadri Layout [23]

NTPC Dadri is India's first 'Integrated Solar Thermal Power Plant' (ISTPP) in India. In this ISTPP, a solar field is being integrated to an existing 210 (MW) coal-fueled thermal power station unit. The solar heat is to be provided to high pressure heater. This will save the extraction steam to heater and thus less steam is required to be generated in the boiler and hence there will be less coal consumption in heating the boiler. The basic information of the project is taken from fourteenth issue of 'Sun Focus', a quarterly newsletter published by MNRE [83].

4.3 CST TECHNOLOGY

The NCPS ISTPP is a Compact Linear Fresnel Reflector (CLFR)-based solar thermal project. The technology in use in this project is being presented by Frenell GmbH, Germany. The technology employed in this project can generate temperature up to 550 ^{0}C. This high temperature can generate hot water, steam, or thermal storage materials. The technology works by focusing the sunlight on the absorber tubes. There is a linear arrangement of field motor driven mirrors, which focus solar thermal energy on

a vacuum tube located at the focus. Few important features of the technology are described below:

- ❖ Flat mirrors with curvature are used to collect solar energy;
- ❖ Lesser ground clearance;
- ❖ Ready to fabricate components;
- ❖ Automatic cleaner of mirrors.

The current setup of CFLR technology at Dadri is designed to produce hot water at 257°C with 64 per cent overall efficiency.

4.4 INTEGRATED SOLAR HYBRID SCHEME AT NCPS

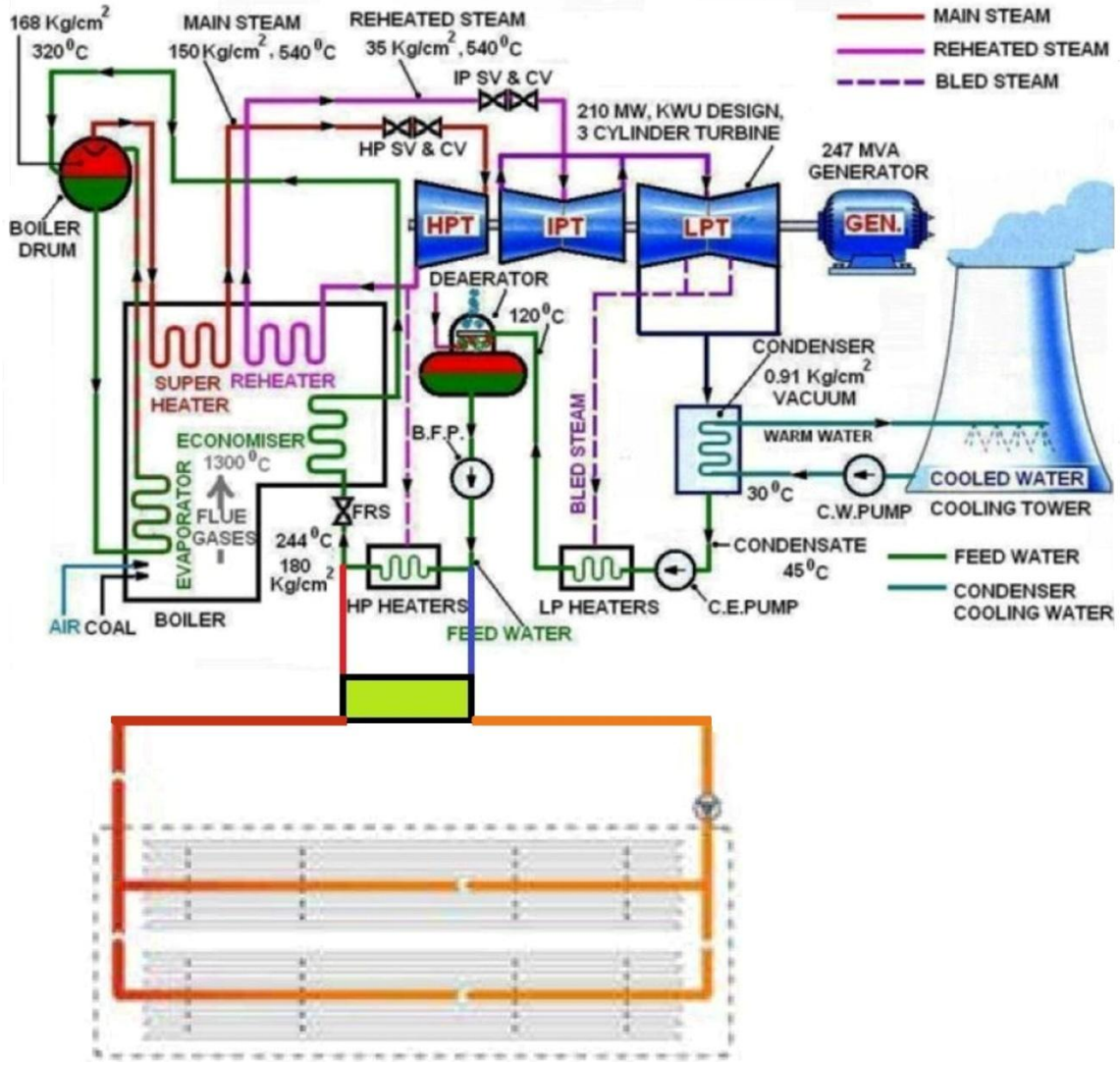

Fig. 4.3 Integrated Hybrid Scheme at NCPS [83]

Thermax Ltd. is integrating the NCPS plant with thermal system. The integration includes placing a solar heater in place of high pressure heater as presented in fig. 4.3. Thus there is no need to extract the steam from turbine. This saved steam shall expand in the cycle further to increase the cycle efficiency. At NPCS ISTPP, the CLFR collectors are placed in seven rows, heating water from 210 °C to 257 °C. This heat is further used to increase temperature of feed water from 200 °C to 247 °C as presented in Fig. 4.4.

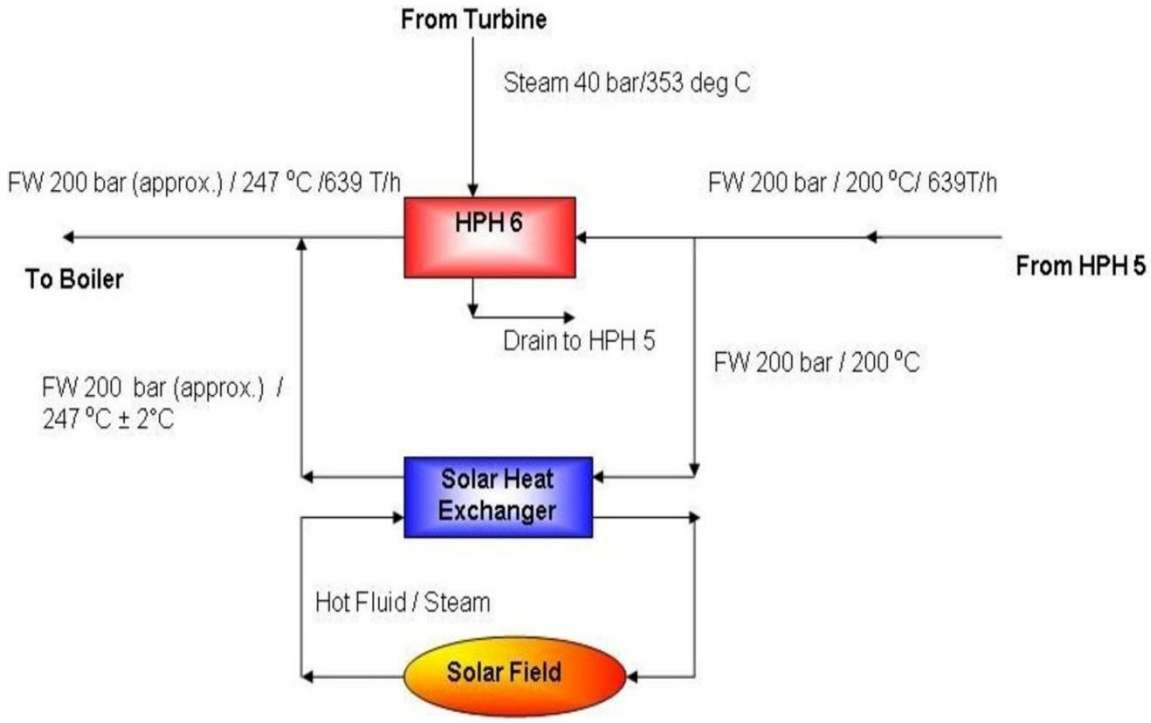

Fig 4.4 Schematic diagram solar integrated of high pressure heater [74]

4.5 ANALYTICAL MODEL OF NCPS 210 MW THERMAL POWER PLANT

4.5.1 Rankine Cycle Analysis of the Base Plant

The analytical model study of a power plant needs plant operational data which is collected from plant survey. Also few assumptions are to be made so as to fit the practically collected data on ideal Rankine cycle. In this analysis the plant operational data is taken from the exergy analysis work of the same unit by S. Sengupta et.al [14].

The data table 4.1 presented in above stated work is as under based on points shown in schematic diagram in fig. 4.5:

Table 4.1 Operating data from plant at different conditions [14]

P. No.	40 % Load			60 % Load			75 % Load			100 Load		
	Pr.	T	ṁ	Pr.	T	ṁ	Pr.	T	ṁ	Pr.	T	ṁ
1	150	537	257.952	150	537	370.595	150	537	457.241	150	537	622.804
2	16.81	306.26	19.769	23.83	313.28	31.93	29.15	318.56	42.189	39.2	342.66	63.437
3	16.81	306.26	238.183	23.83	313.28	338.665	29.15	318.56	415.052	39.2	342.66	559.367
4	15.02	537	238.183	21.28	537	338.665	26.02	537	415.052	34.94	537	559.367
5	7.07	427.34	12.652	9.96	426.02	19.366	12.14	425.26	24.589	16.23	424.1	34.673
6	3.02	312.63	225.531	4.23	310.42	319.299	5.14	309.15	390.463	6.84	307.31	524.694
8	3.02	312.63	215.247	4.23	310.42	302.42	5.14	309.15	368.996	6.84	307.31	492.898
9	1.033	198.18	9.273	1.382	195.57	14.315	1.663	193.92	18.313	2.299	192.2	26.39
10	0.382	107.82	7.586	0.526	105.01	14.221	0.611	103.59	18.943	0.841	102.07	28.343
11	0.127	X = 0.9781	0.000	0.148	X = 0.9642	0.237	0.167	X = 0.9582	1.529	0.215	X = 0.9501	4.388
12	0.103	X = 0.9937	198.562	0.103	X = 0.95	247.25	0.103	X = 0.9427	330.385	0.103	X = 0.9275	432.812
13	0.103	46.09	217.478	0.103	46.09	305.571	0.103	46.09	372.019	0.103	46.09	496.54
14	21.78	46.09	217.478	20.54	46.09	305.571	19.25	46.09	372.019	16.07	46.09	496.54
21	2.753	129.76	258.956	3.84	141.47	371.589	4.66	148.46	458.235	6.15	159.04	623.789
22	157.58	133.4	258.956	160.32	144.33	371.589	163.09	151.18	458.235	170	161.86	623.789
26	157.24	204.41	258.956	159.61	220.46	371.589	162.01	230	458.235	168	244.98	623.789

Base plant layout is given in figure 4.5 below. The steam being outlet from boiler is expanded in HPT. Then it is reheated and expanded in IPT and LPT.

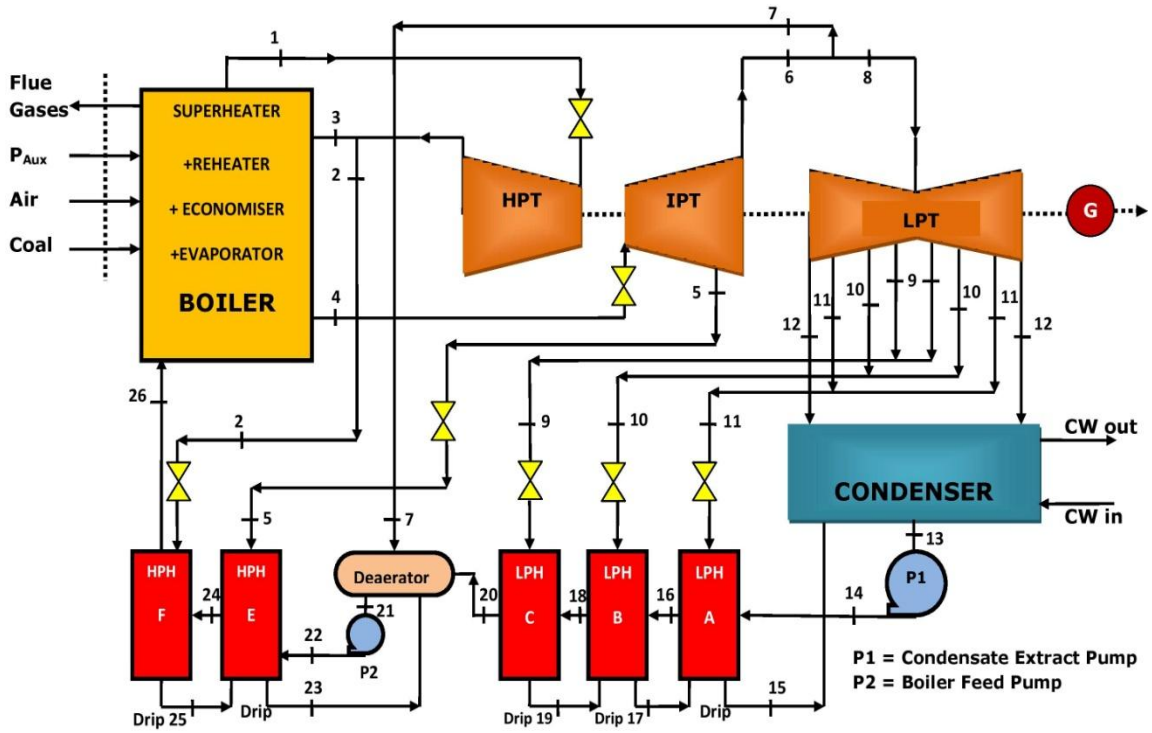

Fig. 4.5 Schematic layout of the base plant for analytical study

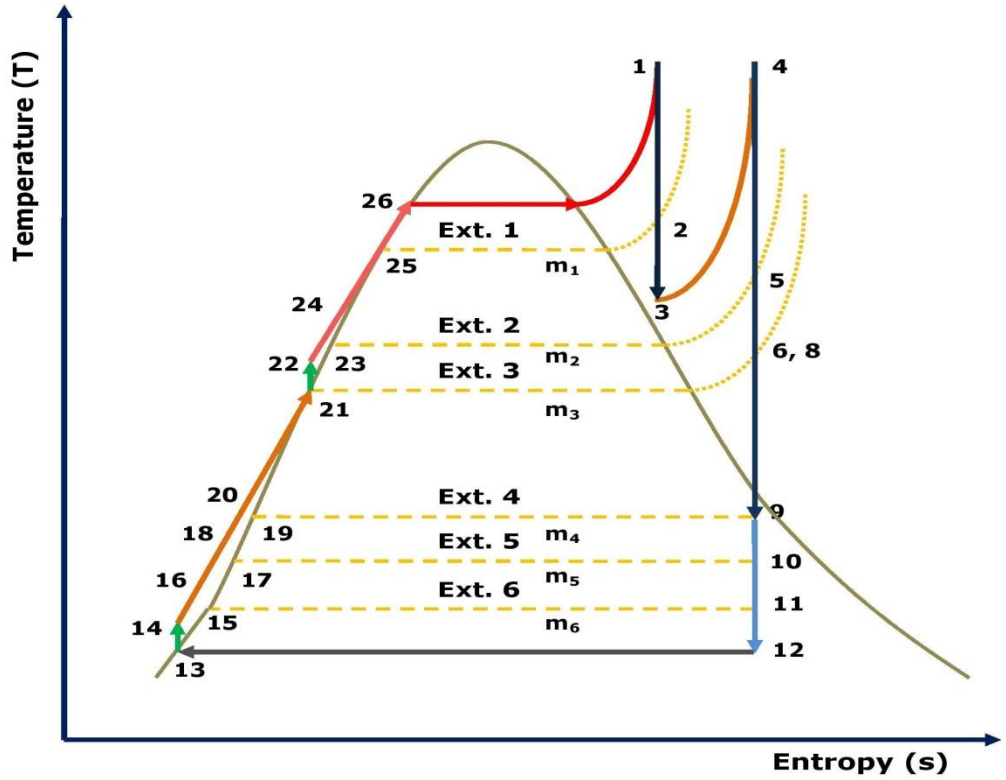

Fig.4.6 Schematic diagram based T-s diagram of NCPS 210 MW Plant

There are six feedwater heaters; one extraction from HPT, one extraction from IPT and three from LPT. The third heater from high pressure side is a deaerator for which steam is extracted from outlet steam coming out from IPT before entering into LPT. All heaters except deaerator are closed heaters.

The Rankine Cycle representation of the above plant is shown in figure 4.6 below. From operational data shown in Table 4.1 the enthalpy values at different points are picked from steam table based on property value at that point.

For points 11 and 12, the temperature value is not known but quality of steam is known. Hence using pressure value at that point saturated liquid specific enthalpy (h_f) and saturated vapour specific enthalpy (h_g) are calculated.

Based on these values,

$$h_{fg} = h_g - h_f$$

Saturated liquid specific volume is taken 0.001.

For heaters as presented in fig. 4.5 energy balance equations are given as under;

Heater F:

$$m_1 (h_2 - h_{25}) = 1 (h_{26} - h_{24})$$

Heater E:

$$m_2 (h_5 - h_{23}) + m_1 (h_{25} - h_{23}) = 1 (h_{24} - h_{22})$$

Deaerator:

$$m_3 (h_7 - h_{21}) + (m_1 + m_2) (h_{23} - h_{21}) = (1 - m_1 - m_2 - m_3) (h_{21} - h_{20})$$

Heater C:

$$m_4 (h_9 - h_{19}) = (1 - m_1 - m_2 - m_3)(h_{20} - h_{18})$$

Heater B:

$$m_5 (h_{10} - h_{17}) + m_4 (h_{19} - h_{17}) = (1 - m_1 - m_2 - m_3 - m_4 - m_5) (h_{18} - h_{16})$$

Heater A:

$$m_6 (h_{11} - h_{15}) + (m_4 + m_5) (h_{17} - h_{15}) = (1 - m_1 - m_2 - m_3 - m_4 - m_5 - m_6) (h_{16} - h_{14})$$

Turbine work of cycle is calculated as;

$$W_T = W_{T_{1-2}} + W_{T_{2-3}} + W_{T_{4-5}} + W_{T_{5-6}} + W_{T_{8-9}} + W_{T_{9-10}} + W_{T_{10-11}} + W_{T_{11-12}}$$

$$W_T = 1\,(h_1 - h_2) + (1 - m_1)\,(h_2 - h_3) + (1 - m_1)\,(h_4 - h_5) + (1 - m_1 - m_2)\,(h_5 - h_6) + (1 - m_1 - m_2 - m_3)\,(h_8 - h_9) + (1 - m_1 - m_2 - m_3 - m_4)\,(h_9 - h_{10}) + (1 - m_1 - m_2 - m_3 - m_4 - m_5)\,(h_{10} - h_{11}) + (1 - m_1 - m_2 - m_3 - m_4 - m_5 - m_6)\,(h_{11} - h_{12})$$

The net pump work of cycle sum of work done in condensate extraction pump, boiler feed pump and drip pump. Mathematically;

$$W_P = W_{CEP} + W_{BFP} + W_{Drip}$$

$$W_P = (h_{14} - h_{13}) + (h_{22} - h_{21}) + W_{Drip}$$

The drip pump work in all cases is calculated as as *vdP*.

Therefore the net work done in the cycle is difference between turbine work and pump work.

Also from the Rankine cycle diagram shown in fig. 4.6, the heat input in the cycle is given as;

$$Q = 1\,(h_1 - h_{26}) + (1 - m_1)\,(h_4 - h_3)$$

From above analysis, the cyclic efficiency of Rankine cycle in fig. 4.6 is calculated as;

$$\eta_{Cycle} = \frac{W_{Net}}{Q} = \frac{W_T - W_P}{Q}$$

4.5.2 Equivalent Coal Consumption based on Steam Requirement at Heaters

As deaerator is an integral part of steam power plant. It is exclusively used for deaerating gases dissolved so deaerator can't be replaced by a solar heater. For calculating coal or fossil fuel consumption based on bypass steam required at heaters following data is used as basic input parameter;

Specific heat of water (*c*) = 1 kcal/kg

'Gross Calorific Value' of coal (CV_G) = 3620 kcal/kg [25] [Appendix 2.4]

Also the mass flow rate of feed water is taken from table 4.1 at different heater locations.

Now, amount of heat that will be saved if heater A is being replaced by solar field;

$$Q_A = m_{14} \,.\, c \,.\, (T_{16} - T_{14})$$

And, amount of coal that would saved if low pressure heater A is being replaced by solar field,

$$F_A = \frac{Q_A}{CV_G}$$

Similarly, the amount of heat that will be saved if heater B is being replaced by solar field;

$$Q_B = m_{16} \,.\, c \,.\, (T_{18} - T_{16})$$

And, amount of coal that would saved if low pressure heater B is being replaced by solar field,

$$F_B = \frac{Q_B}{CV_G}$$

The amount of heat that will be saved if heater C is being replaced by solar field;

$$Q_C = m_{18} \,.\, c \,.\, (T_{20} - T_{18})$$

And, amount of coal that would saved if low pressure heater C is being replaced by solar field,

$$F_C = \frac{Q_C}{CV_G}$$

The amount of heat that will be saved if heater E is being replaced by solar field;

$$Q_E = m_{22} \,.\, c \,.\, (T_{24} - T_{22})$$

And, amount of coal that would saved if low pressure heater E is being replaced by solar field,

$$F_E = \frac{Q_E}{CV_G}$$

And at last, the amount of heat that will be saved if heater F is being replaced by solar field;

$$Q_F = m_{24} \,.\, c \,.\, (T_{26} - T_{24})$$

And, amount of coal that would saved if low pressure heater F is being replaced by solar field,

$$F_F = \frac{Q_F}{CV_G}$$

Following are the calculation results presented in table 4.2 at full load condition;

Table 4.2 Basic calculation results of analytical model at full load condition

Point No.	Pr. [Pa]	T [K]	h [J/kg]	s [J/kg.K]	ṁ [Ton/hr]
1	15000000	810.2	3413314	6476.727	622.804
2	3920000	615.8	3075295	6476.727	63.437
3	3920000	615.8	3075295	6476.727	559.367
4	3494000	810.2	3535001	7264.214	559.367
5	1623000	697.3	3306146	7264.214	34.673
6	684000	580.5	3074287	7264.214	524.694
7	684000	580.5	3074287	7264.214	31.796
8	684000	580.5	3074287	7264.214	492.898
9	229900	465.4	2852751	7264.214	26.39
10	150000	433.0	2792188	7264.214	28.343
11	21500	334.8	2495105	7264.214	4.388
12	10300	319.5	2412333	7264.214	432.812
13	10300	319.5	194170	656.573	496.54
14	1607000	319.5	195767	656.573	496.54
15	21500	334.7	257660	850.663	4.388
16	21500	334.7	257660	850.663	496.54
17	150000	368.0	397401	1248.288	28.343
18	150000	368.0	397401	1248.288	496.54
19	229900	397.8	523729	1578.122	26.39
20	229900	397.8	523729	1578.122	496.54
21	615000	432.9	674348	1939.923	623.789
22	17000000	434.4	690733	1939.923	623.789
23	1623000	452.9	762374	2136.177	34.673
24	1623000	452.9	762374	2136.177	623.789
25	3920000	522.3	1080954	2784.414	63.437
26	16800000	518.1	1062354	2718.111	623.789

4.6 ADVANCES IN THE STUDY OF ISTP PLANT AT NCPS

4.6.1 Organization of Different Cases at FWH Integration

There are six feed water heaters at NCPS as described above. Out of these one is open type FWH or deaerator and rest five are closed FWH. Therefore when the replacement of FWH with solar heating option is considered, there are five heaters that can be replaced as shown in schematic diagram of the plant in fig. 4.7. Based on replacement of FWH there are various possibilities that can be studied as FWH replacement option. To obtain significant study results with trend, following cases are built:

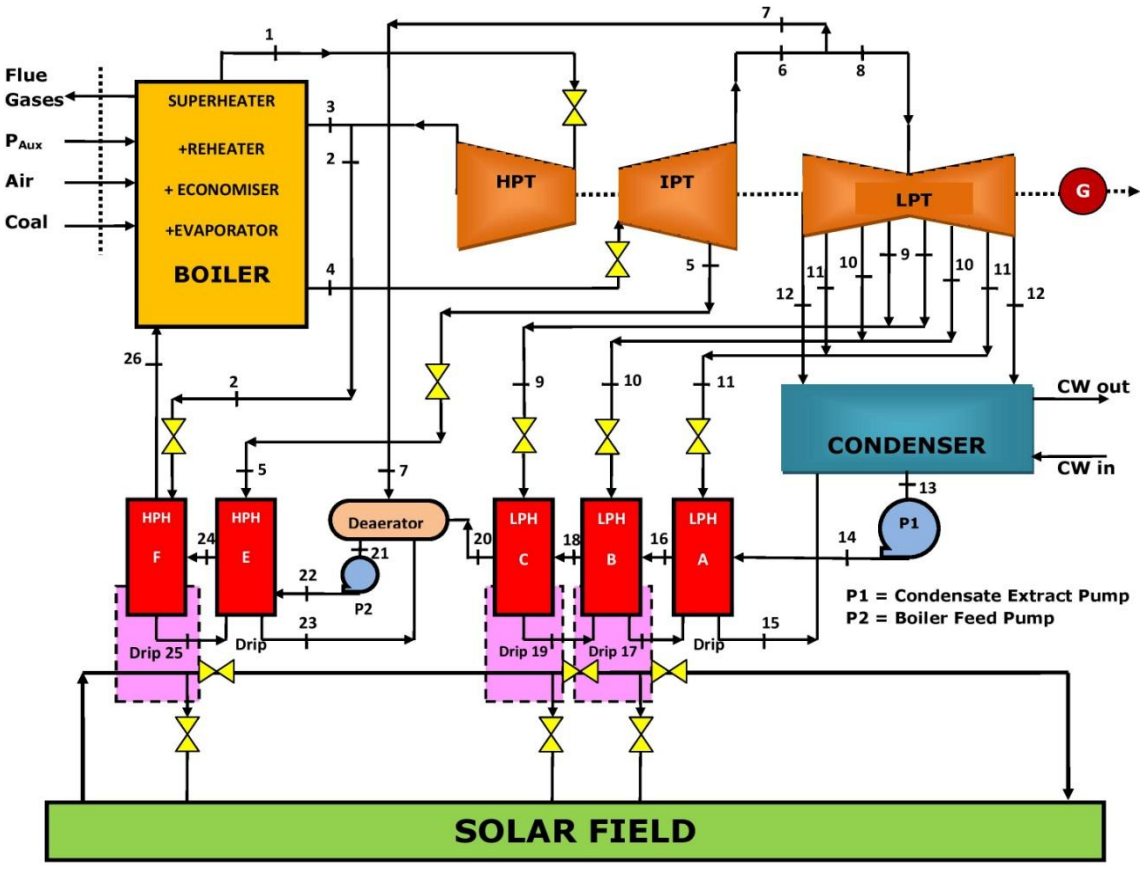

Fig. 4.7 Schematic diagram of NCPS 210 MW plant with most optimal integration scheme using current solar technology

Case I: FWH A is being replaced by solar heating option.

Case II: FWH B is being replaced by solar heating option.

Case III: FWH C is being replaced by solar heating option.

Case IV: FWH E is being replaced by solar heating option.

Case V: FWH F is being replaced by solar heating option.

Case VI: FWH F, C and B together being replaced by solar heating option.

Case VII: All FWH are being replaced by solar heating option.

4.6.2 Indian Solar Resources and Average DNI Availability

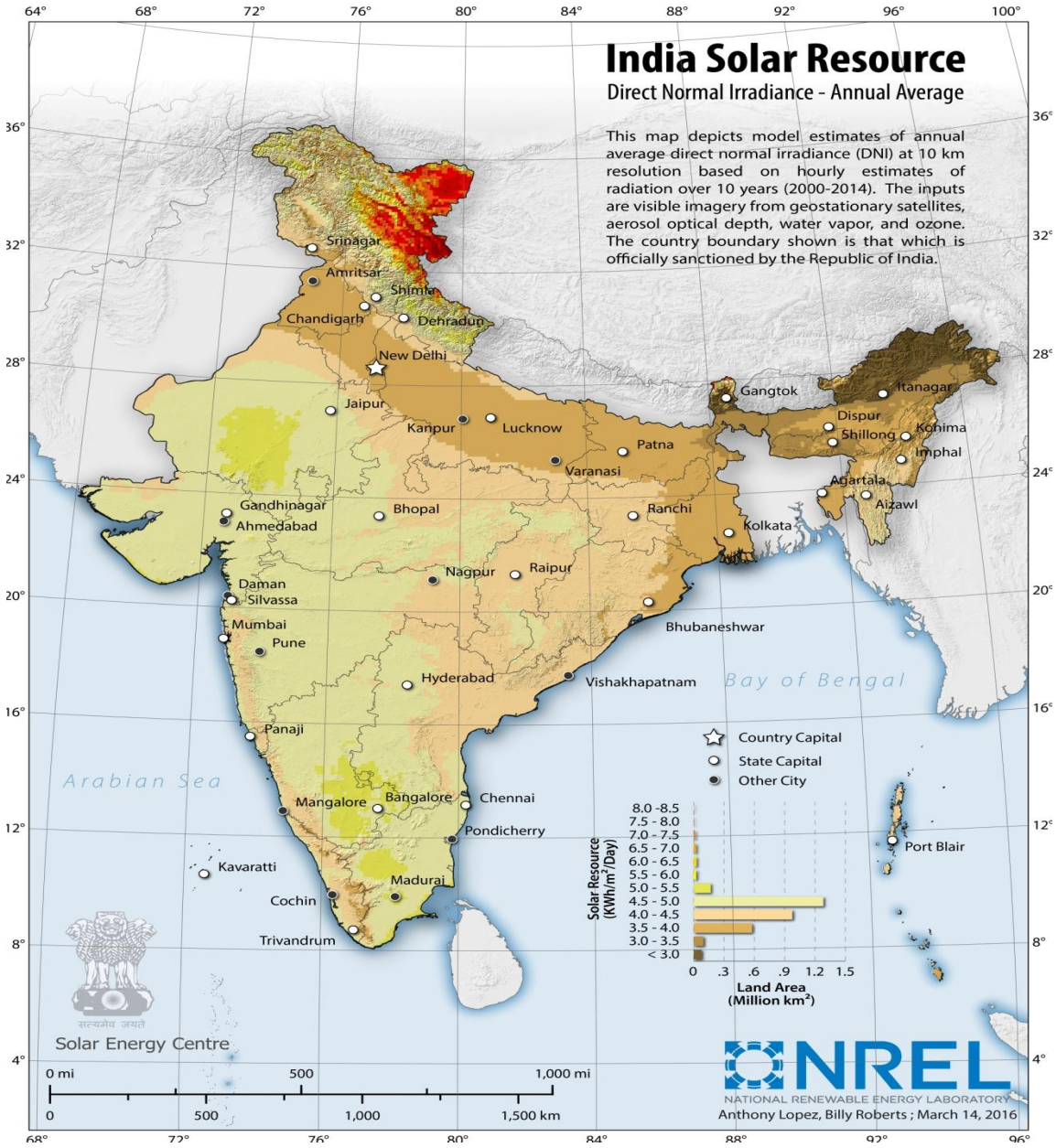

Fig. 4.8 Average DNI in Indian context (Source: NREL)

The solar thermal analysis of ISTPP is based on calculation and comparison of different parameters that are important to understand the design and performance of the ISTPP.

Also the solar energy depends upon the DNI value at a particular location. The average solar map of India is shown below in fig. 4.8.

4.7 SOLAR PROSPECT OF CLFR ANALYTICAL MODEL

The solar prospect of analytically integrated model is the first and foremost point to be considered. The results of this analysis are provided in result section of this report.

4.7.1 Solar Irradiance variation in Relation to Inlet Solar Heat at Plant Location

The solar irradiance at the plant location in this context is very important parameter. It is calculated based on long term observation of weather data and solar insolation value. The solar insolation value considered in this report is taken from NREL DNI Calculator shown in fig. 4.9.

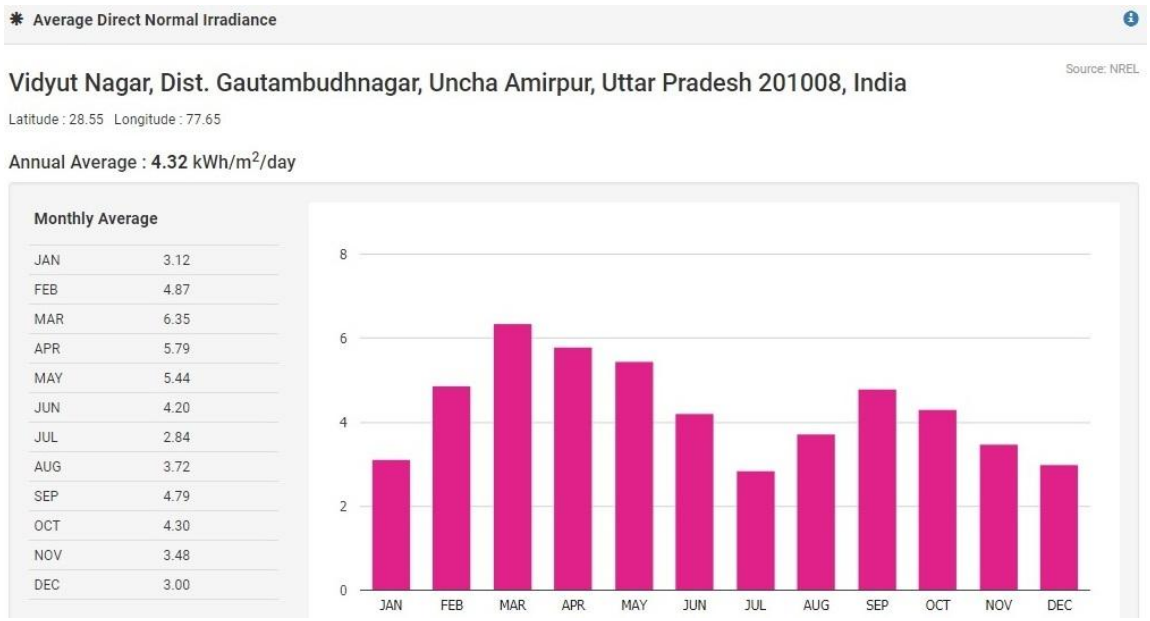

Fig. 4.9 DNI at plant location (Source: NREL)

Solar collector efficiency given in above is collection efficiency of LFR. It is taken from Appendix 2.3 for LFR. The solar collector area for each case is calculated on

annual average DNI. Then based upon this area the inlet solar heat at given solar irradiance is calculated for each case using following formula;

$$Solar\ Heat\ at\ Given\ Irradiance$$
$$= Collector\ Area\ based\ on\ Avg.DNI\ X\ Collector\ Efficiency\ X\ Solar\ Irrdiance$$
$$SH_I = A_C\ X\ \eta_C\ X\ s_d$$

The average value of DNI taken in this report is 0.18 (kW/m^2) based on above DNI Data. The value of DNI varies between 0.09 (kW/m^2) to 0.27 (kW/m^2) as shown in above fig. 4.9. Thus these values are divided in 10 equal intervals for trend analysis.

The solar collector area based on annual average value of DNI can be calculated as below;

$$Collector\ area = \frac{Heat\ Requirement\ at\ Heater}{Solar\ Irrdiance\ X\ Solar\ Collector\ Efficiency}$$
$$A_C = \frac{Q_{Case}}{s_d\ X\ \eta_c}$$

Solar collector efficiency given in above is collection efficiency of LFR. It is taken from Appendix 2.3 for LFR. The solar collector area for each case is calculated on annual average DNI. Then based upon this area the inlet solar heat at given solar irradiance is calculated for each case using following formula;

$$Solar\ Heat\ at\ Given\ Irradiance$$
$$= Collector\ Area\ based\ on\ Avg.DNI\ X\ Collector\ Efficiency\ X\ Solar\ Irrdiance$$
$$SH_I = A_C\ X\ \eta_C\ X\ s_d$$

4.7.2 Analysis of Different Cases with Respect to Energy Efficiency

The calculation of analysis of cases with respect to energy efficiency depends on the results shown in table 6.2. From there, the fuel utilization of base case as well as the seven cases we have mentioned earlier is taken.

Now, as mentioned earlier, the GCV that we have taken in this report is 3620 kcal/kg or 15156.22 kJ/kg [25]. Latent heat required for vaporization at inlet pressure of heater A is taken 1933.19 (kJ/kg). From these two values, LCV of fuel is calculated using following formula;

$$Lower\ Calorific\ Value$$
$$= Gross\ Calorific\ Value\ of\ Fuel$$
$$- Latent\ heat\ of\ vaporisation\ at\ inlet\ pressure\ of\ heater\ A$$
$$CV_L = CV_G - L$$

Now, energy efficiency of plant is calculated as,

$$Energy\ Efficency = \left(\frac{P_{gen}\ X\ 3600}{F\ X\ CV_L}\right) X\ 100$$

For different cases, the fuel utilization value and LCV is different and hence energy efficiency is different.

4.7.3 Heat Rate in Different Cases

Heat rate of a plant is defined as ratio of net heat input to the net plant power output. In this case heat rate is calculated using following formula;

$$Heat\ Rate = \frac{F\ X\ CV_L}{P_{gen}}$$

4.7.4 Area calculation in Different Cases

Area requirement for collector and land area required are discussed in this section for the ISTP. The solar irradiation value and collector efficiency are taken same as discussed above. The area requirement for a particular case is calculated using following formulae;

$$Area\ of\ Solar\ Collector\ Required$$
$$= \frac{Heat\ Requirement\ from\ Solar\ Field\ in\ that\ Case}{Average\ Solar\ Irrdiance * Collector\ Efficiency}$$
$$A_C = \frac{Q}{s_d\ X\ \eta_C}$$

Now, the land area requirement is approximately three times of solar collector area requirements [32].

4.7.5 Variation in the Area of Solar Collector with Solar Irradiance

Variation of requirement of solar collector with the variation of solar irradiation is to be shown in this section. For this, the collection efficiency of LFR is already

known. Also the heat requirement in each case is known. We have already divided the DNI value range so that the trend analysis could be done. For each case area of solar collector at a specific value of DNI is to be calculated by following formula;

$$Collector\ Area\ for\ a\ Case\ at\ Specific\ DNI = \frac{Heat\ Required\ in\ that\ Case}{Specific\ value\ of\ Solar\ Irradiance\ X\ Collector\ Efficiency}$$

$$A_C = \frac{Q}{s_d\ X\ \eta_c}$$

4.7.6 Effect of Fluid Inlet Temperature on Collection Efficiency

To find out the most feasible mass flow rate of fluid, a relation between fluid inlet temperature and collection efficiency has been found. With increase in fluid temperature, the solar absorber temperature also increases, as the same fluid circulates in the circuit. Thus there are losses because of radiation along with convection, which in turn decreases the efficiency. This also decreases the heat gain rate to the absorber. To visualize this phenomenon, computations are made with fluid inlet temperature range (518.1 K and 319 K) to the solar field. Following trend is found:

- There is significant reduction in collection efficiency with Increase in temperature.
- The decrease is slightly irregular (non-linear).

The non-linearity comes as there is slight increase in value of overall loss coefficient with increase in temperature. The value of collection efficiency with varying area of collector based on needs is also calculated, which is constant in all cases. The difference of the two values at each point of curve represents the loss incurred (due to convection and radiation).

The calculations have been done on the previously defined values of collection efficiency of LFR collector and average annual solar irradiance at plant location. Also area of solar collector is taken as maximum calculated area of solar collector requirement to replace all the heaters at the annual average DNI. Now, the heat requirement in this case is defined in a different manner. At first, the heater F is to be replaced by solar field. F and E are together to be replaced. Similarly all the heaters are to be replaced gradually. Also, the outlet temperature of fluid in each case has to be

noted for graphical study. The collector efficiency has also to be calculated for each condition described above.

4.7.7 Variation in Mass Flow Rate with Energy Efficiency

In this case, the mass flow rate known in each case and energy efficiency calculated previously are compared.

4.8 Pollution Prospect of Analytical Integrated Model

The rate of carbon dioxide and sulphur dioxide production indifferent cases ate presented in this section. The results of this analysis are presented in result section of this report.

The rate of CO_2 and SO_2 production in all cases is studied. To analyze rate of CO_2 and SO_2 production in all cases, first of all the basic data required is needed. The net power output of the plant is same i.e. 210 MW. The fuel requirement in base case and equivalent amount of fuel utilization in heaters is also known. The ultimate analysis results of coal used are taken from table appendix 2.4.

Theoretical air requirement to completely burn fuel used in kg of air per kg of fuel is calculated as;

$$A_{th} = 11.5\,C + 34.5\left(H - \frac{O}{8}\right) + 4.3\,S$$

After this, actual amount of air supplied for complete combustion of 1 kg fuel assuming 30% excess air is required for complete combustion of fuel is calculated to be;

$$A_{act} = 1.3\,X\,A_{th}$$

Then water vapour entering with air per kg of fuel is found out;

$$V_{WF} = A_{act}\,X\,M$$

Thus, Total water vapour formed per kg fuel is;

$$V_{WT} = 9\,H + M + V_{WF}$$

Then Mass of combustion gases per kg of fuel is obtained,

$$M_{CO_2} = \frac{44}{12}\,X\,C$$

$$M_{SO_2} = \frac{64}{32} X S$$

Finally, the rate of CO2 and SO2 production kg/kWh calculation is done;

$$R_{CO_2} = \frac{F X M_{CO_2} X 1000}{P_{gen}}$$

$$R_{SO_2} = \frac{F X M_{SO_2} X 1000}{P_{gen}}$$

CHAPTER 5

HFC BASED MODEL OF THE NCPS SOLAR INTEGRATED PLANT WITH THERMAL STORAGE

5.1 LIMITATIONS OF CLFR BASED MODEL AND NEED OF NEW COLLECTOR

Following are the limitations of the LFR base model:

- CLFR technology uses linear arrangement of mirrors hence larger space area is required to establish mirror rows.
- In context of case study, the variation of inlet temperature of fluid to the solar field with solar collection efficiency of collector of an area is discussed in previous chapter for CFLR case in NCPS model. The results show that the inlet fluid temperature to the solar field should be as low as possible for best results. This needs the replacement of all the feedwater heaters from solar field. Using the present CLFR technology, the replacement of all the FWH with solar field is not possible due to land area limitations of the case.
- The fluid temperature of the CLFR reflector moderate and thus the overall energy efficiency is low.
- Due to moderate temperature, the thermal storage integration is not much feasible.

The above shortcomings indicate some more research to the present model for optimization of results.

5.2 SELECTION OF NEW SOLAR COLLECTOR BASED ON NEEDS OF THIS PROJECT

Following is the most optimal integration scheme shown in fig. 5.1, for project discussed under case study:

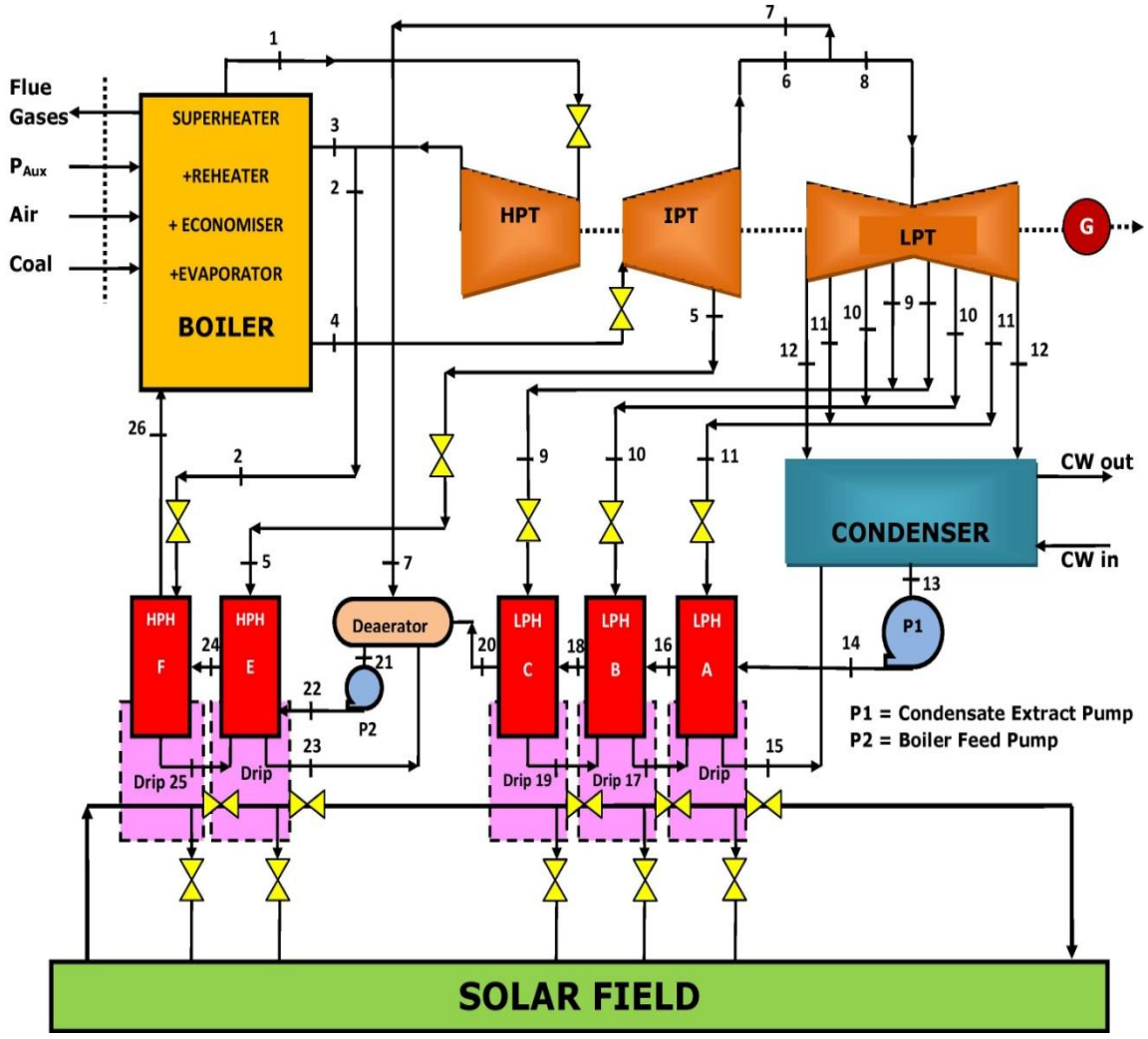

Fig. 5.1 Optimal integration of solar thermal to base case power station

- In the above layout shown, all the feed water heaters are shown to be replaced by solar field. Suitable valve arrangement is provided for flexible operation of integrated plant. As the solar field is expected to replace all the FWH, a solar

collector with higher collector efficiency is needed for the plant, area being constraint for the model.

- The storage system should be integrated for higher solar output and hence integration benefits.

The new collector proposed in this project is 'Heliostat Field Collector' (HFC) which approximately meets all the demands of desired basic parameters as described in Appendix 2.3. The the modified analysis is needed to be done for few parameters which is described below.

5.3 SOLAR THERMAL PROSPECT OF THE NEW HFC BASED MODEL

5.3.1 Analysis of Cases in Light of Area Requirement

Area requirement for collector and land area required are discussed in this section for the ISTP. The solar irradiation value and collector efficiency are taken same as discussed above.

The area requirement for a particular case is calculated using following formulae;

$$Area\ of\ Solar\ Collector\ Required = \frac{Heat\ Requirement\ from\ Solar\ Field\ in\ that\ Case}{Average\ Solar\ Irrdiance * Collector\ Efficiency}$$

$$A_C = \frac{Q}{s_d\ X\ \eta_C}$$

Now, the land area requirement is about 3 times area of solar collector required. [55]

5.3.2 Area of Solar Collector at Different Solar Irradiance Values

Variation of requirement of solar collector with the variation of solar irradiation is to be shown in this section. For this, the collection efficiency of LFR is already known. Also the heat requirement in each case is known. We have already divided the

DNI value range so that the trend analysis could be done. For each case area of solar collector at a specific value of DNI is to be calculated by following formula;

$$Collector\ Area\ for\ a\ Case\ at\ Specific\ DNI = \frac{Heat\ Required\ in\ that\ Case}{Specific\ value\ of\ Solar\ Irradiance\ X\ Collector\ Efficiency}$$

$$A_C = \frac{Q}{s_d\ X\ \eta_c}$$

5.4 ANALYTICAL INTEGRATION OF THE SOLAR THERMAL STORAGE

The size of storage tank is the most important calculation with area constraint.

5.4.1 Volume of the Storage Tanks

Once the Rankine cycle and solar thermal system is designed, the thermal storage system is to be integrated to the system to optimize the performance of integrated system. The volume of the two tanks could be calculated based on the model input performance, its robustness, discharge time, salt properties etc. Following procedure is to be adopted in calculating the volume of storage tanks;

At first the higher and lower temperature of water in the solar field is calculated. Then time of operating storage tank is to be specified as a design consideration i.e. for how much time, the storage is expected to deliver power. The specific heat and density of the salt being used for thermal storage purpose is to be taken from property charts. At last, the energy requirement expected from the tank is also set as an input parameter.

Mass flow rate of the salts is calculated as;

$$m_{Salt} = \frac{Q_{Tank} * Time}{C_{p_{Salt}}\ (T_{HT} - T_{CT})}$$

Maximum volume of the hot tank is calculated as;

$$V_{HT} = \frac{m_{Salt} * Time}{\rho_{HT}}$$

Maximum volume of the cold tank is calculated as;

$$V_{CT} = \frac{m_{Salt} * Time}{\rho_{CT}}$$

Then volume of tank is calculated, area and volume of tank are distributed based on space required and need of the project.

5.4.2 Solar Heat Available for Storage based on Monthly Analysis

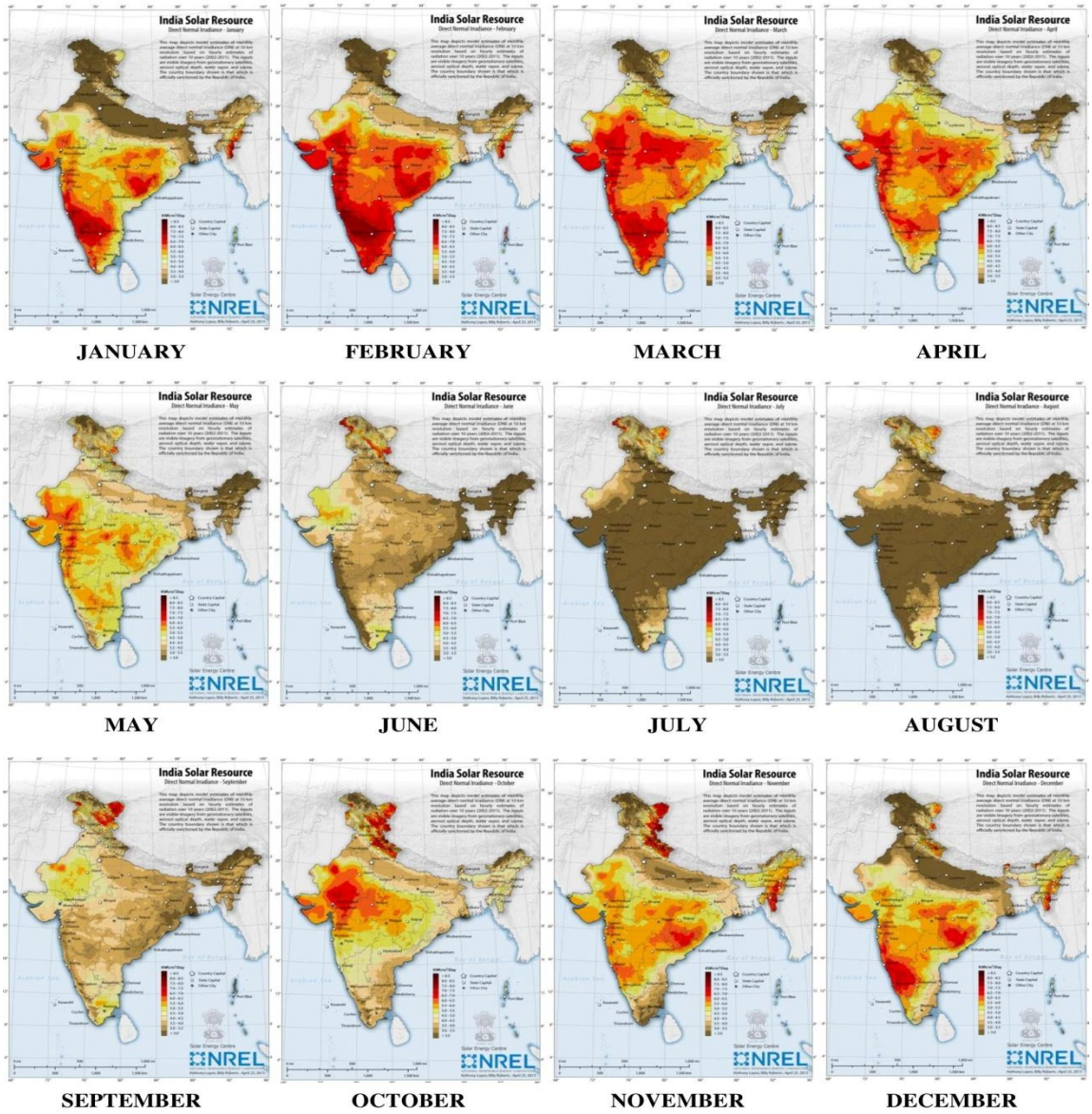

Fig. 5.2 Monthly solar irradiance variance map (Source: NREL)

As the previous analysis shows that integrated solar field to the ISTPP is designed based on annual average DNI value. The DNI value is not constant over the year. It increases significantly in summers as compared to winters in India. Also the DNI value at day time varies on hourly basis. Thus, the solar heat available at current setup is analyzed on two different levels. One is monthly level and other is hourly level.

The previously defined value of annual average value of DNI in chapter 4 at plant location is 4.32 ($kWh/m^2/day$). The distinct value of DNI average value at months is presented in Fig. 5.2.

Taking the solar irradiance data provided by NREL at plant location (Latitude: 28.55, Longitude: 77.65), the monthly average value of DNI is presented at following Table. 5.1.

Table 5.1 Monthly available DNI at design condition (Source: NREL)

MONTH	MONTHLY AVERAGE DNI ($kWh/m^2/day$)
JANUARY	3.12
FEBRUARY	4.87
MARCH	6.35
APRIL	5.79
MAY	5.44
JUNE	4.20
JULY	2.84
AUGUST	3.72
SEPTEMBER	4.79
OCTOBER	4.30
NOVEMBER	3.48
DECEMBER	3.00

From comparison of annual energy demand and monthly availability, it is clear that there are minimum five to six months in which storage energy is easily available

without any design modification. For energy storage in rest of the months, number of solar collectors has to be increased.

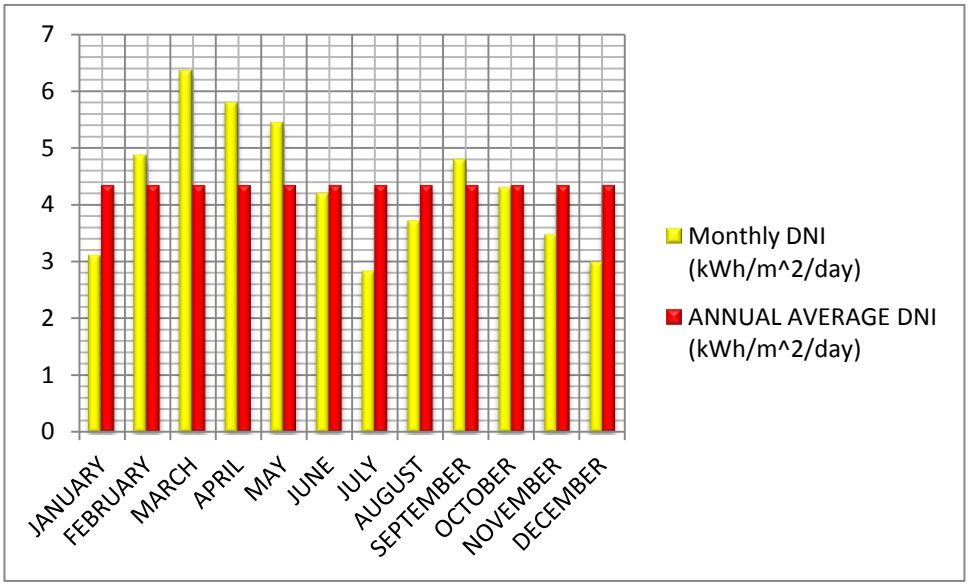

Fig. 5.3 Graph to show surplus availability of DNI for storage suitability

5.5 COMPUTATIONAL MODELLING AND SIMULATION OF HFC BASED SOLAR FIELD

Theoretically the above presented model of HFC based ISTPP seems a promising technology to meet the optimal results. Simulation of HFC based model is done in this work on 'System Advisor Model' (SAM) simulation software of NREL, U.S. Before the simulation process of actual model, there needs a brief introduction to the SAM software itself.

5.5.1 System Advisor Model (SAM): Brief Overview

SAM (Version 2014.1.14) was released on 14 January 2014 by NREL; a national laboratory of the U.S. DoE, U.S.A. SAM is software that prepares computational model of renewable energy systems for technical and economical study of the same. SAM is used to prepare both performance and financial model. The financial model includes

residential and commercial projects, power purchase agreements (PPA) projects, levelised cost of electricity and cash flow and incentives.

5.5.2 Simulation of Analytical Data on Software

The simulation of the project is made based on per MW of electricity generation. The advantage of doing so is it helps in trend analysis and also it can be interpolated for needed power production from solar system. The simulation of the project is done in using following methodology:

5.5.2.1 Defining Location and resources

At first, the location of the plant is defined based on geographical longitude and latitude of the plant. In case of out plant, the location is NTPC, Dadri, Gautam Buddh Nagar, Uttar pradesh with Latitude 28.55^0 and Longitude 77.65^0. These are defined so that the software can fetch weather data of the location.

5.5.2.2 System Design

The next step is system design. The system design depends on its components. In our project, the DNI at plant location is specified 180 W/m^2. The thermal storage is specified to provide power to 10 hours. These input conditions are set for further steps.

5.5.2.3 Heliostat Field

The heliostat field design is made in two steps:

- Generating heliostat layout
- Optimizing solar field geometry

The choice of size of single heliostat is kept same as the default value. Based on our calculated area of heliostat field, there should be 210 collectors for required power production. Now, the next process is to optimize solar field. The optimization results in the arrangement of 581 heliostats for the same area and higher output. Both the results are provided ahead. The comparisons of the two arrangements are also provided.

5.5.2.4 Tower and Receiver

After finding the optimized values of tower and receiver height, the next step is to simulate the data with the default values of solar field properties.

5.5.2.5 Thermal Storage

In next step of simulation, storage system is simulated. The storage medium for our simulation is made on solar salt (60% $NaNO_3$ + 40% KNO_3) at a pre specified value of 10 hours of storage.

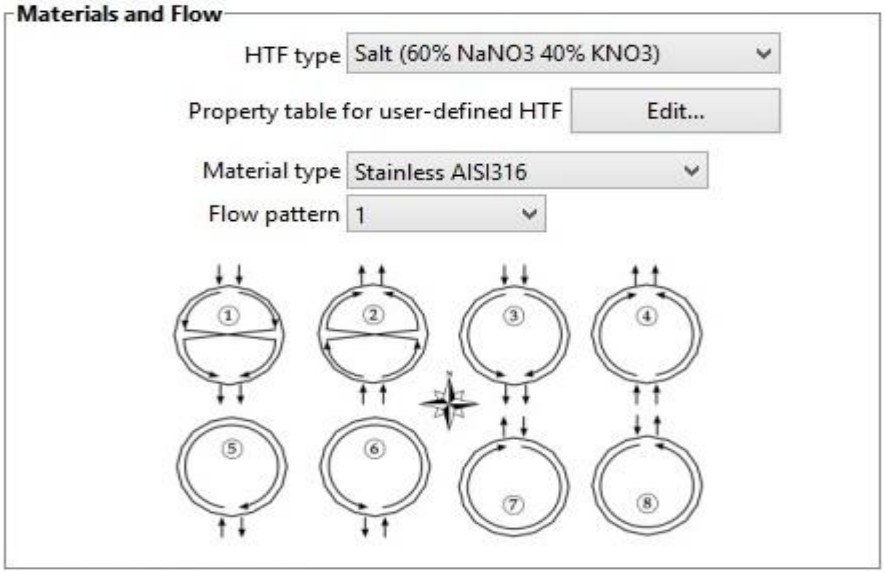

Fig. 5.4 Solar thermal storage material specification

5.5.2.6 Other Simulation Parameters

The other simulation parameters such as system controls, system costs and lifetime of the solar system, the financial parameters, and the time of delivery factor, incentives and depreciations are kept to their default values for trend analysis.

The various trends resulting from above simulation is shown in the next chapter.

CHAPTER 6

RESULTS AND DISCUSSION

The study presented in this dissertation is focused on performance improvement of an existing ISTPP by analytical and simulation method. For this, basic Rankine cycle of the plant is studied first. Then the presented integrated model of the plant is analytically simulated. The shortcomings of the current model are also discussed. Then a higher collection efficiency based model is presented and analyzed. Also the software simulation of the new model is studied. The new model is also having an integrated solar storage for added benefits. Some important results are obtained in above analysis. Those results are outlined below:

- Rankine cycle analysis of the base plant results,
- Fuel saving results in various predefined cases,
- Analytical results of CLFR integrated model; this includes study of solar irradiance, energy efficiency, heat rate, collector area, land area requirements, mass flow rate, fluid inlet temperature to the solar field and rate of CO_2 and SO_2 production in all cases.
- Analytical results of HFC integrated model including collector area and land area requirement. The analytical results of storage integration are also presented in this section.
- Simulation results of HFC based model on SAM. This provides an optimization of heliostat field and also solar thermal simulation.

The above outlined results are also presented in graphical view for better trend analysis. These trends present improvement pattern of the model. The detailed results are presented in coming sections.

6.1 RANKINE CYCLE ANALYSIS OF THE BASE PLANE RESULTS

The Engineering Equation Solver (EES) based results of base case Rankine cycle for hourly plant operation are shown in the table 6.1 below. The base case study is important to get a platform for comparison of integrated model results.

Table 6.1 Base case results of Rankine cycle analysis.

Heat Input (Q)	**2741.52 (kJ/kg)**
Turbine Work (W_T)	**1219.14 (kJ/kg)**
Pump Work (W_P)	**20.49 (kJ/kg)**
Cycle Efficiency (η_{Cycle})	**43.72 (%)**

6.2 FUEL SAVING RESULTS IN VARIOUS CASES

The integration of solar heat to thermal power station is directly linked with fuel saving in overall performance. The fuel saving in integrated model is nothing but reduced load on boiler heat. It is assumed that this reduction in heat required at boiler is equivalent with coal utilization in generating boiler heat. The EES based results of fuel saving on yearly basis are shown in table 6.2. The plant size and steam consumption are borrowed from previous chapter of the dissertation for comparison. The energy efficiency is also presented for each case for comparative study.

Table 6.2 Fuel saving results of various cases of analysis with plant energy efficiency

Parameters	Base Case Design	Case I	Case II	Case III	Case IV	Case V	Case VI	Case VII
Plant Size (MW)	210	210	210	210	210	210	210	210

Steam Consumption (Ton/hr)	622.8	618.4	594.4	596.4	588.1	559.3	504.6	465.5
Coal Consumption (Ton/hr)	135	132.9	130.4	130.9	131.8	123.8	115.1	109.8
Fuel Saving (Ton/hr)	0	2.1	4.6	4.1	3.2	11.2	19.9	25.2
Energy Efficiency of Plant	42.4	43.0	45.3	44.7	44.2	46.2	51.3	52.1

6.3 ANALYTICAL RESULTS OF CLFR INTEGRATED MODEL

The analysis of CLFR integrated solar thermal plant as a base case is done in the previous sections. The analysis results are presented in the various sections as presented below:

6.3.1 Results of Variation Solar Irradiance on Inlet Solar Heat at Plant Location

Assuming the area of solar collector constant at each case, the variation of solar heat with variation of incident solar irradiance can be shown as below:

Table 6.3 Variation of solar heat with incident irradiance

Solar Irradiance (kW/m^2)	**Inlet Solar Heat (kW)**						
	CASE I	**CASE II**	**CASE III**	**CASE IV**	**CASE V**	**CASE VI**	**CASE VII**
0.09	15728	34608	31014	24141	85208	150829	190698

0.11	19223	42299	37906	29506	104143	184347	233076
0.13	22718	49989	44798	34870	123078	217865	275453
0.15	26213	57680	51690	40235	142013	251382	317830
0.17	29708	65371	58581	45600	160948	284900	360208
0.19	33203	73062	65473	50965	179883	318418	402585
0.21	36698	80752	72365	56329	198818	351935	444963
0.23	40193	88443	79257	61694	217753	385453	487340
0.25	43688	96134	86149	67059	236688	418971	529717
0.27	47183	103824	93041	72423	255623	452488	572095

The graph of the above result plotted in EES shows the following trend:

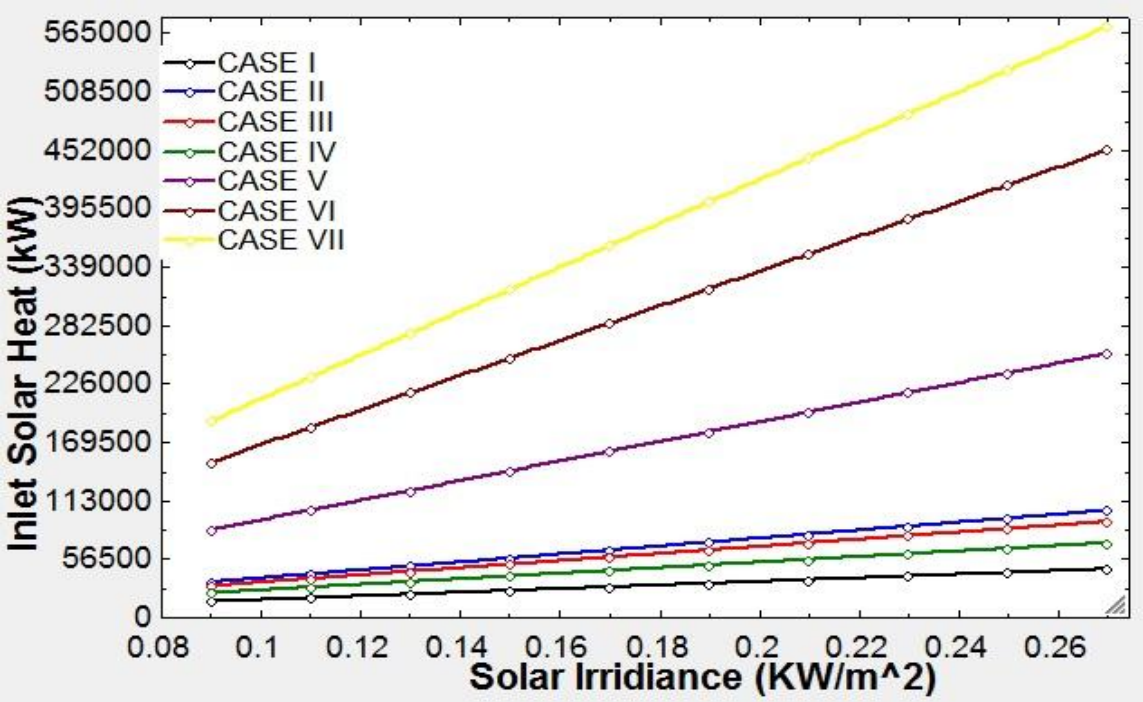

Fig. 6.1 Trend of variation of solar heat with Incident Irradiance

From the trends presented above it is clear that the inlet solar heat to the solar field is a direct function of soar irradiance.

6.3.2 Results of Variation of Energy Efficiency, Heat Rate, Collector Area, Land Area and Mass Flow Rate in Different Cases

The results of variation of energy efficiency, heat rate, collector area, land area and mass flow rate in different cases are presented in a single table 6.4. Such a tabulated presentation is best suited for single window comparison of several parameters.

Table 6.4 Results of variation of energy efficiency, heat rate, collector area, land area and mass flow rate in different cases.

Parameters	CASE I	CASE II	CASE III	CASE IV	CASE V	CASE VI	CASE VII
Latent Heat of Vaporization (kJ/kg)	1933	2358	2226	2189	1933	2358	1933
Lower Calorific Value (kJ/kg)	13223	12798	12930	12967	13223	12798	13223
Mass Flow Rate (Ton/hr)	4.4	28.3	26.4	34.7	63.4	118.2	157.2
Energy Efficiency (%)	43.0	45.3	44.7	44.2	46.2	51.3	52.1
Coal based Heat Rate (Kj/kWh)	8370	7949	8060	8139	7793	7014	6916

Collector area Required (Acres)	1.2	2.6	2.4	1.8	6.5	11.5	14.5
Land Area Required (Acres)	3.6	7.92	7.1	5.5	19.5	34.5	43.6

The above results show the calculated values of different cases of solar integration to the base plant. These parameters are base of analysis of integrated solar thermal plant. The Advantages of such integration can be predicted based on these results. However, these results specify some fixed values. To reach at certain output, some trend on results should also be in mind. Hence some trend analysis is also done and depicted in graphs. These graphs are shown in the coming pages. They also clearly depict solar-thermal integration benefits. The above tabulated results are also presented in various graphs for trend analysis. These trends are in comparison with all cases.

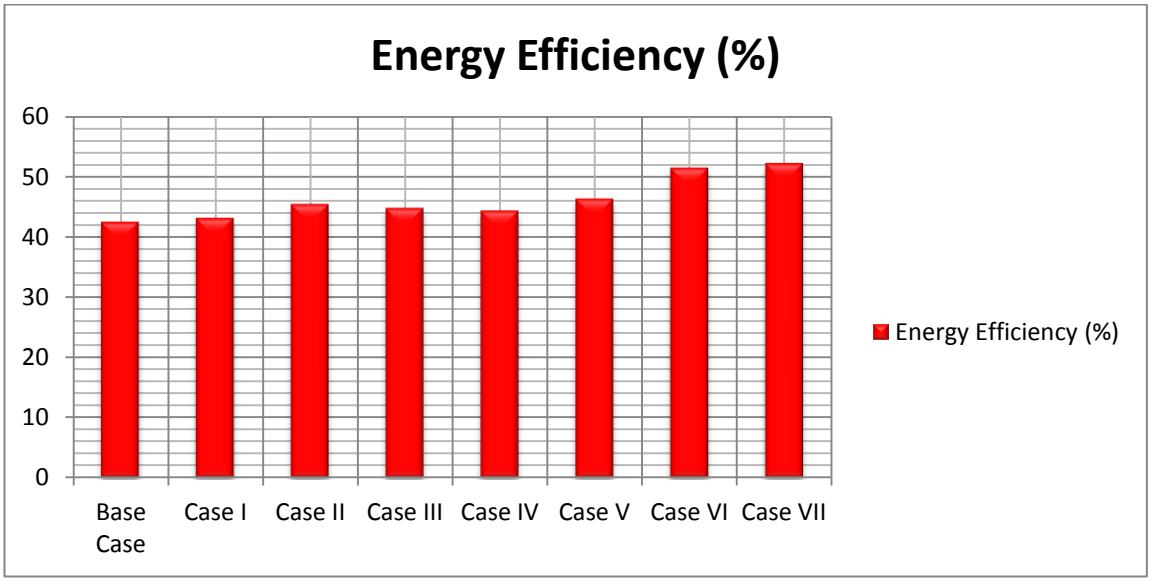

Fig.6.2 Energy efficiency variation in different cases

From above graph of fig. 6.2 it is evident that energy efficiency is increasing with level of solar integration and is at peak when all FWH are replaced by solar field.

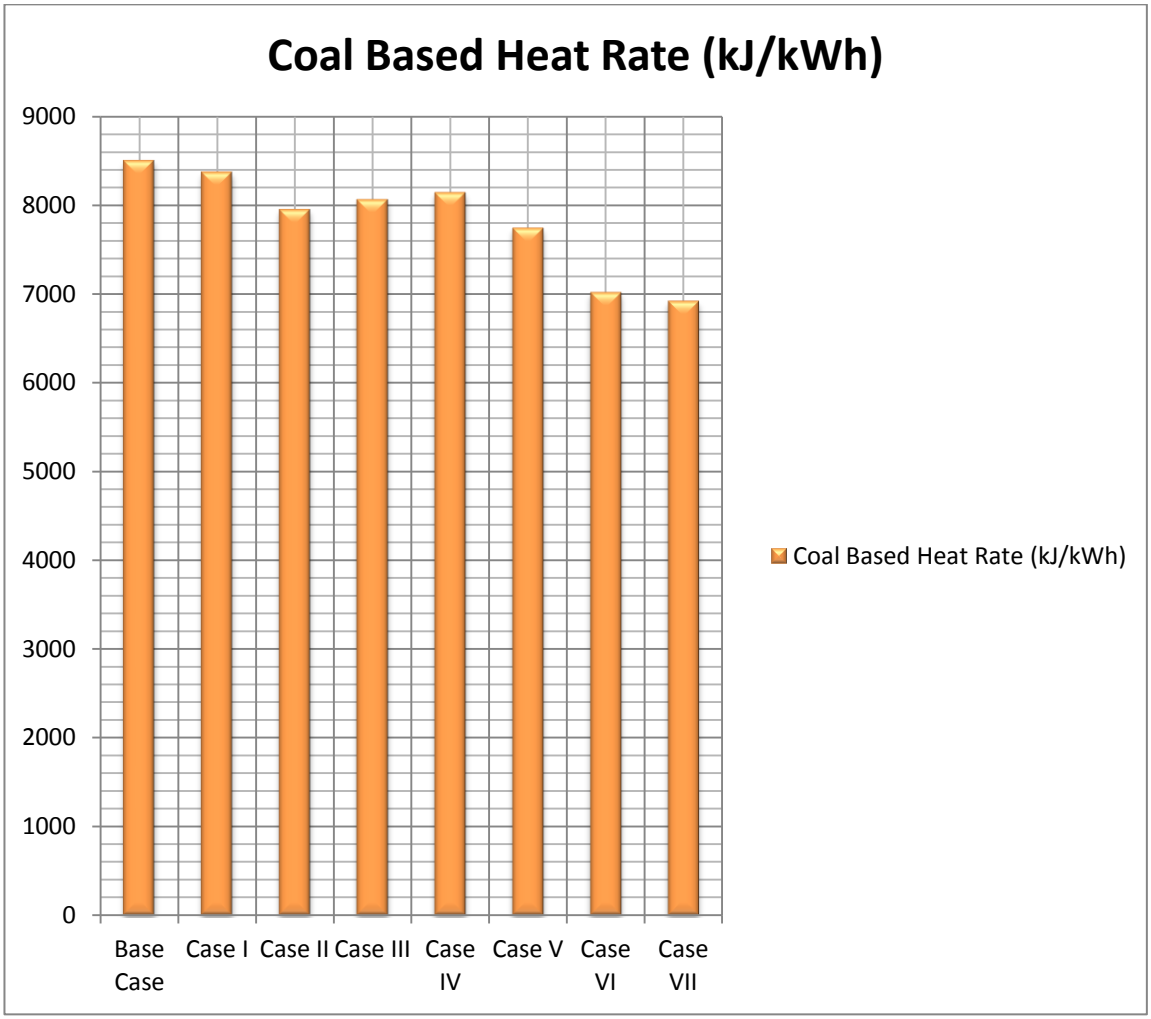

Fig. 6.3 Heat rate required from coal burning in different cases.

In above graph of fig. 6.3 the heat rate obtained from coal firing is compared for different cases. Trends show decrement in heat requirement from coal burning on higher level of solar integration.

The collector area and respective land area requirement for different cases are graphically presented in fig. 6.4. Larger collector and land areas are required for higher levels of integration.

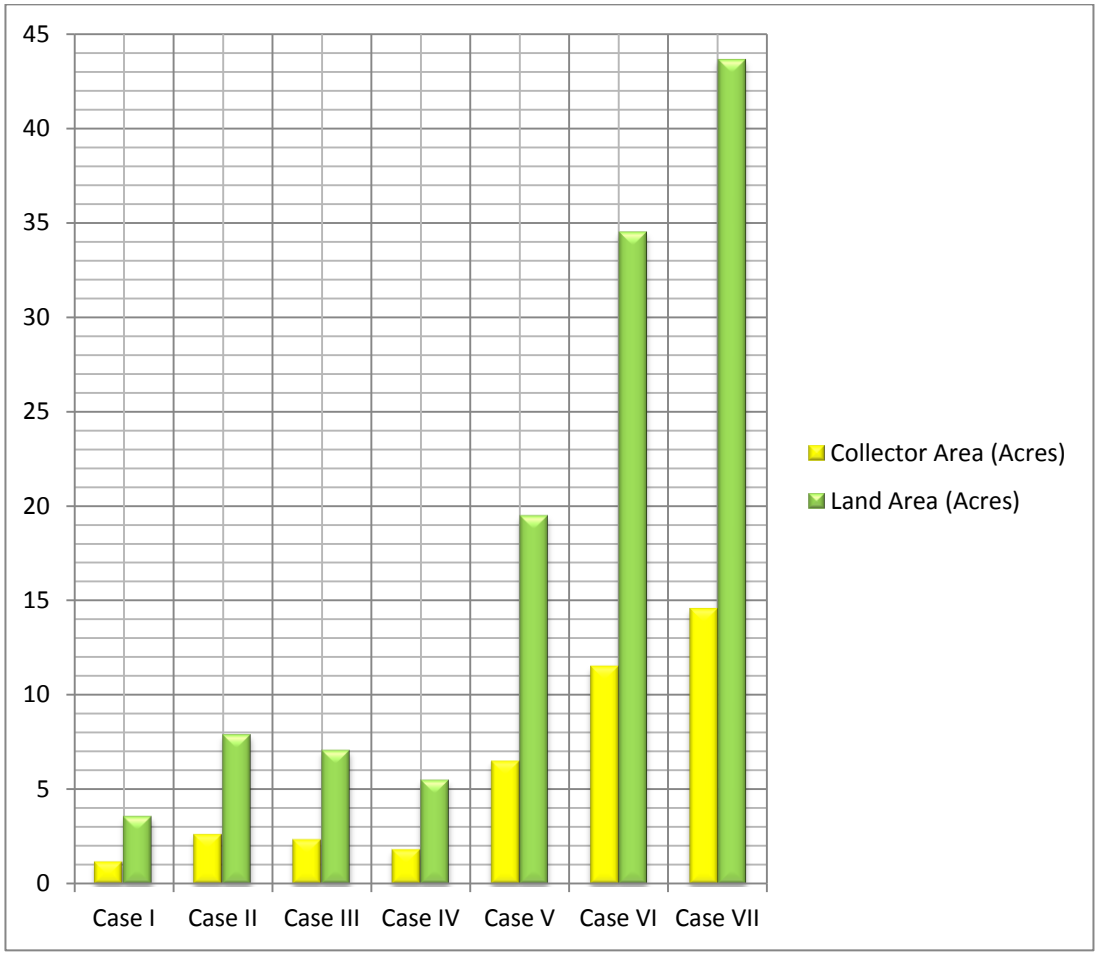

Fig. 6.4 Collector and land area requirement in different cases

6.3.3 Optimal Area of Solar Collector on Varying Solar Irradiance

The solar irradiance at each location is non-uniform throughout the year. These vary between ranges of irradiance values. The minimum and maximum irradiance values are subdivided in ten equal parts for continuality of analysis. The optimal area of solar collector is calculated for each case using EES from analytical model.

Table 6.5 Effect of varying solar irradiance on optimal area required of solar collector.

Solar Irradiance (kW/m^2)	**Optimal Area of Solar Collector (Acres)**						
	CASE I	CASE II	CASE III	CASE IV	CASE V	CASE VI	CASE VII

0.09	2.39	5.27	4.73	3.68	12.99	23.00	29.08
0.11	1.96	4.31	3.87	3.01	10.63	18.82	23.79
0.13	1.66	3.65	3.27	2.54	8.99	15.92	20.13
0.15	1.43	3.16	2.83	2.20	7.79	13.80	17.45
0.17	1.27	2.79	2.50	1.94	6.88	12.17	15.39
0.19	1.13	2.50	2.24	1.74	6.15	10.89	13.77
0.21	1.02	2.26	2.02	1.57	5.57	9.85	12.46
0.23	0.93	2.06	1.85	1.44	5.08	9.00	11.38
0.25	0.86	1.90	1.70	1.32	4.67	8.28	10.47
0.27	0.79	1.75	1.57	1.22	4.33	7.66	9.69

The table 6.5 presented above presented above the effect of variation in solar irradiance on optimal area requirement of solar collector.

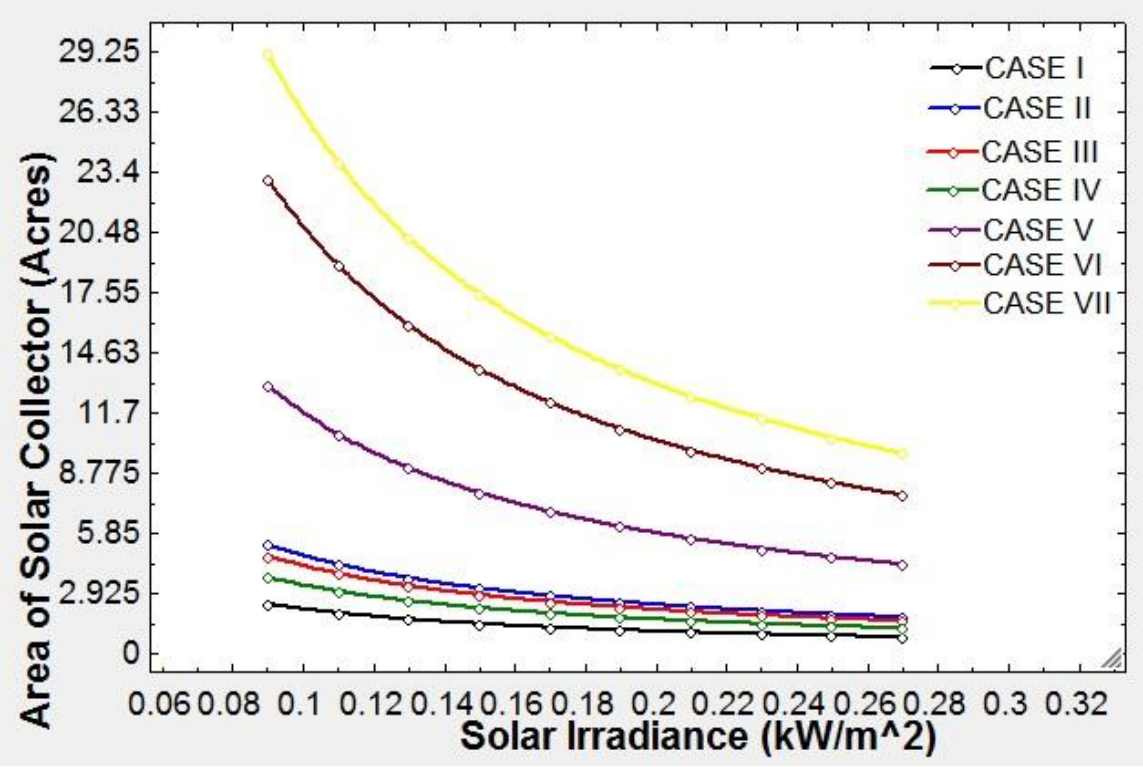

Fig. 6.5 Variation of area of solar collector with solar irradiance value

The results tabulated above are plotted in fig. 6.5 using EES for trend analysis. The EES results present that on increasing solar irradiance value the area requirement for solar collector is reduced significantly.

6.3.4 Effect of Fluid Inlet Temperature on Collection Efficiency

Solar field heat is collected to heat water for heating the FWH condensate in integrated model. The solar heated water is allowed to exchange its heat at FWH and water then again circulates back in the separate solar cycle. The fluid entering in solar field is also important parameter when compared with collector efficiency. This comparison is tabulated below.

Table 6.6 Collection efficiency of solar collector on different fluid inlet temperature to the solar field

Fluid Inlet temperature to the Solar System (K)	Collection Efficiency with Case Based Constant Collector Area (%)	Collection Efficiency with Case Based Variable Collector Area (%)
319	36	36
334	33.03	36
368	26.49	36
434	20.64	36
452	16.08	36

Following result is found based of analysis of this section:

- There is significant reduction in collection efficiency with Increase in temperature.
- The decrease is slightly irregular (non-linear).

The non-linearity comes as there is slight increase in value of overall loss coefficient with increase in temperature. The value of collection efficiency with varying area of collector based on needs is also calculated, which is constant in all cases. The difference of the two values at each point of curve represents the loss incurred (due to convection and radiation).

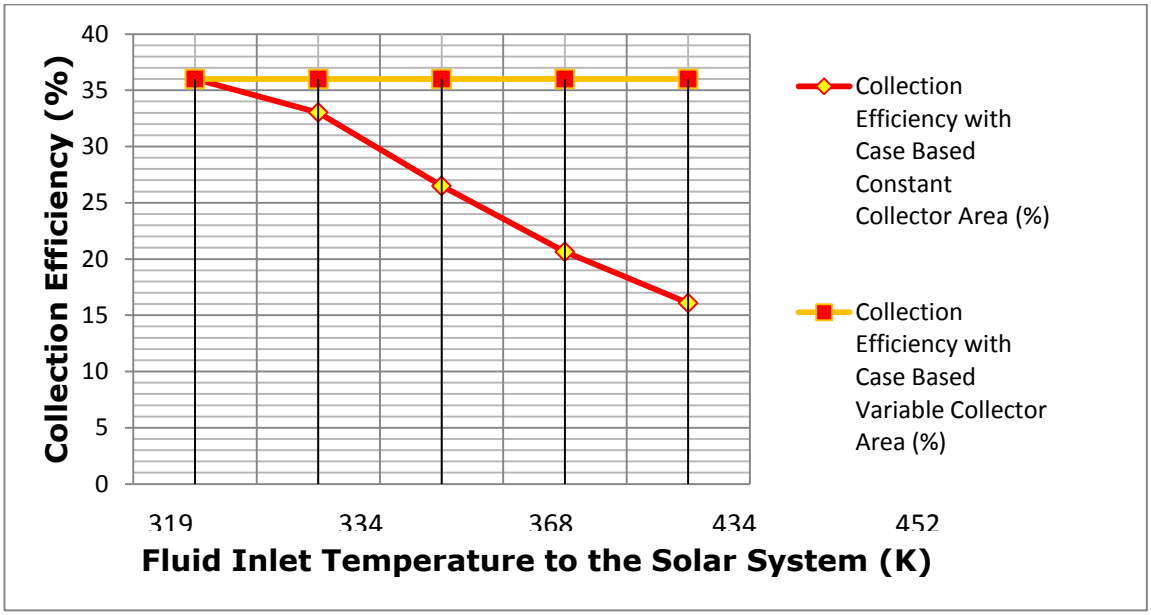

Fig. 6.6 variation of collection efficiency of solar collector with fluid inlet temperature to the solar system

6.3.5 Rate of CO_2 and SO_2 Production in all Cases

While discussing the environmental front of integration benefits, it is the first important object to measure the CO_2 and SO_2 production. These pollutants are important to be reduced. The analytical model of pollutant production are developed and analyzed on EES. The results are tabulated below.

Table 6.7 Rate of carbon dioxide and sulphur dioxide production in all cases.

Pollutant	Base Case	CASE I	CASE II	CASE III	CASE IV	CASE V	CASE VI	CASE VII
Carbon Dioxide (kg/kWh)	0.93	0.92	0.90	0.90	0.91	0.85	0.79	0.76
Sulphur Dioxide (kg/kWh)	0.0069	0.0068	0.0067	0.0067	0.0067	0.0063	0.0059	0.0056

The results presented above are also plotted the graphs for trends.

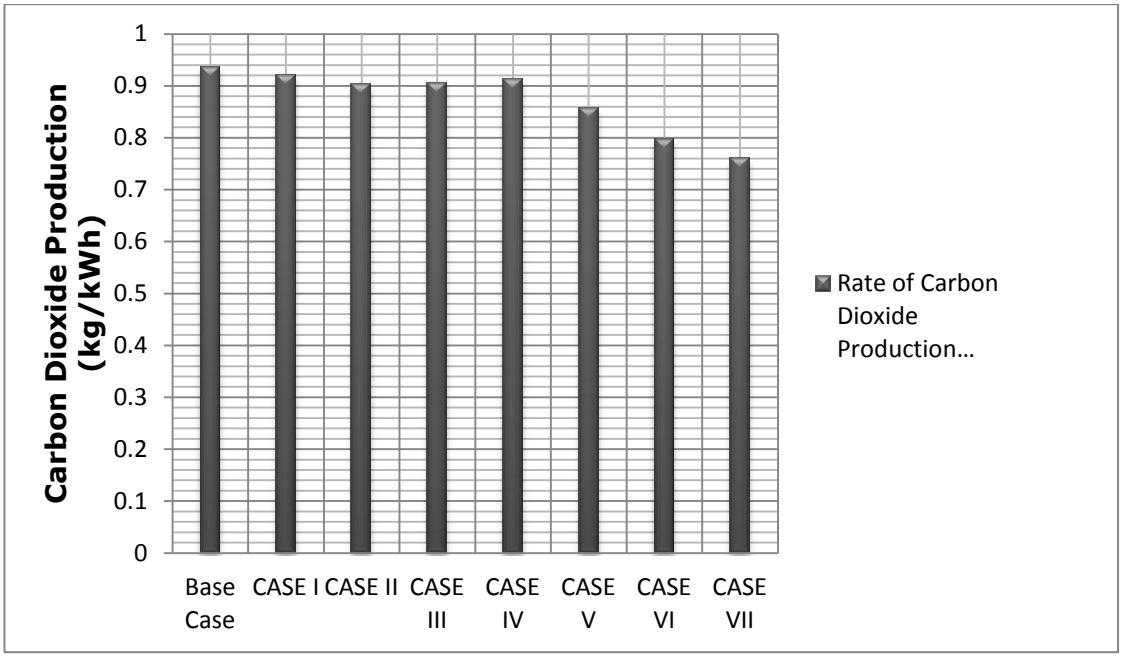

Fig. 6.7 Graphical representation of carbon dioxide production in all cases

The graph plotted in fig. 6.7 shows the carbon dioxide production in various cases. The carbon dioxide emission is reduced significantly in higher integration modes.

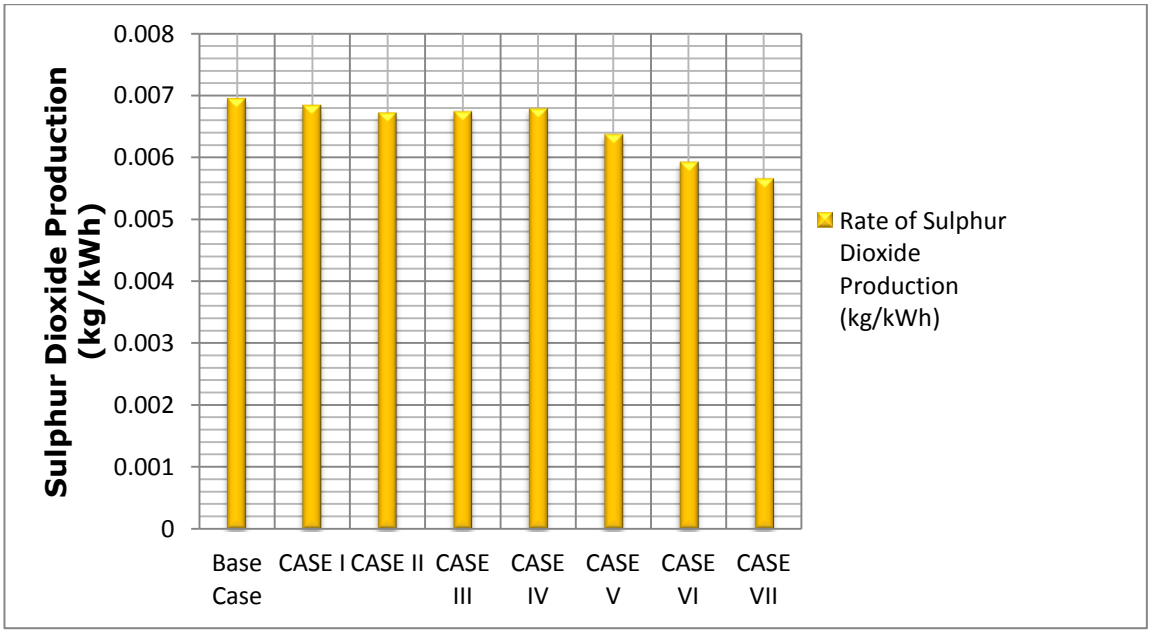

Fig.6.8 Graphical representation of carbon dioxide production in all cases

The graph plotted in fig. 6.8 shows the sulphur dioxide production in various cases. The sulphur dioxide emission is reduced significantly in higher integration modes.

6.4 ANALYTICAL RESULTS OF HFC INTEGRATED MODEL

The efficiency improvement is directly linked with higher level of integration. This requires higher availability of solar heat. The solar heat available in CLFR model is not sufficient for best integration mode due to land area constraint to expand CLFR field further. This indicates the improvements required in solar thermal collection efficiency of existing model. A new HFC based model with better collection efficiency is analyzed to get best integration mode advantages. The integration advantages shall remain unchanged as detailed in previous section but the current integration is designed for case V and new integration can support case VII also. The integrated model presented is also flexible and easy switching of integration modes can be done based on input and output constraints.

6.4.1 Variation of solar collector areas in all cases

The parameter such as collector and land area requirement shall vary with solar collector efficiency. The new area of collector and land requirement are tabulated below.
Table 6.8 Analytical results of solar collector area requirement in different cases.

Parameters	CASE I	CASE II	CASE III	CASE IV	CASE V	CASE VI	CASE VII
Collector area Required (Acres)	0.59	1.31	1.18	0.92	3.24	5.75	7.27
Land Area Required (Acres)	1.79	3.95	3.54	2.76	9.74	17.25	21.81

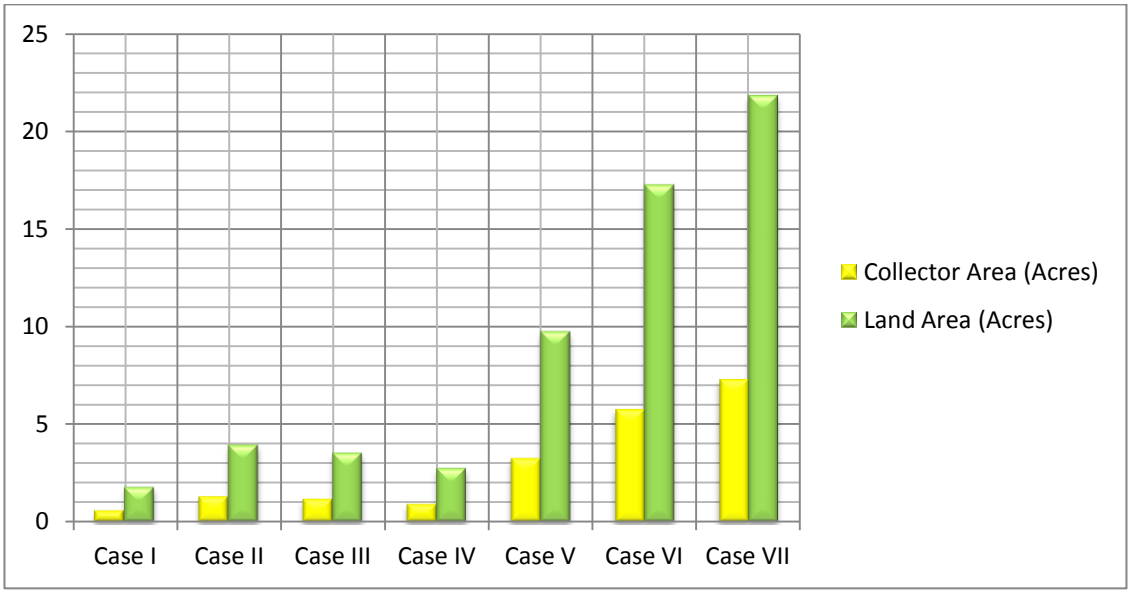

Fig. 6.9 Analytical Graphical Representation of solar collector area requirement in different cases.

The graph shown above represents the analytical results of solar collector and land area requirement for new model. It is less than the previous model. This clearly shows that more heat is available here with lesser area requirement.

6.4.2 Optimal Area of Solar Collector at Different Solar Irradiances

The analytical result of EES model for optimal area of solar collector required are tabulated below. The significant reduction in area is evident here.

Table 6.9 Optimal area of solar collector at different values of solar irradiance

Solar Irradiance (kW/m^2)	Optimal Area of Solar Collector (Acres)						
	CASE I	CASE II	CASE III	CASE IV	CASE V	CASE VI	CASE VII
0.09	0.11	0.26	0.23	0.18	0.64	1.15	1.45
0.11	0.09	0.21	0.19	0.15	0.53	0.94	1.19
0.13	0.08	0.18	0.16	0.12	0.44	0.79	1.00
0.15	0.07	0.15	0.14	0.11	0.38	0.69	0.87

0.17	0.06	0.13	0.12	0.09	0.34	0.60	0.76
0.19	0.05	0.12	0.11	0.08	0.30	0.54	0.68
0.21	0.05	0.11	0.10	0.07	0.27	0.49	0.62
0.23	0.04	0.10	0.09	0.07	0.25	0.45	0.56
0.25	0.04	0.09	0.08	0.06	0.23	0.41	0.52
0.27	0.03	0.08	0.07	0.06	0.21	0.38	0.48

The graph plotted in fig. 6.10 shows that the solar collector of lesser area are sufficient at higher solar irradiances.

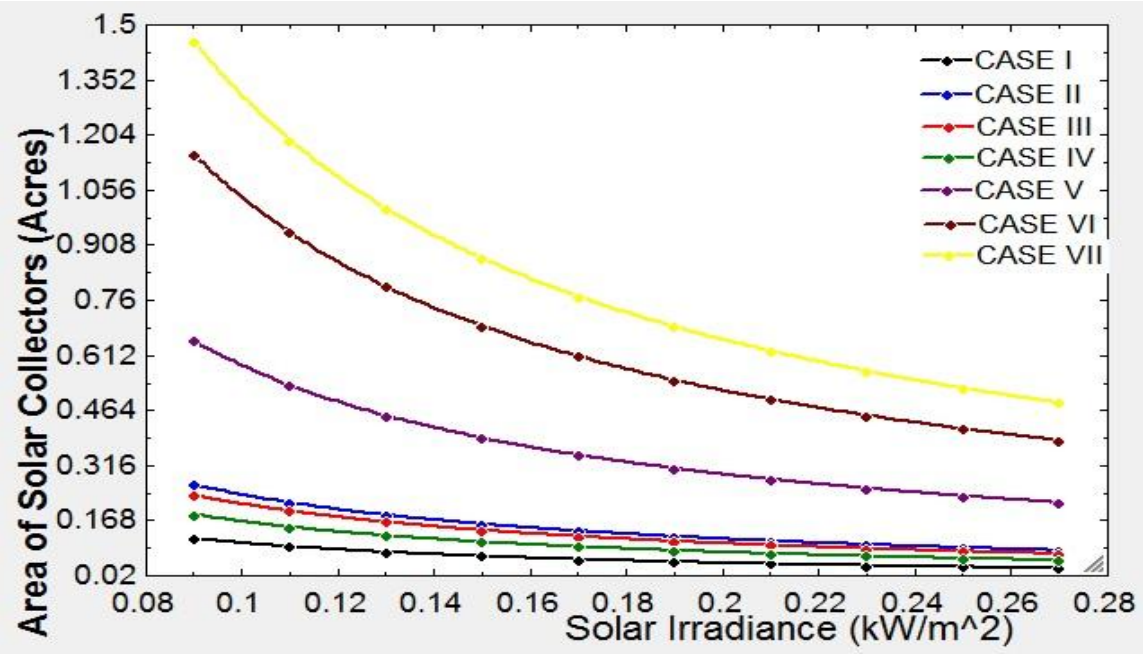

Fig. 6.10 Trends of optimal solar collector areas at different solar irradiances.

6.4.3 Analytical Storage Integration Results

As discussed in previous section that the area requirements in new model are lesser than the existing model. This provides land area availability for adding thermal storage to solar integrated model. To aid the benefits of solar thermal storage, a storage model of ten hours of supply is integrated analytically. The analytical integration results

of EES model are presented in table below. The mass of salt required and volume of storage tanks are calculated.

Table 6.10 Results of storage dimension and other calculations

Parameters	Values
Mass of Salt Required (kg)	9525.38
Peak Thermal Storage in the tank (kJ)	381397
Storage Time (hours)	10
Volume of Hot Tank (m^3)	43.46
Volume of Cold Tank (m^3)	45.45

6.5 SIMULATION RESULTS OF HFC BASED MODEL

The heliostat based model is simulated on SAM software that is freely accessible to NREL website for research simulation uses. The various results are presented and discussed below. This software works on location co-ordinates for weather data fetching.

6.5.1 Heliostat Field Simulation Results

The heliostat field is simulated on SAM with basic collector model and optimized collector model. The base case and optimized results of the heliostat arrangement in the solar field is compared in table 6.8 below.

Table 6.11 Optimization of heliostat field at area available

Parameter	Units	Base value	Optimized Value
Receiver Height	m	21.60	5.97
Receiver Diameter	m	17.65	3.65
Tower Height	m	193.45	50.53
Heliostat Count		210	581

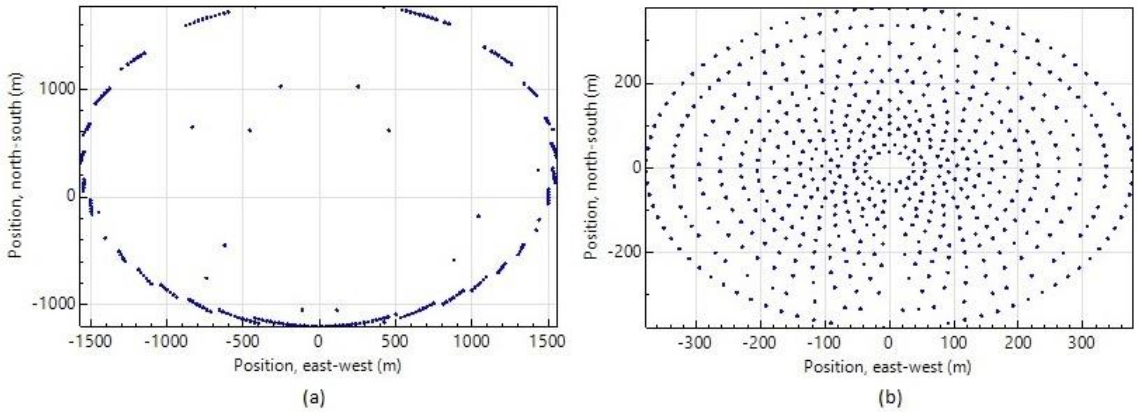

Fig. 6.11 (a) Simulation results of heliostat field. (b) Optimized simulation results of heliostat field.

Fig. 6.11 shows that using the same area, there is possibility of optimization of solar collector arrangement. The new arrangement can have higher number of collectors for improved heat collection.

6.5.2 Solar Thermal Simulation Results

The various trends of solar thermal simulation per MW of electricity integrating HFC is shown below in different graphs. These graphs are based on annual profile of study.

6.5.2.1 Solar Resource Beam Normal Irradiance (W/m^2)

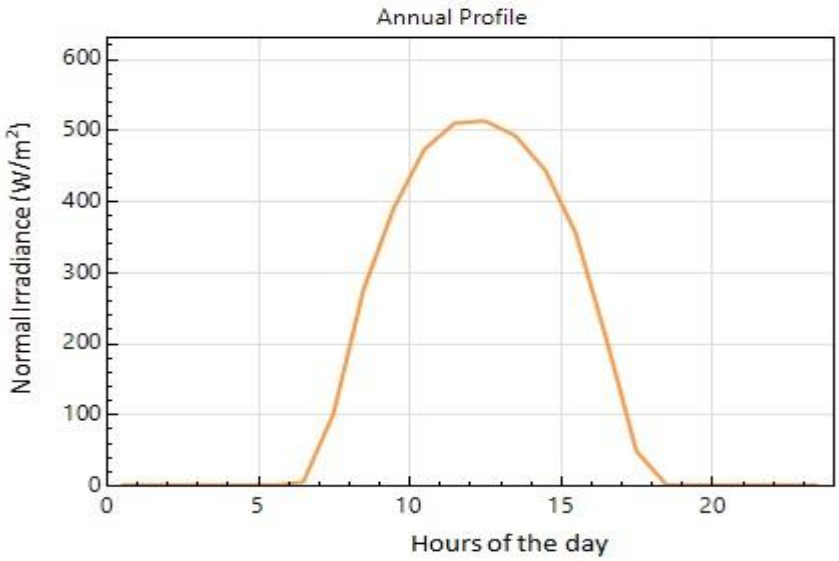

Fig. 6.12 Solar normal irradiation based on location co-ordinate at different hours

The solar irradiance available at the location on hourly basis is shown in fig. 6.12 in the result below. The graph shows that irradiance value is at peak between 10 am to 3 pm at plant location.

6.5.2.2 Receiver Thermal Efficiency

The thermal efficiency of receiver is shown at different hours of day. The graph shows steep drop in receiver thermal efficiency just around reaching the 3 pm of day. It is due to increased convective and radiation losses and reduced collection efficiency at higher temperatures.

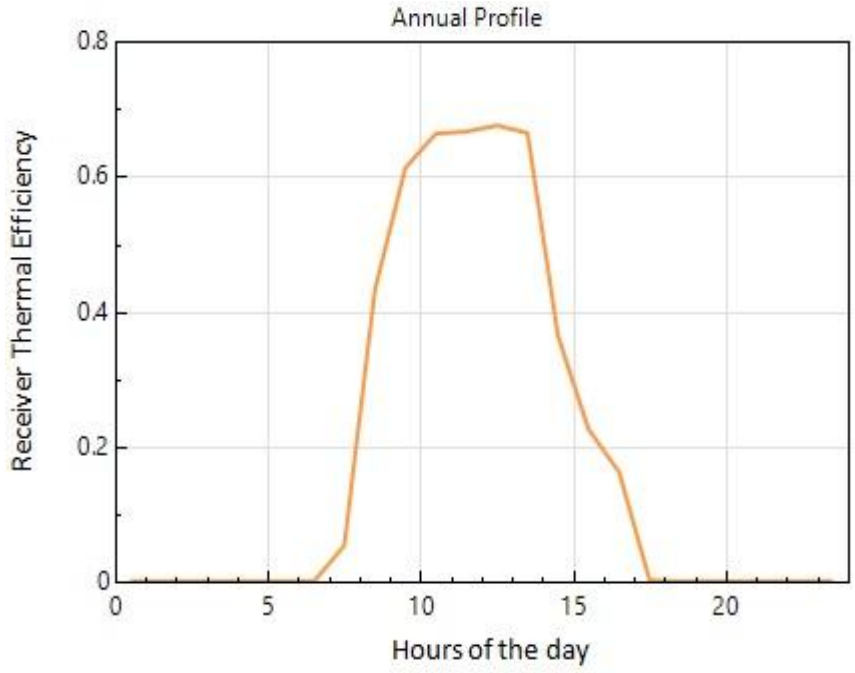

Fig. 6.13 Recever thermal efficiency at different hours of day

6.5.2.3 Outlet Temperature of HTF

The outlet temperature of HTF is having similar trend as receiver thermal efficiency as the heat received at receiver is taken by fluid and hence it drops as the receiver thermal efficiency drops.

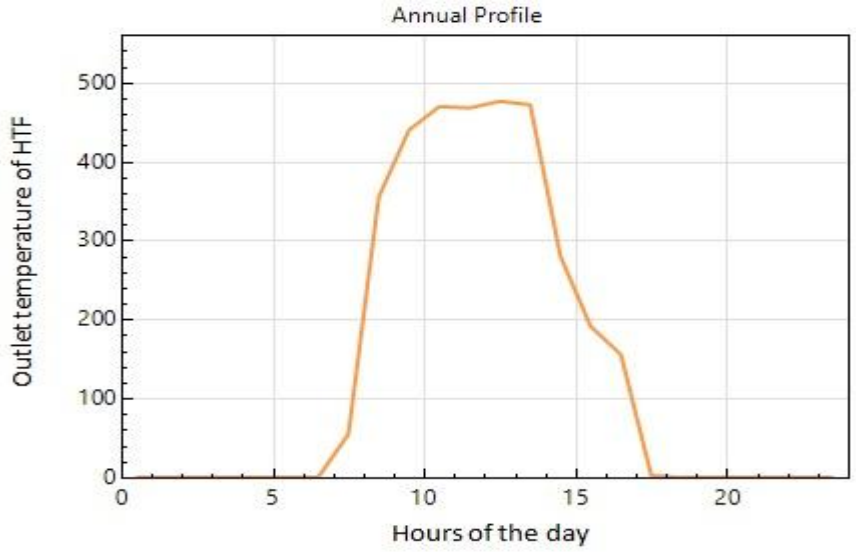

Fig. 6.14 Outlet temperature of high temperature fluid at different hours of day

6.5.2.4 TES Charge and Discharge Thermal Power

The thermal storage simulation results are presented for both charging and discharging case in fig. 6.15 shown below. The charging rate is higher after 7 am and is continued approximately up to 4 pm. After this time there is rapid discharge of stored heat and it drops to zero after completion of storage time of 10 hours.

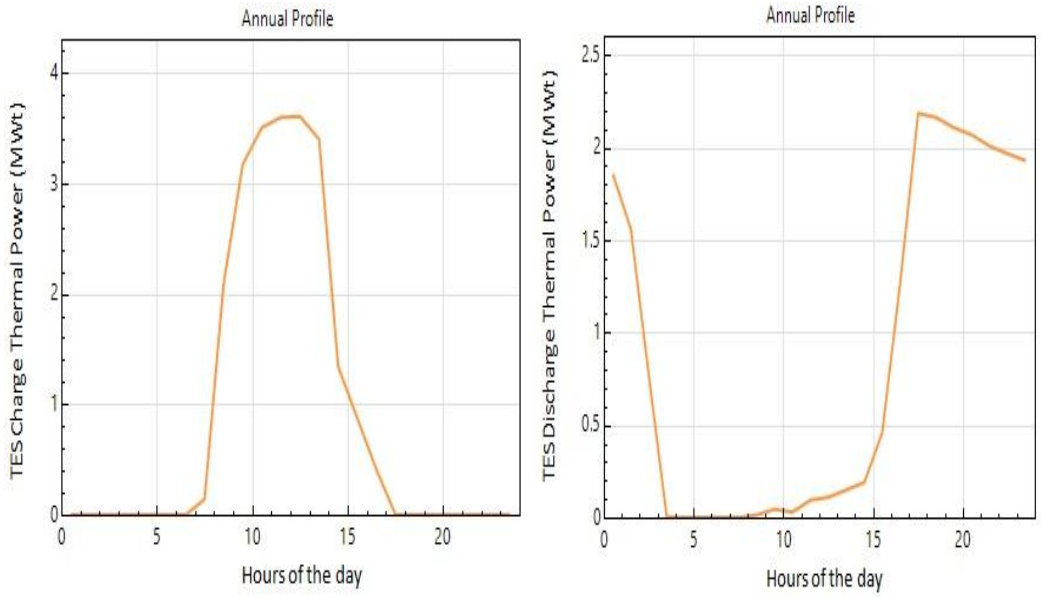

Fig. 6.15 (a and b) Thermal energy storage charging and discharging thermal power availability.

6.4.2.5 Most Optimal Hours of the Day

The profile to summaries simulation of integrated model is presented at last. It shows a continuous availability of maximized output for six hours and integration option availability for day and night duration. Fig. 6.16 presents the same. The delivery of different output factors are comparatively studied to get the most beneficial hours of the day.

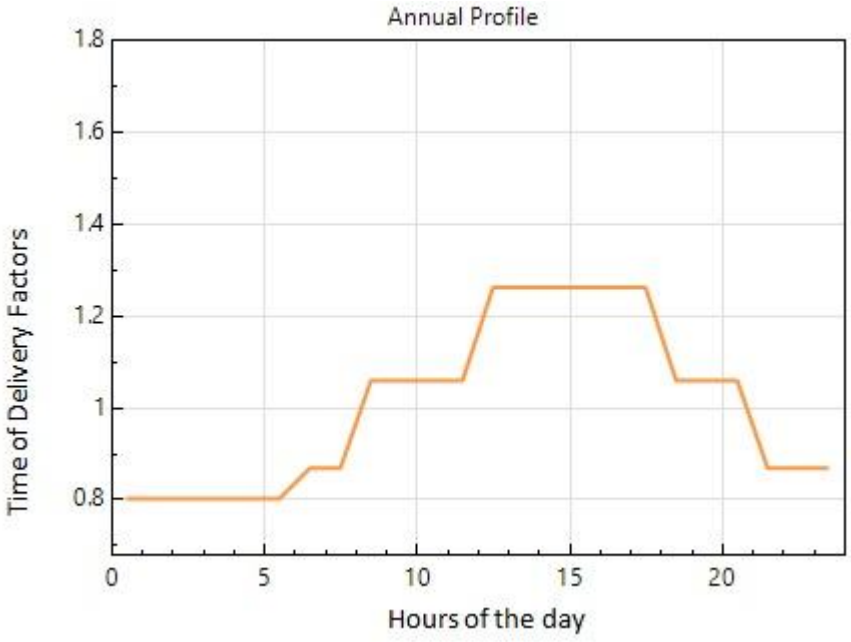

Fig. 6.16 Time of delivery of integrated system at different hours

CHAPTER 7

CONCLUSION AND FORTHCOMMING OUTLOOK TO THE ANALYSIS

7.1 CONCLUSION

The modern day electricity consumption is rising rapidly. The need to boost the electricity production with environmental friendliness is the most important challenge before modern power engineers. The ongoing research in numerous fields associated with electrical power production, distribution and consumption is aimed at maximizing production and minimizing losses and consumption without neglecting environmental front. The solar integration of a power production project is one such attempt. It is not only increase production but also minimizes environmental losses. The challenges in integrating solar energy to thermal power station are concluded in fig. 7.1 below;

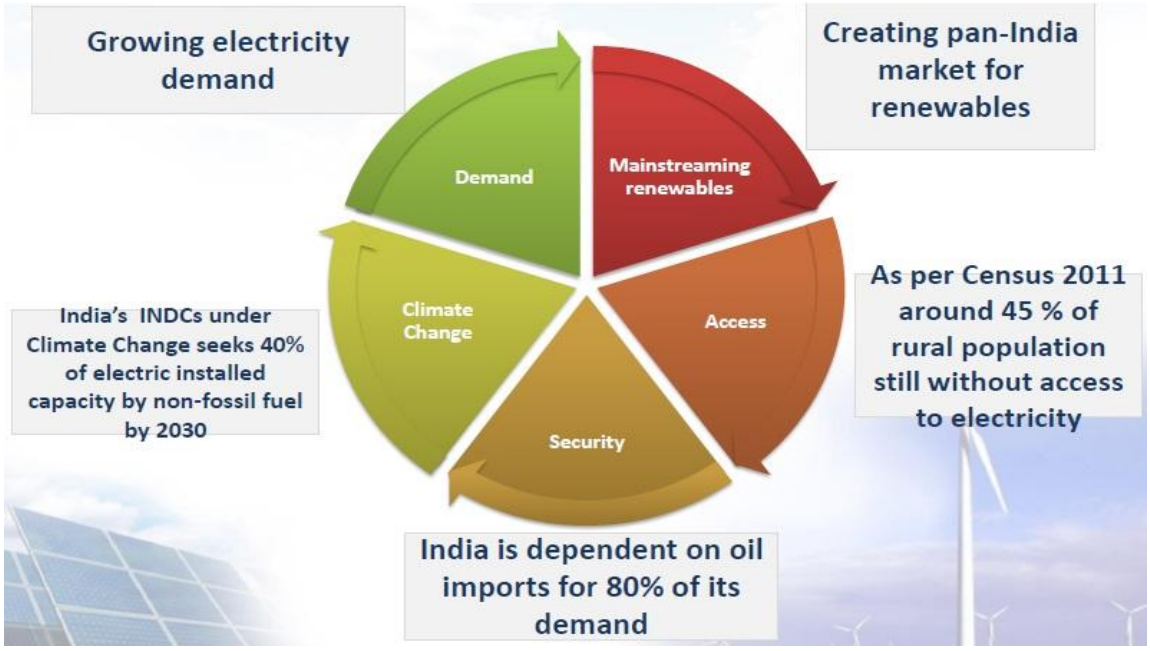

Fig. 7.1 solar thermal integration challenges [9].

The steam power plant solar integration can be done in many ways detailed in this project. One such method is to replace feed water heaters of a regenerative steam power plant with solar heating system. This is the most recent scheme and requites least modification in existing plant. It is also very flexible integration scheme as the control systems provide methods to operate plant in solar integrated mode as well as base mode.

Also the method detailed in this dissertation involves many possible configurations with their respective analysis. This analysis is done based on two methods; analytical method and simulation method. The analysis is performed by formulating entire case and then analyzing it with data available with on Engineering Equation Solver (EES) software. The concept of solar thermal energy storage to increase the overall efficiency of the integrated model is also introduced and analyzed. This model is then simulated in System Analyzer Model (SAM) software to get the trend analysis results of the project. The trends obtained in this analysis are presented in the results section of this report.

The integrated solar thermal power plant, Dadri is chosen as the base model of this work. The solar thermal integration at this plant is based on Compact Linear Fresnel Reflector (CLFR) Technology. In this work the CLFR is replaced with Heliostat Field Collector (HFC). This model is having higher solar thermal collection efficiency as well as more heat available to aid the steam cycle. The solar thermal storage addition had added system ability to operate with integrated mode for a longer duration. Talking to the environmental front, the emission of carbon dioxide and sulphur dioxide is reduced in the integrated mode as obtained from the analysis results. The other pollutants are also assumed to be reduced in the same pattern. In economical terms, hourly coal saving in different integration modes is provided. This shows the economical benefits of the project. Carbon dioxide emission reduction will save carbon tax as well.

The optimal solar integration data includes:

- Reduced steam consumption from 622.8 (Ton/hr) to 465.5 (Ton/hr) at peak load in main cycle.
- Reduced coal consumption from 135 (Ton/hr) to 109.8 (Ton/hr).

- Increase in energy efficiency of plant from 42.2% to 52.1%.
- Reduced land area required as 19.5 acres in base case with one FWH replacement mode to 21.81 acres in all FWH replacement mode of new model.
- Reduced carbon dioxide emission from 0.93 (kg/kWh) to 0.76 (kg/kWh).
- Reduced sulphur dioxide production from 0.0069 (kg/kWh) to 0.0056 (kg/kWh).
- Addition of solar thermal storage for 10 hours of aided integrated operation.

Thus the benefits of such schemes are worth noting and further research should also be continued on the technology for betterment of existing results.

7.2 Future Scope

The betterment of a technology is a continuous process. In this project also a detailed component level analysis with computational simulation is to be studied in future. Such an analysis shall help in component level optimization and also the entire scheme optimization.

The future scope of work can be pointed out as below:

- Simulation of base case at variable mass flow rate for solar integrated condition.
- Solar field analysis and simulation based solar cycle using TRANSYS or other simulation software.
- CFD analysis of storage to optimize the dimensions of storage.
- Entire integrated plant cycle simulation and optimization.

REFERENCES

[1] https://www.hindustantimes.com/business-news/india-is-world-s-sixth-largest-economy-at-2-6-trillion-says-imf/story-7wXZPXSWlvvImlAvpLKeNL.html (Updated: Apr 19, 2018 10:40 IST) (Retrieved May 1, 2018.)

[2] https://www.business-standard.com/article/economy-policy/now-india-is-the-third-largest-electricity-producer-ahead-of-russia-japan-118032600086_1.html (Updated at March 26, 2018 08:48 IST) (Retrieved April 8, 2018)

[3] https://powermin.nic.in/en/content/power-sector-glance-all-india (Retrieved May 2, 2018)

[4] Raghuvanshi, S. P., Chandra, A., & Raghav, A. K. (2006). Carbon dioxide emissions from coal based power generation in India. Energy Conversion and Management, 47(4), 427-441.

[5] https://www.hitachi.com/environment/showcase/solution/energy/coal_thermal_power.html (Retrieved March 2, 2018)

[6] Mittal, M. L., Sharma, C., & Singh, R. (2012, August). Estimates of emissions from coal fired thermal power plants in India. In 2012 International emission inventory conference (pp. 13-16).

[7] Mishra, U. C. (2004). Environmental impact of coal industry and thermal power plants in India. Journal of environmental radioactivity, 72(1-2), 35-40.

[8] http://www.ren21.net/wp-content/uploads/2018/06/17-8652_GSR2018_FullReport_web_-1.pdf (Retrieved June 3, 2018)

[9] Maithni, P.C., (2015). Renewable energy development in India, World Energy Outlook, IEA.

[10] https://mnre.gov.in/sites/default/files/uploads/Tentative-State-wise-break-up-of-Renewable-Power-by-2022.pdf (Retrieved April 12, 2018)

[11] Central Electricity Authority, (2017) Plan for integration of 175 GW RE capacity in the Indian Grid, International O&M Conference, IPS

[12] Sharma, B.D., (2011). Performance of solar power plants in India. Central Electricity Regulatory Commission, CERC.

[13] Mahtta, R., Joshi, P. K., & Jindal, A. K. (2014). Solar power potential mapping in India using remote sensing inputs and environmental parameters. Renewable Energy,

71, 255-262.

[14] Sengupta, S., Datta, A., & Duttagupta, S. (2007). Exergy analysis of a coal-based 210 MW thermal power plant. International Journal of Energy Research, 31(1), 14-28.

[15] Hashimoto, T., Tanaka, Y., Hokano, M., & Hirasaki, D. (2008). Latest technology of highly efficient coal-fired thermal power plants and future prospects. Mitsubishi Heavy Industries Technical Review, 45(1).

[16] Graus, W., & Worrell, E. (2011). Methods for calculating CO2 intensity of power generation and consumption: A global perspective. Energy Policy, 39(2), 613-627.

[17] Coal Industry Advisory Board, (2010) Power generation from coal, IEA.

[18] Murehwa, G., Zimwara, D., Tumbudzuku, W., & Mhlanga, S. (2012). Energy efficiency improvement in thermal power plants. International Journal of Innovative Technology and Exploring Engineering, 2, 20-25.

[19] Geete, A., & Khandwawala, A. I. (2013). Thermodynamic analysis of 120 MW thermal power plant with combined effect of constant inlet pressure (124.61 bar) and different inlet temperatures. Case Studies in Thermal Engineering, 1(1), 17-25.

[20] Kumar, R., Sharma, A. K., & Tewari, P. C. (2014). Thermal performance and economic analysis of 210 MWe coal-fired power plant. Journal of Thermodynamics.

[21] Wu, X., Shen, J., Li, Y., & Lee, K. Y. (2015). Steam power plant configuration, design, and control. Wiley Interdisciplinary Reviews: Energy and Environment, 4(6), 537-563.

[22] Satish, V., Raju, V.D. (2016). Energy and exergy analysis of thermal power plant, IJESC, 8(6), 2636-2644.

[23] Buckley, T. (2017). NTPC as a force in India's electricity transition, IEEFA.

[24] Schesack, M. (2017). Flexibility case study at Dadri and Simhadri boiler, combustion and coal, Steag, IGEF.

[25] Sutrakar, A. K., Dhingra, D. (2018). Combustion of co-firing biomass with pulverized coal in NTPC power plant, NTPC Energy Technology Research Alliance.

[26] https://mnre.gov.in/ (Retrieved Jun 15, 2018)

[27] Solar Thermal Power Plants, (2013). BINE-Themeninfo II/2013, DLR, 1610-8302

[28] Feuermann, D., & Gordon, J. M. (1991). Analysis of a two-stage linear Fresnel

reflector solar concentrator. Journal of solar energy engineering, 113(4), 272-279.

[29] Kalogirou, S. A. (2004). Solar thermal collectors and applications. Progress in energy and combustion science, 30(3), 231-295.

[30] Ho, C. K. (2008). Software and codes for analysis of concentrating solar power technologies (No. SAND2008-8053). Sandia National Laboratories.

[31] Fan, J., Chen, Z., Furbo, S., Perers, B., & Karlsson, B. (2009, October). Efficiency and lifetime of solar collectors for solar heating plants. In 29th ISES Biennial Solar World Congress.

[32] Nixon, J. D., Dey, P. K., & Davies, P. A. (2010). Which is the best solar thermal collection technology for electricity generation in north-west India? Evaluation of options using the analytical hierarchy process. Energy, 35(12), 5230-5240.

[33] Manikumar, R., & Arasu, A. V. (2012). Design and theoretical performance analysis of linear Fresnel reflector solar concentrator with a tubular absorber. International Journal of Renewable Energy Technology, 3(3), 221-236.

[34] Zhu, G., Wendelin, T., Wagner, M. J., & Kutscher, C. (2014). History, current state, and future of linear Fresnel concentrating solar collectors. Solar Energy, 103, 639-652.

[35] Montes, M. J., Rubbia, C., Abbas, R., & Martínez-Val, J. M. (2014). A comparative analysis of configurations of linear Fresnel collectors for concentrating solar power. Energy, 73, 192-203.

[36] McGovern, R. K., & Smith, W. J. (2012). Optimal concentration and temperatures of solar thermal power plants. Energy conversion and management, 60, 226-232.

[37] Gakkhar, N., & Soni, M. S. (2014). Techno-economic parametric assessment of CSP power generations technologies in India. Energy Procedia, 54, 152-160.

[38] Ahmed, M. H., & Amin, A. M. (2016). Thermal Analysis of the Performance of Linear Fresnel Solar Concentrator. Journal of Clean Energy Technologies, 4(5).

[39] Tikariha, M. K. ,Gupta, K.V. S. S., (2018). Solar energy forecasting- A pathway for successful renewable energy integration, Indian Power Sector (IPS)

[40] Mills, D. R., & Morrison, G. L. (2000). Compact linear Fresnel reflector solar thermal powerplants. Solar energy, 68(3), 263-283.

[41] Suresh, M. V. J. J., Reddy, K. S., & Kolar, A. K. (2010). 4-E (Energy, Exergy, Environment, and Economic) analysis of solar thermal aided coal-fired power plants. Energy for sustainable development, 14(4), 267-279.

[42] Popov, D. (2011). An option for solar thermal repowering of fossil fuel fired power plants. Solar Energy, 85(2), 344-349.

[43] Patel, V., Saha, B., & Chatterjee, K. (2014, December). Fuel saving in coal-fired power plant with augmentation of solar energy. In Power, Control and Embedded Systems (ICPCES), 2014 International Conference on (pp. 1-5). IEEE.

[44] Zhai, R., Zhu, Y., Yang, Y., Tan, K., & Hu, E. (2013). Exergetic and parametric study of a solar aided coal-fired power plant. Entropy, 15(3), 1014-1034.

[45] Peterseim, J. H., White, S., Tadros, A., & Hellwig, U. (2013). Concentrated solar power hybrid plants, which technologies are best suited for hybridization?. Renewable Energy, 57, 520-532.

[46] Junjie, W., Hongjuan, H., & Yongping, Y. (2014). Research on the performance of coal-fired power system integrated with solar energy. Energy Procedia, 61, 791-794.

[47] Zhao, H., & Bai, Y. (2014). Thermodynamic performance analysis of the coal-fired power plant with solar thermal utilizations. International Journal of Energy Research, 38(11), 1446-1456.

[48] Zhao, Y., Hong, H., & Jin, H. (2014). Evaluation criteria for enhanced solar–coal hybrid power plant performance. Applied Thermal Engineering, 73(1), 577-587.

[49] Van Rooy, W. L., & Storm, C. P. (2015). Solar augmentation at supercritical coal-fired power stations. 3rd Southern African Solar Energy Conference, South Africa, 11-13 May, 2015.

[50] Zhai, R., Zhao, M., Tan, K., & Yang, Y. (2015). Optimizing operation of a solar-aided coal-fired power system based on the solar contribution evaluation method. Applied Energy, 146, 328-334.

[51] Khana, N. H., Jamala, R., Awanb, W. Q., & Rajac, M. A. Z. (2016). 168. Design of Solar Coal Hybrid Power Plant: Techno-economic Analysis.

[52] Qin, J., Hu, E., & Nathan, G. J. (2016). The performance of a Solar Aided Power Generation plant with diverse “configuration-operation” combinations. Energy

Conversion and Management, 124, 155-167.

[53] Feng, L., Chen, H., Zhou, Y., Zhang, S., Yang, T., & An, L. (2016). The development of a thermo-economic evaluation method for solar aided power generation. Energy Conversion and Management, 116, 112-119.

[54] Duan, L., Yu, X., Jia, S., Wang, B., & Zhang, J. (2017). Performance analysis of a tower solar collector-aided coal-fired power generation system. Energy Science & Engineering, 5(1), 38-50.

[55] Ahmadi, G., Toghraie, D., & Akbari, O. A. (2017). Solar parallel feed water heating repowering of a steam power plant: a case study in Iran. Renewable and Sustainable Energy Reviews, 77, 474-485.

[56] Qin, J., Hu, E., & Nathan, G. J. (2017). Impact of the operation of non-displaced feedwater heaters on the performance of Solar Aided Power Generation plants. Energy Conversion and Management, 135, 1-8.

[57] Zhong, W., Chen, X., Zhou, Y., Wu, Y., & López, C. (2017). Optimization of a solar aided coal-fired combined heat and power plant based on changeable integrate mode under different solar irradiance. Solar Energy, 150, 437-446.

[58] Zhao, Y., Hong, H., & Jin, H. (2017). Optimization of the solar field size for the solar–coal hybrid system. Applied Energy, 185, 1162-1172.

[59] Bishoyi, D., & Sudhakar, K. (2017). Modeling and performance simulation of 100 MW LFR based solar thermal power plant in Udaipur India. Resource-Efficient Technologies, 3(4), 365-377.

[60] Behar, O. (2018). Solar thermal power plants–A review of configurations and performance comparison. Renewable and Sustainable Energy Reviews, 92, 608-627.

[61] Habibollahzade, A., Houshfar, E., Ashjaee, M., Behzadi, A., Gholamian, E., & Mehdizadeh, H. (2018). Enhanced power generation through integrated renewable energy plants: Solar chimney and waste-to-energy. Energy Conversion and Management, 166, 48-63.

[62] Zhu, Y., Pei, J., Cao, C., Zhai, R., Yang, Y., Reyes-Belmonte, M. A., ... & Romero, M. (2018). Optimization of solar aided coal-fired power plant layouts using multi-criteria assessment. Applied Thermal Engineering, 137, 406-418.

[63] Kuravi, S., Trahan, J., Goswami, D. Y., Rahman, M. M., & Stefanakos, E. K. (2013). Thermal energy storage technologies and systems for concentrating solar power plants. Progress in Energy and Combustion Science, 39(4), 285-319.

[64] Ravaghi-Ardebilli, Z., Maneti, F., Lima, N. M., & Zuniga Linan, L. (2013). Study of direct thermal energy storage technologies for effectiveness of concentrating solar power plants. The Italian Association of Chemical Engineering (AIDIC), 32.

[65] Steinmann, W. D. (2015). Thermal energy storage systems for concentrating solar power (CSP) technology. In Advances in Thermal Energy Storage Systems (pp. 511-531).

[66] [66] Nunes, V. M. B., Queirós, C. S., Lourenço, M. J. V., Santos, F. J. V., & de Castro, C. N. (2016). Molten salts as engineering fluids–a review: Part I. Molten alkali nitrates. Applied energy, 183, 603-611.

[67] Stutz, B., Le Pierres, N., Kuznik, F., Johannes, K., Del Barrio, E. P., Bédécarrats, J. P. & Mazet, N. (2017). Storage of thermal solar energy. Comptes Rendus Physique, 18(7), 401-414.

[68] Seitz, M., Johnson, M., & Hübner, S. (2017). Economic impact of latent heat thermal energy storage systems within direct steam generating solar thermal power plants with parabolic troughs. Energy Conversion and Management, 143, 286-294.

[69] Walczak, M., Pineda, F., Fernández, Á. G., Mata-Torres, C., & Escobar, R. A. (2018). Materials corrosion for thermal energy storage systems in concentrated solar power plants. Renewable and Sustainable Energy Reviews, 86, 22-44.

[70] Cáceres, G., Fullenkamp, K., Montané, M., Naplocha, K., & Dmitruk, A. (2017). Encapsulated Nitrates Phase Change Material Selection for Use as Thermal Storage and Heat Transfer Materials at High Temperature in Concentrated Solar Power Plants. Energies, 10(9), 1318.

[71] Rodat, S., Bavière, R., Bruch, A., & Camus, A. (2018). Dynamic simulation of a Fresnel solar power plant prototype with thermocline thermal energy storage. Applied Thermal Engineering, 135, 483-492.

[72] Zhao, B. C., Cheng, M. S., Liu, C., & Dai, Z. M. (2018). System-level performance optimization of molten-salt packed-bed thermal energy storage for concentrating

solar power. Applied Energy, 226, 225-239.

[73] Peiró, G., Prieto, C., Gasia, J., Jové, A., Miró, L., & Cabeza, L. F. (2018). Two-tank molten salts thermal energy storage system for solar power plants at pilot plant scale: Lessons learnt and recommendations for its design, start-up and operation. Renewable Energy, 121, 236-248.

[74] Kulshreshtha, A., (2013). Integration of Solar Thermal with Fossil Fuel Plant, Indian Power Sector (I.P.S.) Conference.

[75] Rajput, R. K., (2017). Power Plant Engineering, Laxmi Publications, New Delhi, India

[76] Raja, A. K., Srivastava, A. P., Dwivedi, M., (2016), Power Plant Engineering, New Age International Publications, New Delhi, India.

[77] Nag, P. K., (2017), Power Plant Engineering, McGraw-Hill Education, New Delhi, India.

[78] Nag, P. K., (2017), Engineering Thermodynamics, McGraw-Hill Education, New Delhi, India.

[79] Nag, P. K., (2017), Heat and Mass Transfer, McGraw-Hill Education, New Delhi, India

[80] http://indianpowersector.com/home/power-station/thermal-power-plant/ (Retrieved March 1, 2018)

[81] Goswami, D. Y., (2015). Principles of Solar Engineering, CRC Press, Taylor & Francis Group, Boca Raton London, New York

[82] Sukhatme, S. P., Sukhatme, K., (1996). Solar Energy: Principles of Thermal Collection and Storage, Tata McGraw-Hill Education, New Delhi, India.

[83] Sun Focus (2016), Magazine on Concentrated Solar Heat, Vol.4, Issue, 2, MNRE, GoI

[84] Pelay, U., Luo, L., Fan, Y., Stitou, D., & Rood, M. (2017). Thermal energy storage systems for concentrated solar power plants. Renewable and Sustainable Energy Reviews, 79, 82-100.

APPENDIX 1

1.1 EES Model of Base Case Analysis with Equivalent Coal Saving Calculations

```
$UnitSystem SI Pa K J Mass {Declaring unit system that we'll be using}
$TabStops 2 cm
{INPUTS}
f$ = 'Water'    {Water as working fluid}
T[1]=810.15 [K]
P[1]=15000000 [Pa]
s[1]=entropy(f$, T=T[1], P=P[1])
h[1]=enthalpy(f$, T=T[1], P=P[1])
s[1]=s[2]
s[1]=s[3]
T[4]=810.15 [K]
P[4]=3494000 [Pa]
s[4]=entropy(f$, T=T[4], P=P[4])
h[4]=enthalpy(f$, T=T[4], P=P[4])
s[4]=s[5]
s[4]=s[6]
s[4]=s[7]
s[4]=s[8]
s[4]=s[9]
s[4]=s[10]
s[4]=s[11]
s[4]=s[12]
T[2]=615.81 [K]
P[2]=3920000 [Pa]
h[2]=enthalpy(f$, T=T[2], P=P[2])
T[3]=615.81 [K]
P[3]=3920000 [Pa]
h[3]=enthalpy(f$, T=T[3], P=P[3])
T[5]=697.25 [K]
P[5]=1623000 [Pa]
h[5]=enthalpy(f$, T=T[5], P=P[5])
T[6]=580.46 [K]
P[6]=684000 [Pa]
h[6]=enthalpy(f$, T=T[6], P=P[6])
T[7]=580.46 [K]
P[7]=684000 [Pa]
h[7]=enthalpy(f$, T=T[7], P=P[7])
T[8]=580.46 [K]
P[8]=684000 [Pa]
h[8]=enthalpy(f$, T=T[8], P=P[8])
T[9]=465.35 [K]
P[9]=229900 [Pa]
h[9]=enthalpy(f$, T=T[9], P=P[9])
T[10]=433 [K]
P[10]=150000 [Pa]
h[10]=enthalpy(f$, T=T[10], P=P[10])
P[11]=21500 [Pa]
x[11]=0.9501
```

```
h_f[11]=258000 [J/kg] {specific enthalpy of saturated liquid}
h_g[11]=2612600 [J/kg] {specific enthalpy of saturated vapour}
h_fg[11]=h_g[11]-h_f[11]
h[11]=h_f[11]+x[11]*h_fg[11]
T[11]=temperature(f$, h=h[11], P=P[11])
P[12]=10300 [Pa]
x[12]=0.9275
h_f[12]=194170 [J/kg] {Specific enthalpy of saturated liquid}
h_g[12]=2585720 [J/kg] {Specific enthalpy of saturated vapour}
h_fg[12]=h_g[12]-h_f[12]
h[12]=h_f[12]+x[12]*h_fg[12]
T[12]=temperature(f$, h=h[12], P=P[12])
h[13]=h_f[12]
P[13]=P[12]
T[13]=temperature(f$, h=h[13], P=P[13])
s[13]=entropy(f$, h=h[13], P=P[13])
P[14]=1607000 [Pa]
v_f[13]= 0.001 {Specific volume of saturated liquid at pressure 10300 Pa}
h[14]=h[13]+v_f[13]*(P[14]-P[13])
T[14]=Temperature(f$, P=P[14], h=h[14])
s[14]=entropy(f$, h=h[14], P=P[14])
T[15]=334.705 [K]
P[15]=P[11]
h[15]=enthalpy(f$, P=P[15], T=T[15])
s[15]=entropy(f$, T=T[15], P=P[15])
h[16]=h[15]
T[16]=T[15]
P[16]=pressure(f$, h=h[16], T=T[16])
s[16]=entropy(f$, T=T[16], h=h[16])
T[17]=368 [K]
P[17]=P[10]
h[17]=enthalpy(f$, T=T[17], P=P[17])
s[17]=entropy(f$, T=T[17], P=P[17])
h[18]=h[17]
T[18]=T[17]
P[18]=pressure(f$, h=h[18], T=T[18])
s[18]=entropy(f$, T=T[18], h=h[18])
T[19]=397.836 [K]
P[19]=P[9]
h[19]=enthalpy(f$, T=T[19], P=P[19])
s[19]=entropy(f$, T=T[19], P=P[19])
h[20]=h[19]
T[20]=T[19]
P[20]=pressure(f$, h=h[20], T=T[20])
s[20]=entropy(f$, T=T[20], h=h[20])
T[21]=432.85 [K]
P[21]=615000 [Pa]
h[21]=enthalpy(f$, T=T[21], P=P[21])
s[21]=entropy(f$, T=T[21], P=P[21])
P[22]=17000000 [Pa]
v_f[21]=0.001 {Specific volume of saturated liquid at pressure 615000 Pa}
h[22]=h[21]+v_f[21]*(P[22]-P[21])
T[22]=Temperature(f$, P=P[22], h=h[22])
s[22]=entropy(f$, P=P[22], h=h[22])
```

T[23]=452.88[K]
P[23]=P[5]
h[23]=enthalpy(f$, T=T[23], P=P[23])
s[23]=entropy(f$, T=T[23], P=P[23])
h[24]=h[23]
T[24]=T[23]
P[24]=pressure(f$, h=h[24], T=T[24])
s[24]=entropy(f$, T=T[24], h=h[24])
T[25]=522.25 [K]
P[25]=P[2]
h[25]=enthalpy(f$, T=T[25], P=P[25])
s[25]=entropy(f$, T=T[25], P=P[25])
T[26]=518.13 [K]
P[26]=16800000 [Pa]
h[26]=enthalpy(f$, T=T[26], P=P[26])
s[26]=entropy(f$, T=T[26], P=P[26])
{Heater F}
m_1*(h[2]-h[25])=1*(h[26]-h[24])
{Heater E}
m_2*(h[5]-h[23])+m_1*(h[25]-h[23])=1*(h[24]-h[22])
{Heater D}
m_3*(h[7]-h[21])+(m_1+m_2)*(h[23]-h[21])=(1-m_1-m_2-m_3)*(h[21]-h[20])
{Heater C}
m_4*(h[9]-h[19])=(1-m_1-m_2-m_3)*(h[20]-h[18])
{Heater B}
m_5*(h[10]-h[17])+m_4*(h[19]-h[17])=(1-m_1-m_2-m_3-m_4-m_5)*(h[18]-h[16])
{Heater A}
m_6*(h[11]-h[15])+(m_4+m_5)*(h[17]-h[15])=(1-m_1-m_2-m_3-m_4-m_5-m_6)*(h[16]-h[14])
{Turbine Work}
W_T=1*(h[1]-h[2])+(1-m_1)*(h[2]-h[3])+(1-m_1)*(h[4]-h[5])+(1-m_1-m_2)*(h[5]-h[6])+(1-m_1-m_2-m_3)*(h[8]-h[9])+(1-m_1-m_2-m_3-m_4)*(h[9]-h[10])+(1-m_1-m_2-m_3-m_4-m_5)*(h[10]-h[11])+(1-m_1-m_2-m_3-m_4-m_5-m_6)*(h[11]-h[12])
{Drip Pump 1 Work}
W_D1=0.001*(P[25]-P[23])
{Drip Pump 2 Work}
W_D2=0.001*(P[19]-P[17])
{Drip Pump 3 Work}
W_D3=0.001*(P[17]-P[15])
{Drip Pump 4 Work}
W_D4=0.001*(P[15]-P[13])
{Net Pump Work}
W_P=(h[14]-h[13])+(h[22]-h[21])+W_D1+W_D2+W_D3+W_D4
{Net Work Done}
W_Net=W_T-W_P
{Heat Input}
Q=1*(h[1]-h[26])+(1-m_1)*(h[4]-h[3])
{Cycle Eficiency}
eta_Cycle=W_Net/Q
c=1 [Kcal/kg] {Specific heat of water}
CV_G=3620[Kcal/kg] {Gross Calorific Value of coal}
{The amount of heat Q_A and coal F_A to be saved in the boiler if Low Pressure heater A is to be replaced by the Solar Field}
m[14]=496.54 [Ton/hr] {Weight of feed water}
Q_A=m[14]*c*(T[16]-T[14])
F_A=Q_A/CV_G

{The amount of heat Q_B and coal F_B to be saved in the boiler if Low Pressure heater B is to be replaced by the Solar Field}
m[16]=496.54 [Ton/hr] {Weight of feed water}
Q_B=m[16]*c*(T[18]-T[16])
F_B=Q_B/CV_G
{The amount of heat Q_C and coal F_C to be saved in the boiler if Low Pressure heater C is to be replaced by the Solar Field}
m[18]=496.54 [Ton/hr] {Weight of feed water}
Q_C=m[18]*c*(T[20]-T[18])
F_C=Q_C/CV_G
{The amount of heat Q_E and coal F_E to be saved in the boiler if High Pressure heater E is to be replaced by the Solar Field}
m[22]=623.798 [Ton/hr] {Weight of feed water}
Q_E=m[22]*c*(T[24]-T[22])
F_E=Q_E/CV_G
{The amount of heat Q_F and coal F_F to be saved in the boiler if High Pressure heater F is to be replaced by the Solar Field}
m[24]=623.798 [Ton/hr] {Weight of feed water}
Q_F=m[24]*c*(T[26]-T[24])
F_F=Q_F/CV_G

1.2 EES Model of Variation of Inlet Solar Energy with Variation of Solar Irradiances in all Cases for CLFR/HFC

"Variation of inlet solar energy with the variation of solar irradiation in all cases"
eta_c=36/72 {Percentage solar collector efficiency in all cases}
S_d=0.18 [KW/m^2] {Average annual solar irradiance at plant location based on DNI data}
s_d1=0.09 [KW/m^2] {Minimum solar irradiance at plant location based on DNI data}
s_d2=0.11 [KW/m^2] {Typical value of solar irradiance at plant location based on DNI data}
s_d3=0.13 [KW/m^2] {Typical value of solar irradiance at plant location based on DNI data}
s_d4=0.15 [KW/m^2] {Typical value of solar irradiance at plant location based on DNI data}
s_d5=0.17 [KW/m^2] {Typical value of solar irradiance at plant location based on DNI data}
s_d6=0.19 [KW/m^2] {Typical value of solar irradiance at plant location based on DNI data}
s_d7=0.21 [KW/m^2] {Typical value of solar irradiance at plant location based on DNI data}
s_d8=0.23 [KW/m^2] {Typical value of solar irradiance at plant location based on DNI data}
s_d9=0.25 [KW/m^2] {Typical value of solar irradiance at plant location based on DNI data}
s_d10=0.27 [KW/m^2] {Maximum solar irradiance at plant location based on DNI data}
{Case I}
Q_I=31455.4284 [KJ] {Heat required at heater A}
A_CI=Q_I/(S_d*eta_c) {Collector area in case I at average annual solar irrdiance}
SH_I1=A_CI*eta_c*s_d1 {Inlet solar heat at given solar irradiance}
SH_I2=A_CI*eta_c*s_d2 {Inlet solar heat at given solar irradiance}
SH_I3=A_CI*eta_c*s_d3 {Inlet solar heat at given solar irradiance}
SH_I4=A_CI*eta_c*s_d4 {Inlet solar heat at given solar irradiance}
SH_I5=A_CI*eta_c*s_d5 {Inlet solar heat at given solar irradiance}
SH_I6=A_CI*eta_c*s_d6 {Inlet solar heat at given solar irradiance}
SH_I7=A_CI*eta_c*s_d7 {Inlet solar heat at given solar irradiance}
SH_I8=A_CI*eta_c*s_d8 {Inlet solar heat at given solar irradiance}
SH_I9=A_CI*eta_c*s_d9 {Inlet solar heat at given solar irradiance}
SH_I10=A_CI*eta_c*s_d10 {Inlet solar heat at given solar irradiance}

{Case II}
Q_II=69216.1776 [KJ] {Heat required at heater B}

A_CII=Q_II/(S_d*eta_c) {Collector area in case II at average annual solar irrdiance}
SH_II1=A_CII*eta_c*s_d1 {Inlet solar heat at given solar irradiance}
SH_II2=A_CII*eta_c*s_d2 {Inlet solar heat at given solar irradiance}
SH_II3=A_CII*eta_c*s_d3 {Inlet solar heat at given solar irradiance}
SH_II4=A_CII*eta_c*s_d4 {Inlet solar heat at given solar irradiance}
SH_II5=A_CII*eta_c*s_d5 {Inlet solar heat at given solar irradiance}
SH_II6=A_CII*eta_c*s_d6 {Inlet solar heat at given solar irradiance}
SH_II7=A_CII*eta_c*s_d7 {Inlet solar heat at given solar irradiance}
SH_II8=A_CII*eta_c*s_d8 {Inlet solar heat at given solar irradiance}
SH_II9=A_CII*eta_c*s_d9 {Inlet solar heat at given solar irradiance}
SH_II10=A_CII*eta_c*s_d10 {Inlet solar heat at given solar irradiance}
{Case III}
Q_III=62027.442 [KJ] {Heat required at heater C}
A_CIII=Q_III/(S_d*eta_c) {Collector area in case III at average annual solar irrdiance}
SH_III1=A_CIII*eta_c*s_d1 {Inlet solar heat at given solar irradiance}
SH_III2=A_CIII*eta_c*s_d2 {Inlet solar heat at given solar irradiance}
SH_III3=A_CIII*eta_c*s_d3 {Inlet solar heat at given solar irradiance}
SH_III4=A_CIII*eta_c*s_d4 {Inlet solar heat at given solar irradiance}
SH_III5=A_CIII*eta_c*s_d5 {Inlet solar heat at given solar irradiance}
SH_III6=A_CIII*eta_c*s_d6 {Inlet solar heat at given solar irradiance}
SH_III7=A_CIII*eta_c*s_d7 {Inlet solar heat at given solar irradiance}
SH_III8=A_CIII*eta_c*s_d8 {Inlet solar heat at given solar irradiance}
SH_III9=A_CIII*eta_c*s_d9 {Inlet solar heat at given solar irradiance}
SH_III10=A_CIII*eta_c*s_d10 {Inlet solar heat at given solar irradiance}
{Case IV}
Q_IV=48282.1776 [KJ] {Heat required at heater E}
A_CIV=Q_IV/(S_d*eta_c) {Collector area in case IV at average annual solar irrdiance}
SH_IV1=A_CIV*eta_c*s_d1 {Inlet solar heat at given solar irradiance}
SH_IV2=A_CIV*eta_c*s_d2 {Inlet solar heat at given solar irradiance}
SH_IV3=A_CIV*eta_c*s_d3 {Inlet solar heat at given solar irradiance}
SH_IV4=A_CIV*eta_c*s_d4 {Inlet solar heat at given solar irradiance}
SH_IV5=A_CIV*eta_c*s_d5 {Inlet solar heat at given solar irradiance}
SH_IV6=A_CIV*eta_c*s_d6 {Inlet solar heat at given solar irradiance}
SH_IV7=A_CIV*eta_c*s_d7 {Inlet solar heat at given solar irradiance}
SH_IV8=A_CIV*eta_c*s_d8 {Inlet solar heat at given solar irradiance}
SH_IV9=A_CIV*eta_c*s_d9 {Inlet solar heat at given solar irradiance}
SH_IV10=A_CIV*eta_c*s_d10 {Inlet solar heat at given solar irradiance}
{Case V}
Q_V=170415.3204 [KJ] {Heat required at heater F}
A_CV=Q_V/(S_d*eta_c) {Collector area in case V at average annual solar irrdiance}
SH_V1=A_CV*eta_c*s_d1 {Inlet solar heat at given solar irradiance}
SH_V2=A_CV*eta_c*s_d2 {Inlet solar heat at given solar irradiance}
SH_V3=A_CV*eta_c*s_d3 {Inlet solar heat at given solar irradiance}
SH_V4=A_CV*eta_c*s_d4 {Inlet solar heat at given solar irradiance}
SH_V5=A_CV*eta_c*s_d5 {Inlet solar heat at given solar irradiance}
SH_V6=A_CV*eta_c*s_d6 {Inlet solar heat at given solar irradiance}
SH_V7=A_CV*eta_c*s_d7 {Inlet solar heat at given solar irradiance}
SH_V8=A_CV*eta_c*s_d8 {Inlet solar heat at given solar irradiance}
SH_V9=A_CV*eta_c*s_d9 {Inlet solar heat at given solar irradiance}
SH_V10=A_CV*eta_c*s_d10 {Inlet solar heat at given solar irradiance}
{Case VI}
Q_VI=301658.940 [KJ] {Heat required at heater F+C+B}
A_CVI=Q_VI/(S_d*eta_c) {Collector area in case VI at average annual solar irrdiance}
SH_VI1=A_CVI*eta_c*s_d1 {Inlet solar heat at given solar irradiance}
SH_VI2=A_CVI*eta_c*s_d2 {Inlet solar heat at given solar irradiance}

SH_VI3=A_CVI*eta_c*s_d3 {Inlet solar heat at given solar irradiance}
SH_VI4=A_CVI*eta_c*s_d4 {Inlet solar heat at given solar irradiance}
SH_VI5=A_CVI*eta_c*s_d5 {Inlet solar heat at given solar irradiance}
SH_VI6=A_CVI*eta_c*s_d6 {Inlet solar heat at given solar irradiance}
SH_VI7=A_CVI*eta_c*s_d7 {Inlet solar heat at given solar irradiance}
SH_VI8=A_CVI*eta_c*s_d8 {Inlet solar heat at given solar irradiance}
SH_VI9=A_CVI*eta_c*s_d9 {Inlet solar heat at given solar irradiance}
SH_VI10=A_CVI*eta_c*s_d10 {Inlet solar heat at given solar irradiance}
{Case VII}
Q_VII=381396.546 [KJ] {Heat required at heater F+E+C+B+A}
A_CVII=Q_VII/(S_d*eta_c) {Collector area in case VII at average annual solar irrdiance}
SH_VII1=A_CVII*eta_c*s_d1 {Inlet solar heat at given solar irradiance}
SH_VII2=A_CVII*eta_c*s_d2 {Inlet solar heat at given solar irradiance}
SH_VII3=A_CVII*eta_c*s_d3 {Inlet solar heat at given solar irradiance}
SH_VII4=A_CVII*eta_c*s_d4 {Inlet solar heat at given solar irradiance}
SH_VII5=A_CVII*eta_c*s_d5 {Inlet solar heat at given solar irradiance}
SH_VII6=A_CVII*eta_c*s_d6 {Inlet solar heat at given solar irradiance}
SH_VII7=A_CVII*eta_c*s_d7 {Inlet solar heat at given solar irradiance}
SH_VII8=A_CVII*eta_c*s_d8 {Inlet solar heat at given solar irradiance}
SH_VII9=A_CVII*eta_c*s_d9 {Inlet solar heat at given solar irradiance}
SH_VII10=A_CVII*eta_c*s_d10 {Inlet solar heat at given solar irradiance}

1.3 EES Model of Energy Efficiency and Heat Rate in All Cases

"Net Energy Efficiencies and Heat Rate in All Cases"
CV_G=15156.22[KJ/kg] {Gross Calorific Value of coal}
P_gen=210 [MW] {Net power output of the plant}
F=135 [Ton/hr] {Based on data collected from actual plant operation}
F_A= 2.075 [Ton/hr] {Equivalent amount of fuel utilization in heater A}
F_B= 4.567 [Ton/hr] {Equivalent amount of fuel utilization in heater B}
F_C= 4.092 [Ton/hr] {Equivalent amount of fuel utilization in heater C}
F_E= 3.186 [Ton/hr] {Equivalent amount of fuel utilization in heater E}
F_F= 11.24 [Ton/hr] {Equivalent amount of fuel utilization in heater F}
F_FCB= 19.899 [Ton/hr] {Equivalent amount of fuel utilization in heater F+C+B}
F_FECBA= 25.16 [Ton/hr] {Equivalent amount of fuel utilization in heater F+E+C+B+A}
L=1933.19 [KJ/kg] {Latent heat of vapourisation at inlet pressure of heater A}
CV_L=CV_G-L {Lower calorific value of fuel}
eta=((P_gen*3600*1000)/(F*1000*CV_L))*100 {Energy efficiency of plant in normal operation}
H_Rate=((F*1000*CV_L)/(P_gen*1000)) {Heat rate of plant in normal operation}
{CASE I}
L_I=1933.19 [KJ/kg] {Latent heat of vapourisation at inlet pressure of heater A for case I}
CV_LI=CV_G-L_I {Lower calorific value of fuel at case I}
F_I=F-F_A {Amount of fuel requirement in case I}
eta_I=((P_gen*3600*1000)/(F_I*1000*CV_LI))*100 {Energy efficiency in case I}
H_RateI=((F_I*1000*CV_LI)/(P_gen*1000)) {Heat rate of plant in case I}
{CASE II}
L_II=2358.40 [KJ/kg] {Latent heat of vapourisation at inlet pressure of heater B for case II}
CV_LII=CV_G-L_II {Lower calorific value of fuel at case II}
F_II=F-F_B {Amount of fuel requirement in case II}
eta_II=((P_gen*3600*1000)/(F_II*1000*CV_LII))*100 {Energy efficiency in case II}
H_RateII=((F_II*1000*CV_LII)/(P_gen*1000)) {Heat rate of plant in case II}
{CASE III}
L_III=2226.23 [KJ/kg] {Latent heat of vapourisation at inlet pressure of heater C for case III}
CV_LIII=CV_G-L_III {Lower calorific value of fuel at case III}
F_III=F-F_C {Amount of fuel requirement in case III}

eta_III=((P_gen*3600*1000)/(F_III*1000*CV_LIII))*100 {Energy efficiency in case III}
H_RateIII=((F_III*1000*CV_LIII)/(P_gen*1000)) {Heat rate of plant in case III}
{CASE IV}
L_IV=2188.94 [KJ/kg] {Latent heat of vapourisation at inlet pressure of heater E for case IV}
CV_LIV=CV_G-L_IV {Lower calorific value of fuel at case IV}
F_IV=F-F_E {Amount of fuel requirement in case IV}
eta_IV=((P_gen*3600*1000)/(F_IV*1000*CV_LIV))*100 {Energy efficiency in case IV}
H_RateIV=((F_IV*1000*CV_LIV)/(P_gen*1000)) {Heat rate of plant in case IV}
{CASE V}
L_V=1933.19 [KJ/kg] {Latent heat of vapourisation at inlet pressure of heater F for case V}
CV_LV=CV_G-L_V {Lower calorific value of fuel at case V}
F_V=F-F_F {Amount of fuel requirement in case V}
eta_V=((P_gen*3600*1000)/(F_V*1000*CV_LV))*100 {Energy efficiency in case V}
H_RateV=((F_V*1000*CV_LV)/(P_gen*1000)) {Heat rate of plant in case V}
{CASE VI}
L_VI=2358.40 [KJ/kg] {Latent heat of vapourisation at inlet pressure of heater B for case VI}
CV_LVI=CV_G-L_VI {Lower calorific value of fuel at case VI}
F_VI=F-F_FCB {Amount of fuel requirement in case VI}
eta_VI=((P_gen*3600*1000)/(F_VI*1000*CV_LVI))*100 {Energy efficiency in case VI}
H_RateVI=((F_VI*1000*CV_LVI)/(P_gen*1000)) {Heat rate of plant in case VI}
{CASE VII}
L_VII=1933.19 [KJ/kg] {Latent heat of vapourisation at inlet pressure of heater A for case VII}
CV_LVII=CV_G-L_VII {Lower calorific value of fuel at case VII}
F_VII=F-F_FECBA {Amount of fuel requirement in case VII}
eta_VII=((P_gen*3600*1000)/(F_VII*1000*CV_LVII))*100 {Energy efficiency in case VII}
H_RateVII=((F_VII*1000*CV_LVII)/(P_gen*1000)) {Heat rate of plant in case VII}

1.5 EES Model of Area Requirement for Collector and Land Area for CLFR/HFC

"Area Requirement for collector and land area"
s_d=0.18 [kW/m^2] {Average annual Solar Irradiance}
eta_C=36/72 {Collactor efficiency of CLFR/HFC solar Collactor}
{Case I}
Q_I=31455.4284 [kJ] {Heat requirement at Collector in case I}
A_CI=Q_I/(s_d*eta_c) {Area of solar collector required in case I}
A_LI=3*A_CI {Approximate area of land required in case I}
{Case II}
Q_II=69216.1776 [kJ] {Heat requirement at Collector in case II}
A_CII=Q_II/(s_d*eta_c) {Area of solar collector required in case II}
A_LII=3*A_CII {Approximate area of land required in case II}
{Case III}
Q_III=62027.442 [kJ] {Heat requirement at Collector in case III}
A_CIII=Q_III/(s_d*eta_c) {Area of solar collector required in case III}
A_LIII=3*A_CIII {Approximate area of land required in case III}
{Case IV}
Q_IV=48282.1776 [kJ] {Heat requirement at Collector in case IV}
A_CIV=Q_IV/(s_d*eta_c) {Area of solar collector required in case IV}
A_LIV=3*A_CIV {Approximate area of land required in case IV}
{Case V}
Q_V=170415.3204 [kJ] {Heat requirement at Collector in case V}
A_CV=Q_V/(s_d*eta_c) {Area of solar collector required in case V}
A_LV=3*A_CV {Approximate area of land required in case V}
{Case VI}

Q_VI=301658.940 [kJ] {Heat requirement at Collector in case VI}
A_CVI=Q_VI/(s_d*eta_c) {Area of solar collector required in case VI}
A_LVI=3*A_CVI {Approximate area of land required in case VI}
{Case VII}
Q_VII=381396.546 [kJ] {Heat requirement at Collector in case VII}
A_CVII=Q_VII/(s_d*eta_c) {Area of solar collector required in case VII}
A_LVII=3*A_CVII {Approximate area of land required in case VII}

1.6 EES Model of Solar Collector Area Requirement at Different Inlet Irradiance Conditions

"Variation of requirement of solar collector with the variation of solar irradiation"
eta_C=36/72 {Collaction efficiency of CLFR/HFC Collector}
S_d=0.18 [KW/m^2] {Average annual solar irradiance at plant location based on DNI data}
s_d1=0.09 [KW/m^2] {Minimum solar irradiance at plant location based on DNI data}
s_d2=0.11 [KW/m^2] {Typical value of solar irradiance at plant location based on DNI data}
s_d3=0.13 [KW/m^2] {Typical value of solar irradiance at plant location based on DNI data}
s_d4=0.15 [KW/m^2] {Typical value of solar irradiance at plant location based on DNI data}
s_d5=0.17 [KW/m^2] {Typical value of solar irradiance at plant location based on DNI data}
s_d6=0.19 [KW/m^2] {Typical value of solar irradiance at plant location based on DNI data}
s_d7=0.21 [KW/m^2] {Typical value of solar irradiance at plant location based on DNI data}
s_d8=0.23 [KW/m^2] {Typical value of solar irradiance at plant location based on DNI data}
s_d9=0.25 [KW/m^2] {Typical value of solar irradiance at plant location based on DNI data}
s_d10=0.27 [KW/m^2] {Maximum solar irradiance at plant location based on DNI data}
{CASE I}
Q_I=31455.4284 [kJ] {Heat requirement at solar collector in case I}
A_I1=Q_I/(s_d1*eta_C) {Area of solar collcctor required in hectares}
A_I2=Q_I/(s_d2*eta_C) {Area of solar collcctor required in hectares}
A_I3=Q_I/(s_d3*eta_C) {Area of solar collcctor required in hectares}
A_I4=Q_I/(s_d4*eta_C) {Area of solar collcctor required in hectares}
A_I5=Q_I/(s_d5*eta_C) {Area of solar collcctor required in hectares}
A_I6=Q_I/(s_d6*eta_C) {Area of solar collcctor required in hectares}
A_I7=Q_I/(s_d7*eta_C) {Area of solar collcctor required in hectares}
A_I8=Q_I/(s_d8*eta_C) {Area of solar collcctor required in hectares}
A_I9=Q_I/(s_d9*eta_C) {Area of solar collcctor required in hectares}
A_I10=Q_I/(s_d10*eta_C) {Area of solar collcctor required in hectares}
{CASE II}
Q_II=69216.1776 [kJ] {Heat requirement at solar collector in case II}
A_II1=Q_II/(s_d1*eta_C) {Area of solar collcctor required in hectares}
A_II2=Q_II/(s_d2*eta_C) {Area of solar collcctor required in hectares}
A_II3=Q_II/(s_d3*eta_C) {Area of solar collcctor required in hectares}
A_II4=Q_II/(s_d4*eta_C) {Area of solar collcctor required in hectares}
A_II5=Q_II/(s_d5*eta_C) {Area of solar collcctor required in hectares}
A_II6=Q_II/(s_d6*eta_C) {Area of solar collcctor required in hectares}
A_II7=Q_II/(s_d7*eta_C) {Area of solar collcctor required in hectares}
A_II8=Q_II/(s_d8*eta_C) {Area of solar collcctor required in hectares}
A_II9=Q_II/(s_d9*eta_C) {Area of solar collcctor required in hectares}
A_II10=Q_II/(s_d10*eta_C) {Area of solar collcctor required in hectares}
{CASE II}
Q_III=62027.442 [kJ] {Heat requirement at solar collector in case III}
A_III1=Q_III/(s_d1*eta_C) {Area of solar collcctor required in hectares}
A_III2=Q_III/(s_d2*eta_C) {Area of solar collcctor required in hectares}
A_III3=Q_III/(s_d3*eta_C) {Area of solar collcctor required in hectares}
A_III4=Q_III/(s_d4*eta_C) {Area of solar collcctor required in hectares}

A_III5=Q_III/(s_d5*eta_C) {Area of solar collcctor required in hectares}
A_III6=Q_III/(s_d6*eta_C) {Area of solar collcctor required in hectares}
A_III7=Q_III/(s_d7*eta_C) {Area of solar collcctor required in hectares}
A_III8=Q_III/(s_d8*eta_C) {Area of solar collcctor required in hectares}
A_III9=Q_III/(s_d9*eta_C) {Area of solar collcctor required in hectares}
A_III10=Q_III/(s_d10*eta_C) {Area of solar collcctor required in hectares}
{CASE IV}
Q_IV=48282.1776 [kJ] {Heat requirement at solar collector in case IV}
A_IV1=Q_IV/(s_d1*eta_C) {Area of solar collcctor required in hectares}
A_IV2=Q_IV/(s_d2*eta_C) {Area of solar collcctor required in hectares}
A_IV3=Q_IV/(s_d3*eta_C) {Area of solar collcctor required in hectares}
A_IV4=Q_IV/(s_d4*eta_C) {Area of solar collcctor required in hectares}
A_IV5=Q_IV/(s_d5*eta_C) {Area of solar collcctor required in hectares}
A_IV6=Q_IV/(s_d6*eta_C) {Area of solar collcctor required in hectares}
A_IV7=Q_IV/(s_d7*eta_C) {Area of solar collcctor required in hectares}
A_IV8=Q_IV/(s_d8*eta_C) {Area of solar collcctor required in hectares}
A_IV9=Q_IV/(s_d9*eta_C) {Area of solar collcctor required in hectares}
A_IV10=Q_IV/(s_d10*eta_C) {Area of solar collcctor required in hectares}
{CASE V}
Q_V=170415.3204 [kJ] {Heat requirement at solar collector in case V}
A_V1=Q_V/(s_d1*eta_C) {Area of solar collcctor required in hectares}
A_V2=Q_V/(s_d2*eta_C) {Area of solar collcctor required in hectares}
A_V3=Q_V/(s_d3*eta_C) {Area of solar collcctor required in hectares}
A_V4=Q_V/(s_d4*eta_C) {Area of solar collcctor required in hectares}
A_V5=Q_V/(s_d5*eta_C) {Area of solar collcctor required in hectares}
A_V6=Q_V/(s_d6*eta_C) {Area of solar collcctor required in hectares}
A_V7=Q_V/(s_d7*eta_C) {Area of solar collcctor required in hectares}
A_V8=Q_V/(s_d8*eta_C) {Area of solar collcctor required in hectares}
A_V9=Q_V/(s_d9*eta_C) {Area of solar collcctor required in hectares}
A_V10=Q_V/(s_d10*eta_C) {Area of solar collcctor required in hectares}
{CASE VI}
Q_VI=301658.940 [kJ] {Heat requirement at solar collector in case VI}
A_VI1=Q_VI/(s_d1*eta_C) {Area of solar collcctor required in hectares}
A_VI2=Q_VI/(s_d2*eta_C) {Area of solar collcctor required in hectares}
A_VI3=Q_VI/(s_d3*eta_C) {Area of solar collcctor required in hectares}
A_VI4=Q_VI/(s_d4*eta_C) {Area of solar collcctor required in hectares}
A_VI5=Q_VI/(s_d5*eta_C) {Area of solar collcctor required in hectares}
A_VI6=Q_VI/(s_d6*eta_C) {Area of solar collcctor required in hectares}
A_VI7=Q_VI/(s_d7*eta_C) {Area of solar collcctor required in hectares}
A_VI8=Q_VI/(s_d8*eta_C) {Area of solar collcctor required in hectares}
A_VI9=Q_VI/(s_d9*eta_C) {Area of solar collcctor required in hectares}
A_VI10=Q_VI/(s_d10*eta_C) {Area of solar collcctor required in hectares}
{CASE VII}
Q_VII=381396.546 [kJ] {Heat requirement at solar collector in case VII}
A_VII1=Q_VII/(s_d1*eta_C) {Area of solar collcctor required in hectares}
A_VII2=Q_VII/(s_d2*eta_C) {Area of solar collcctor required in hectares}
A_VII3=Q_VII/(s_d3*eta_C) {Area of solar collcctor required in hectares}
A_VII4=Q_VII/(s_d4*eta_C) {Area of solar collcctor required in hectares}
A_VII5=Q_VII/(s_d5*eta_C) {Area of solar collcctor required in hectares}
A_VII6=Q_VII/(s_d6*eta_C) {Area of solar collcctor required in hectares}
A_VII7=Q_VII/(s_d7*eta_C) {Area of solar collcctor required in hectares}
A_VII8=Q_VII/(s_d8*eta_C) {Area of solar collcctor required in hectares}
A_VII9=Q_VII/(s_d9*eta_C) {Area of solar collcctor required in hectares}
A_VII10=Q_VII/(s_d10*eta_C) {Area of solar collcctor required in hectares}

1.7 EES Model of Effect of Fluid Inlet Temperature in Solar Field on Collector Efficiency

"Effect of inlet fluid temperature on instantaneous collection efficiency for optimum mass flow rate"
eta_C=36 {collection efficiency of LFR collector}
s_d=0.18 [kW/m^2] {Average annual solar irradiance at plant location}
A=58857.4916 [m^2] {maximum calculated area of solar collector requirement to replace all the heaters}
{HEATER F}
T_oF=518.1 [K] {outlet temperature of fluid in heater F}
Q_F=170415.3204 [kJ] {heat required at heater F}
eta_CF=Q_F/(s_d*A) {Instantaneous collection efficiency of solar collector after replacing heater F}
{HEATER F+E}
T_oFE=434 [K] {outlet temperature of fluid in heater F+E}
Q_FE=218697.489 [kJ] {heat required at heater F+E}
eta_CFE=Q_FE/(s_d*A) {Instantaneous collection efficiency of solar collector after replacing heaters F+E}
{HEATER F+E+C}
T_oFEC=368 [K] {outlet temperature of fluid in heater F+E+C}
Q_FEC=280724.94 [kJ] {heat required at heater F+E+C}
eta_CFEC=Q_FEC/(s_d*A) {Instantaneous collection efficiency of solar collector after replacing heaters F+E+C}
{HEATER F+E+C+B}
T_oFECB=334 [K] {outlet temperature of fluid in heater F+E+C+B}
Q_FECB=349491.118 [kJ] {heat required at heater F+E+C+B}
eta_CFECB=Q_FECB/(s_d*A) {Instantaneous collection efficiency of solar collector after replacing heaters F+E+C+B}
{HEATER F+E+C+B+A}
T_oFECBA=319 [K] {outlet temperature of fluid in heater F+E+C+B+A}
Q_FECBA=381396.546 [kJ] {heat required at heater F+E+C+B+A}
eta_CFECBA=Q_FECBA/(s_d*A) {Instantaneous collection efficiency of solar collector after replacing heaters F+E+C+B+A}

1.8 EES Model of Rate of CO_2 and SO_2 Production in All Cases

"The rate of CO2 and SO2 production in all the cases"
P_gen=210*10^3 [kW] {Net power output of the plant}
F=135 [Ton/hr] {Based on data collected from actual plant operation}
F_A= 2.075 [Ton/hr] {Equivalent amount of fuel utilization in heater A}
F_B= 4.567 [Ton/hr] {Equivalent amount of fuel utilization in heater B}
F_C= 4.092 [Ton/hr] {Equivalent amount of fuel utilization in heater C}
F_E= 3.186 [Ton/hr] {Equivalent amount of fuel utilization in heater E}
F_F= 11.24 [Ton/hr] {Equivalent amount of fuel utilization in heater F}
F_FCB= 19.899 [Ton/hr] {Equivalent amount of fuel utilization in heater F+C+B}
F_FECBA= 25.16 [Ton/hr] {Equivalent amount of fuel utilization in heater F+E+C+B+A}
{Ultimate analysis results of coal in airdried condition}
M=0.0636
Ash=0.4105
C=0.3964
H=0.0318
N=0.0086

```
S=0.0054
O=0.0837
{Theoratical air required for complete combustion of fuel used}
A_th=(11.5*C)+(34.5*(H-(O/8)))+(4.3*S) {kg of air per kg of fuel}
{Actual amount of air supplied for complete combustion of 1 kg fuel}
A_act=1.3*A_th {Assuming 30% excess air is required for complete combustion of fuel}
{Water vapour entering with air per kg of fuel}
V_WF=A_act*M
{Total water vapour formed per kg fuel}
V_WT=9*H+M+V_WF
{Mass of combustion gases per kg of fuel}
M_CO2=(44/12)*C
M_SO2=(64/32)*S
{The rate of CO2 and SO2 production kg/kWh calculation}
{For base case}
R_CO2=(F*M_CO2*1000)/P_gen
R_SO2=(F*M_SO2*1000)/P_gen
{CASE I}
R_CO2I=((F-F_A)*M_CO2*1000)/P_gen
R_SO2I=((F-F_A)*M_SO2*1000)/P_gen
{CASE II}
R_CO2II=((F-F_B)*M_CO2*1000)/P_gen
R_SO2II=((F-F_B)*M_SO2*1000)/P_gen
{CASE III}
R_CO2III=((F-F_C)*M_CO2*1000)/P_gen
R_SO2III=((F-F_C)*M_SO2*1000)/P_gen
{CASE IV}
R_CO2IV=((F-F_E)*M_CO2*1000)/P_gen
R_SO2IV=((F-F_E)*M_SO2*1000)/P_gen
{CASE V}
R_CO2V=((F-F_F)*M_CO2*1000)/P_gen
R_SO2V=((F-F_F)*M_SO2*1000)/P_gen
{CASE VI}
R_CO2VI=((F-F_FCB)*M_CO2*1000)/P_gen
R_SO2VI=((F-F_FCB)*M_SO2*1000)/P_gen
{CASE VII}
R_CO2VII=((F-F_FECBA)*M_CO2*1000)/P_gen
R_SO2VII=((F-F_FECBA)*M_SO2*1000)/P_gen
```

1.9 EES Model of Analytical Integration of TES

```
"Thermal Energy Storage Design"
T_HT= 823.15 [K] {Higher temperature water received at inlet of storage system}
T_CT= 563.15 [K] {Lower temperature of water bypass at low temperature tank}
t= 10 [Hours] {Time of operation through storage}
c_psalt=1.54 [kJ/kgK] {Specifc heat of salt in use}
rho_HT=2096 [kg/m^3] {Density of molten salt at higher temperature}
rho_CT=2192 [kg/m^3] {Density of molten salt at lower temperature}
Q_Tank= 381396.546 [kJ] {Energy required by the tank for Replacement of all FWH}
{Mass Flow of the Salts}
m_Salt=(Q_Tank*t)/(c_psalt*(T_HT-T_CT))
{Maximum volume of the hot tank}
V_HT=(m_Salt*t)/(rho_HT)
{Maximum volume of the cold tank}
V_CT=(m_Salt*t)/(rho_CT)
```

APPENDIX 2

2.1 Comparison between different CSP technologies: [72]

CSP Technology	Operating Temperat--ure (°C)	Solar Concent--ration Ratio	Storage Integration Possibility	Advantage	Disadvantage
Parabolic Trough Collector	20-400	15-45	Possible	- Relatively low installation cost. - Large experimental feedback	- Relatively large area occupied. - Low thermodynamic efficiency due to low operating temperature.
Linear Fresnel Reflector	50-300	10-40	Possible	- Relatively low installation cost.	- Low thermodynamic efficiency due to low operating temperature.
Solar Power Tower	300-1000	150-1500	Highly possible with low storage cost	- High thermodynamic efficiency due to high operating temperature.	- Large space area occupied. - Relatively high installation cost. - High heat loss.
Parabolic Dish Collector	120-1500	100-1000	Difficult	- Relatively small area occupied. - High thermodynamic efficiency due to high operating temperature.	- Relatively high installation cost. - Little experimental feedback.

2.2 Summary of different Thermal Energy Storage Technologies: [84]

Technology	Cost	Energy Density	Occupied Area	Temperature for material Storage	Technology Feedback	Flexibility Charge/ Discharge	Heat Transfer	Advantages	Disadvantages
Sensible	Low Cost Materials	Low	High	High	- Large Experimental Feedback. - Majority of CSP Plants in operation.	Switch within a short time	Quite good	- Large experimental and commercial feedback. - Easy implementation	- Heat loss during storage. - Low energy density - High freezing point for liquid materials. - Variable discharging temperature
Latent	Low Cost Materials	Medium	Medium	High	- More R&D Work needed	Switch within a short time	Slow low thermal conductivity	- Constant charge/ discharge temperatures - Medium energy density	- Low thermal conductivity. - Solid deposits on the PCM/ heat exchanger area.
Thermo-chemical	Low Cost Materials High design and installation costs for the reactor	High	Low	Low (Ambient Temperature)	- No feedback	Switch within a medium time	Slow low thermal conductivity		- Incomplete reversibility - Storage of gaseous products. - Necessity of heat and mass transfer enhancement.

2.3 Characteristic values for solar thermal technologies and their alternatives [32]

PARAMETER	Criteria	Sub- Criteria	Metric	Unit	Alternatives	Parabolic Trough		Heliostat Field Collector			Linear Fresnel reflector		Parabolic Dish Reflector	Compound Parabolic Collector	
					Sub-Alternatives / Comment	Synthetic Oil	DSG	Salt Receiver	Water/ Steam	Volumetric	CLFR	LFR	Glass	CPC	With Linear Fresnel Lens
TECHNICAL	Efficiency	Ideal Conversion Efficiency	-	%	Optical and Carnot efficiency	33%	Higher	45%		Higher	25%	Lower	65%	Lower	22%
		Collector Efficiency		%	Heat transferred based on the ideal system	63%		72%			36%		66%	36	
		Stagnation Temperature		^{0}C		600	Higher	1750			300+		1200+	-	-
		Optical Efficiency		%	Ratio of sunlight capture to incident sunlight	80		Varied		73	67	Lower	94	-	60-65
		Concentration of direct sunlight	Concentration ratio	Number	-	30-100		300-1500		Lower	30+		500-1500	3	10-20
			Capture efficiency	%	-	91		Varied			76	Lower	100	-	40-50
			Half acceptance angle	Degree	Affects required tracking accuracy	0.5		-		-	0.75		0.4	20	3
		Parasitic Load	Fraction of electrical output	%	Eg. for tracking, pumps, etc.	10	Higher	10-20		10	Higher	Low	4	V low	2.3
	Compatibility with working fluid	Pressure Tolerance	-	bar	Flexible hosing, fixed receiver	40-100		100+		10-20	69		20	-	
		Temperature Tolerance		^{0}C	-	100-400	Higher	150-800		1000+	10-300			‹100	‹200

		Chemical Compatibility of heat transfer medium		-	Freezing, Fire hazard, corrosion	Synthetic oil	Water	Molten Salt	Steam	Air	Water		Air	Water	
		2 Phase flow		-	Are difficulties with 2-phase flow encountered	No	Yes	No	Yes	No	Yes		No	Yes	
	Reliability	Reliability	-	% Prediction	Environmental resistance, annual replacement of parts.	5.5 V Low		Medium			Medium		Med-low	Low	High
	Availability	Use of Standard technologies or parts	Number of standard Parts	-	-	Med-Low	Medium	Med-Low	Medium	Med- Low	High		V low	High	Med-high
FINANCIAL	**Affordability**	Capital Cost	-	Dollars/ kW	-	3972	2300	4000+			-	Lower	12578	Lower	-
				Dollars/ m^2	-	424	Lower	476			234	Lower	-	Lower	260
		Total M&O cost		Dollars/ kWh	-	0.012-0.02	Lower	0.034			Low	Lower	0.21	-	
ENVIRONMENTAL	**Resource Usages**	Land Usages	-	m^2/MWh/ Year	Land use per energy output	3.2	Lower	4.6			1.8	Higher	4.15	-	
		Tolerance of slope		Degrees	-	-		Flexible			‹1		Flexible	Level	
		Water Usage	Dependant on system	m^3/MWh	Water Cooled	3.07		2.27	Higher				None	-	
					Dry Cooled	0.3	Higher		Higher		0.04		None	-	
				m^3/m^2/year	Water mirror washing	0.022		0.022			0.022		0.022	-	Lower
	Scalability	Efficiency at different scales	-	-	-	Better		Poor			Better		Better	Better	
		Suitable operating range	Electrical Range	MW	-	0.05-100		0.5-100			0.05-100		0.025-100	Better	

2.4 Discussion on Physical and Chemical Properties of Coal: [25]

Sample ID	Condition	GCV (Kcal/kg)	Proximate Analysis				Ultimate Analysis				
			Moisture %	Ash %	VM %	FC %	C %	H %	N %	S %	O % Diff.
100% Coal	Air Dried	3620	6.36	41.05	22.19	30.40	39.64	3.18	0.86	0.54	8.37
95% Coal + 5% Biomass	Air Dried	3654	6.24	39.70	24.46	29.60	40.45	3.26	0.83	0.45	9.07
90% coal + 10% Biomass	Air Dried	3684	6.09	37.61	26.85	29.45	40.89	3.38	0.75	0.62	10.66
100% Biomass	Air Dried	3850	5.76	10.21	67.29	16.74	42.75	5.42	0.12	0.11	35.63

EVALUATION OF PARALLEL FEED WATER HEATING IN INTEGRATED SOLAR THERMAL POWER PLANT

ORIGINALITY REPORT

2%	1%	2%	1%
SIMILARITY INDEX	INTERNET SOURCES	PUBLICATIONS	STUDENT PAPERS

PRIMARY SOURCES

1	Submitted to Management Development Institute Student Paper	<1%
2	dspace.inha.ac.kr Internet Source	<1%
3	docplayer.net Internet Source	<1%
4	ethesis.nitrkl.ac.in Internet Source	<1%
5	Wina Graus, Ernst Worrell. "Methods for calculating CO2 intensity of power generation and consumption: A global perspective", Energy Policy, 2011 Publication	<1%
6	belco.bm Internet Source	<1%
7	Submitted to University of Sheffield Student Paper	<1%

8	educationdocbox.com Internet Source	<1%
9	Submitted to University of New South Wales Student Paper	<1%
10	Proceedings of ISES World Congress 2007 (Vol I – Vol V), 2009. Publication	<1%
11	Entregado a UC, Irvine el 2012-06-08 Student Paper	<1%
12	Submitted to Institute of Technology, Nirma University Student Paper	<1%
13	V B Khlyupin. "Mathematical modeling of a running cycle of the diesel engine with the additive of water at the intake", IOP Conference Series: Materials Science and Engineering, 2017 Publication	<1%
14	Submitted to Ateneo de Davao University Student Paper	<1%
15	www.secinfo.com Internet Source	<1%
16	www.msubbu.in Internet Source	<1%
	www.ipi.uni-hannover.de	

17	Internet Source	<1%
18	Flavio D.F. Chuahy, Sage L. Kokjohn. "High efficiency dual-fuel combustion through thermochemical recovery and diesel reforming", Applied Energy, 2017 Publication	<1%

Exclude quotes	On	Exclude matches	< 10 words
Exclude bibliography	On		